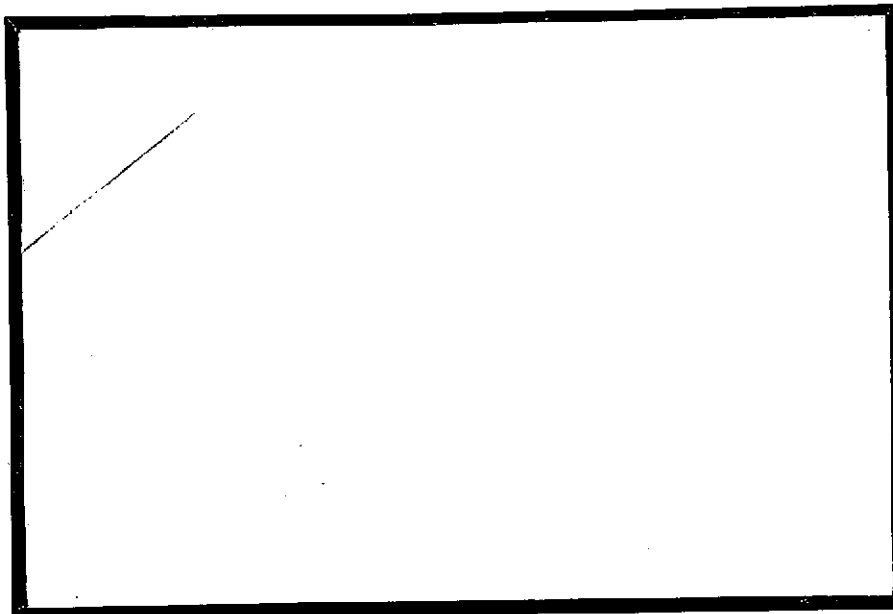


2m14

ELECTRICAL

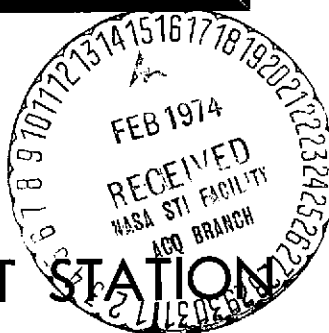
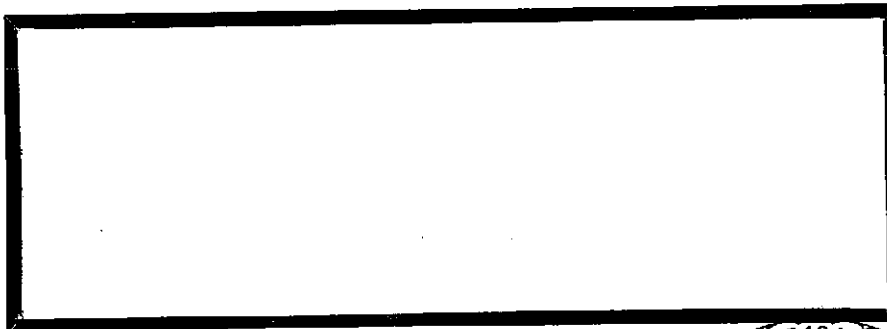


E
N
G
I
N
E
E
R
I
N
G

(NASA-CR-120132) DESIGN IMPLEMENTATION IN
MODEL-REFERENCE ADAPTIVE SYSTEMS (Auburn
Univ.) 212 p HC \$12.75 CACL 22B

N74-16553

Unclas
G3/31 28470



ENGINEERING EXPERIMENT STATION

AUBURN UNIVERSITY

AUBURN, ALABAMA

DESIGN IMPLEMENTATION IN MODEL-REFERENCE
ADAPTIVE SYSTEMS

Prepared By

GUIDANCE AND CONTROL STUDY GROUP

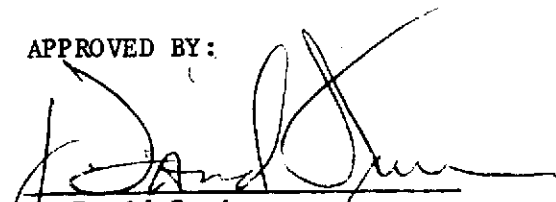
JOSEPH S. BOLAND, III, PROJECT LEADER

FIFTH TECHNICAL REPORT

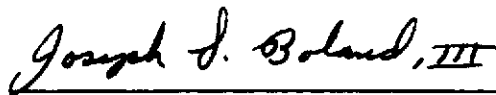
SEPTEMBER 14, 1973

CONTRACT NAS8-26580
GEORGE C. MARSHALL SPACE FLIGHT CENTER
NATIONAL AERONAUTICS AND SPACE ADMINISTRATION
HUNTSVILLE, ALABAMA

APPROVED BY:


J. David Irwin
Associate Professor and Head
Electrical Engineering

SUBMITTED BY:


Joseph S. Boland, III
Associate Professor
Electrical Engineering

FORWARD

The Auburn University Engineering Experiment Station submitted a proposal which resulted in Contract NAS8-26580 being awarded on November 15, 1970. The contract was awarded to the Engineering Experiment Station by the George C. Marshall Space Flight Center, National Aeronautics and Space Administration, Huntsville, Alabama, and was active until September 15, 1973.

This report is a technical summary of the progress made by the Electrical Engineering Department, Auburn, Alabama in the performance of this contract.

ACKNOWLEDGEMENT

The research for this report was performed under Contract NAS8-26580 awarded to the Auburn Engineering Experiment Station, Auburn, Alabama, by the George C. Marshall Space Flight Center of the National Aeronautics and Space Administration. The Project Leader for this work was Associate Professor Joseph S. Boland, III, of the Electrical Engineering Department, Auburn University.

PERSONNEL

The following staff members of Auburn University were active participants in the research for this report:

- J. S. Boland, III - Associate Professor of Electrical Engineering
- B. K. Colburn - Graduate Research Assistant

SUMMARY

The derivation of an approximate error characteristic equation describing the transient system error response is given, along with a procedure for selecting adaptive gain parameters so as to relate to the transient error response. A detailed example of the application and implementation of these methods for a space shuttle type vehicle is included. An extension of the characteristic equation technique is used to provide an estimate of the magnitude of the maximum system error and an estimate of the time of occurrence of this maximum after a plant parameter disturbance.

Techniques for relaxing certain stability requirements and the conditions under which this can be done and still guarantee asymptotic stability of the system error are discussed. Such conditions are possible because the Lyapunov methods used in the stability derivation allow for overconstraining a problem in the process of insuring stability.

Practical implementation problems such as system noise and incomplete state feedback are studied and results given in terms of a bounding criteria on the system error. Under these conditions, asymptotic stability discussions are inappropriate and instead one speaks of bounded stability or stability in the large.

TABLE OF CONTENTS

LIST OF TABLES	viii
LIST OF FIGURES.	ix
I. INTRODUCTION.	1
II. DERIVATION OF A DESIGN IMPLEMENTATION TECHNIQUE	6
Problem Formulation	
Development of the Linearized Error Equation	
Decoupling the Input From the Linearized Error Dynamics	
Application of the Error Equation	
Adaptive Error Estimation	
Design Implementation	
Error Transient Response Determination From Lyapunov Function	
III. DETERMINATION OF STABILITY CRITERIA PROVIDED BY LYAPUNOV THEORY	62
Conventional Technique For Selection of the Q Matrix	
An Extended Stability Bounding Criteria	
An Exact Stability Bounding Technique Employing an Algebraic Equation	
Kleinman's Iterative Method For Determination of Bounds On Q Matrix Elements	
Comparison Between Stability Bounds Obtained From Lyapunov Theory and Linear Methods	
IV. PRACTICAL DIFFICULTIES IN IMPLEMENTING AN MRAS CONTROLLER.	94
MRAS Controllers With Noise	
Parametric Study of the Error Bound As a Function of the Noise Bounds	
Incomplete Adaptation and State Feedback	
An Adjustment Technique For Obtaining Time-Invariant Error Dynamics	

V. RELATED TOPICS.	147
Simulation Results For a Physically Realizeable Space Shuttle Pitch Axis Controller	
RCJ to MRAS Attitude Phase-Over Control During Re-Entry	
On-Board Control Computer Computational Requirement	
Use of More Than One Model During Re-Entry	
VI. SUMMARY AND CONCLUSIONS	172
REFERENCES	176
APPENDICES	178
A. DERIVATION OF DEFINING EQUATION FOR DETERMINING BOUNDS ON THE q_{ij} ELEMENTS	179
B. PHASE-VARIABLE TRANSFORMATION	188
C. DERIVATION OF AN ERROR BOUND WITH STATE AND INPUT NOISES PRESENT.	194

LIST OF TABLES

II-1. Adaptive Gain Values. 39
V-1. Simulation Data for Results Shown in Figure V-2.A 151
V-2. Computation Cycle-Time Equations. 165

LIST OF FIGURES

II-1.C	Various Root Loci Configurations Comparing "Coupled and "Decoupled" Design Techniques	27
II-1.D	Re-Entering Space-Shuttle Vehicle	30
II-2.D	Typical Time-Varying Physical Data Causing Time-Varying Plant Parameters	33
II-3.D	Typical Time Variation of Plant Parameters During Re-Entry (adaptation must compensate for the changes) . .	34
II-4.D	Simulation Diagram of Adapted Attitude Controller	35
II-5.D	Root Loci of the Linearized Error Characteristic Equation.	38
II-6.D	Time Response of the System Error Due to a Plant Disturbance at $t = 150$ seconds (a) Winsor and Roy (b) Gilbert, Monopoli, and Price; Boland and Sutherlin	40
II-1.E	Typical Error Versus Time Trajectory.	44
II-2.E	Error Magnitude Simulation Model.	45
II-3.E	Nonlinear Problem	52
II-4.E	Error Characteristic Equation Root Locus.	55
II-5.E	Error Time Response	55
III-1.C	Root Ordering By Groups	76
III-2.C	Flowchart of QRANGE	79
III-1.E	Routh Hurwitz Array For Third Order $G_m(s)$	88
III-2.E	Illustration of $f(K)$ vs. K Requirement for (III-23.E) . .	91
III-3.E	Allowable "Zero" Root Locations Guaranteeing Asymptotic Error Stability	93
IV-1.A	Adaptive Controller with Stochastic Input and State Noise Present	96

IV-2.A	(a) Error Trajectory C showing Circular Region (b) Trajectory C May Enter Circle of Radius s (c) How p Enters the Physical Problem	101
IV-3.A	State Indeterminacy Due to Noise.	103
IV-4.A	Relationship Between $\frac{\lambda(Q)_{\max}}{\lambda(-A_m^T Q - Q A_m)_{\min}}$ and "a" With "b" as a Parameter.	111
IV-5.A	Error Root Locus for Example With Stochastic Noise.	112
IV-6.A	Adaptive Error Response With Stochastic Noise Present	114
IV-1.B	Model-Plant Layout for Example.	125
IV-2.B	Earth to Orbit Configuration for System in Figure IV-1.B.	125
IV-1.D	Two Means of Keeping Fixed Closed-Loop Error Dynamics (a) Keep the Zeroes and Gain Constant (b) Vary the Zeroes and Gain to Keep Roots Fixed	133
IV-2.D	Adaptation Process Using Dynamic Error Adjustment Technique	138
IV-3.D	Error Reduction Using Lyapunov Adjustment Technique (a), (b) Timing and Error Reduction (c) Typical Error Trajectory Illustrations.	140
IV-4.D	Root Locus Plot.	143
IV-5.D	Saturation Curves for q_{nn} Adjustment.	144
IV-6.D	Error Response Results from Adjustment Scheme for Various Step Inputs	145
IV-7.D	Error Response Using Adjustment Scheme with Sinusoidal Input	146
V-1.A	Practical Implementation of a Shuttle-Type Attitude Controller During Re-Entry Phase.	149
V-2.A	Simulation Results for Incomplete Adaptation and Time-Varying Forward Gain	152
V-1.B	RCJ Pitch Control System.	155

V-2.B	Pitch Axis Control for RCJ to MRAS Phase-Over	157
V-3.B	Circuit to Insure that the Phase-Over Control y Lies Between 0 and 1	161
V-4.B	Control Phase-Over Characteristic	164
V-5.B	Control Phase-Over Response	164
V-1.C	Computation Time/Cycle for the Boland and Sutherlin MRAS Implementation	167
V-2.C	Comparison of Computation Times for Three Adaptation Methods	168
V-3.C	MRAS Attitude Control System Showing the Internal Workings of an All-Analog On-Board Computer	170

I. INTRODUCTION

During the last twenty-five years the theoretical developments making up the classical feedback control theory have been in constant use in the design of automatic controllers. In most commercial applications in the past, using the classical tools of Nyquist and Bode plots, root-locus methods, etc. the designer was able to develop systems satisfying a set of somewhat arbitrary performance indices, i.e. rise time, peak overshoot, bandwidth, etc. With the advent of the U. S. space program, the requirements of guidance and control for space vehicles demanded more and varied analytical tools than were offered by classical theory, and hence was born what is now referred to as modern control theory.

Virtually all of the theory of both the classical and modern control sciences required as a basic assumption that the plant be time-invariant or that it vary in a well described manner. Starting with the ground-breaking work at MIT in 1959 [1], the study of adaptive control systems began. The major reason for interest in such a control area was the knowledge that a large number of physical processes were inherently time-varying and optimal and classical techniques left much to be desired. As a corollary to this, new techniques for system identification were desired.

By the mid - 1960's the groundwork for the study of adaptive control systems was laid. The most promising form of adaptive control studies appeared to center around those methods based on Lyapunov's Second Method and model-reference adaptive systems (MRAS) [2,3,4], a technique which, as part of the design process, can be used to guarantee stability of the adapted control system without need for an analytical description of the solution to the dynamic system.

A particularly promising form of adaptive controller that was based on the idea of on-line, time-varying feedback gains was published in 1968 [5] and then later extended to more general cases [6,7]. These methods suffered from the need for very slowly time-varying plants, although no knowledge of plant parameters was needed. This limitation was later partially removed [8].

Some of the shortcomings of these MRAS design techniques included

- (a) all states must be available
- (b) no noise present
- (c) rate of convergence of the errors was unknown due to the non-linear, time-varying form the closed-loop adaptive controller assumed

Analytical studies of incomplete state feedback [9,10] and stochastic noise [9] were performed to extend the adaptive controller studies to include real-world problems. An approximate solution to the error convergence rate is given in [6] and generalized to a number of different types of MRAS controllers in [11]. At least one study neglected all

physical - realizability conditions and used a controller requiring complete knowledge of the plant in order to adapt the plant [12].

As mentioned earlier, adaptation and identification are similar problems, and using the Lyapunov approach to MRAS type controllers it is possible to develop identification algorithms which can be used in a real-time environment to continuously identify a system without need of disturbing the system [13,14].

Although research was originally financed through the space program, there are a number of areas where adaptive control is presently under active investigation. Some of these areas include (1) anti-skid braking systems where the human driver represents a time-varying, statistically indeterminate plant, (2) chemical processing plants where optimum control of temperature, pressure, humidity, and material flow is extremely important to insure maximum monetary return, (3) a re-entering Space-Shuttle-type vehicle where wide variations in atmospheric conditions cause stability difficulties, (4) high performance aircraft and missiles. Specifically, many of the areas of study covered in this report stem from problem areas related to Space-Shuttle-type vehicles. Corrupted measurements of position, velocity, and acceleration of such a spacecraft, computer and A/D and D/A round-off, incomplete state feedback, and saturation are some of the real-world problems which allow, at best, only a prediction of stability regions.

The purpose of this study was to extend the theoretical work on model-reference adaptive control systems outlined in the Second Technical Report. Specifically, this report is concerned with practical considerations that must be accounted for in implementing an MRAS controller within the framework of real-world problems. These practical considerations include (a) noisy input and state measurement, (b) extending stability bounds and still guarantee asymptotic stability, (c) need for a design method for selecting adaptive gain parameters and relating them to the error dynamic response, (d) stability criterion for the case of incomplete state feedback. Analytical stability results for these cases could then, together, reveal something of the overall stability of a plant in a real-world environment.

There are four chapters subdividing the material into major areas of investigation to the body of this report, in Chapter II is derived an approximate solution to the non-linear time-varying, adaptive error differential equation. This results in a general equation relating the error response to the values of adaptive gain parameters. Using an extension of this idea an approximate method for estimating maximum error magnitude is derived. In Chapter III is outlined procedures for extending the conditions for asymptotic stability of a MRAS controller. This is an important consideration as one of the drawbacks of Lyapunov designed controllers is that sufficient but not necessary conditions are obtained and this may result in an adversely limited stability criterion. Chapter IV outlines the theory for the case of stochastic

systems and incomplete state feedback. Results are available only for very restrictive cases as would be expected. An example is included to illustrate the procedures discussed. Chapter V discusses a few of the practical considerations in physical realizability of adaptive control laws for a Shuttle-type vehicle. Included are results of a control phase-over routine from RCJ to MRAS during atmospheric re-entry. A number of simulation results are included for various practical controller implementations. In addition, a discussion of computer computational requirements is included, resulting in a series of graphs relating computer time to various system parameters.

II. DERIVATION OF A DESIGN IMPLEMENTATION TECHNIQUE

Most proposed model-reference schemes employ Lyapunov's direct method in the design procedure so as to guarantee sufficient conditions for asymptotic tracking of the model by the plant [15]. A number of model-reference schemes have been proposed in the literature [3,5,6,7,16] which work rather well in practice. In all cases, however, no general technique has been put forward for selecting the constants in the adaptive gain equations so as to cause the plant to track the model with a pre-determined error dynamic response. In the past the choice of these constants has been a trial and error procedure at best because of the inherent non-linear nature of the adaptation dynamics, even when the plant is linear. Because of these non-linearities an exact closed-form solution of the error dynamics as a function of the desired constants has not been possible and an intuitive "feel" for the relation between choice of the constants and the resulting response is difficult to obtain. Consequently, simulation studies have invariably been necessary to obtain an acceptable set of adaptive gain constants. In this chapter a straightforward method for choosing these constants is given.

The major result of the derivation which follows is a general error characteristic equation which relates the error dynamic response to the adaptive gain coefficients. Through an extension of this

approach a means of estimating the maximum error and the time after a perturbation from $\underline{e} = 0$ that this maximum error occurs is given.

The results show the error magnitude at time t_2 to be a function of the plant parameter disturbances at time $t_1 < t_2$.

A number of simulation examples are given throughout the chapter to illustrate the implementation of the techniques. An example of the pitch axis of a space shuttle vehicle is given to show the implementation of the adaptive gain parameter design method. A second example is included to illustrate the magnitude estimation procedure.

A. Problem Formulation

The basic equations defining the MRAS controller are considered in this section. The basic plant and model state variable formulations are

$$\dot{\underline{x}}_p(t) = A_p(t)\underline{x}_p(t) + B_p(t)\underline{u}(t) \quad (\text{II-1.A})$$

$$\dot{\underline{x}}_m(t) = A_m\underline{x}_m(t) + B_m\underline{u}(t) \quad (\text{II-2.A})$$

where

$\underline{x}_p(t)$ - $n \times 1$ plant state vector

$\underline{x}_m(t)$ - $n \times 1$ model state vector

$\underline{u}(t)$ - $r \times 1$ input vector

$A_m, A_p(t)$ - $n \times n$ matrices

$B_m, B_p(t)$ - $n \times r$ matrices

It is assumed that the elements of $A_p(t)$, $B_p(t)$ include unknown, slowly time-varying or time-invariant parameters. Adaptive gains $K_{ij}^a(t)$ and $K_{ij}^b(t)$ are to be implemented in the plant controller in order to force the plant states to follow the model states. These gains are defined as

$$[a_{ij}^p(t)] = [c_{ij}^a(t) + K_{ij}^a(t)], \quad (\text{II-3.A})$$

$$[b_{ij}^p(t)] = [c_{ij}^b(t) + K_{ij}^b(t)], \quad (\text{II-4.A})$$

and serve much the same purpose as the fixed optimal control gains obtained using calculus of variations. The major difference in concept is that the adaptive gains must be calculated on-line since the system dynamics are not completely known in advance. The gains are computed so as to cause the response error

$$\underline{e}(t) = \underline{x}_m(t) - \underline{x}_p(t) \quad (\text{II-5.A})$$

to tend toward zero. The basic plant-model dynamics with adaptation are shown in Figure 1.A.

Using (II-5.A), the error state equation is derived as follows:

$$\begin{aligned} \dot{\underline{e}}(t) &= \dot{\underline{x}}_m(t) - \dot{\underline{x}}_p(t) \\ \dot{\underline{e}}(t) &= [A_m \underline{x}_m(t) + B_m \underline{u}(t)] - [A_p(t) \underline{x}_p(t) + B_p(t) \underline{u}(t)] \quad (\text{II-6.A}) \end{aligned}$$

Adding and subtracting $A_m \underline{x}_p(t)$ allows (II-6.A) to be written in the form

$$\dot{\underline{e}}(t) = \underline{A}_m \underline{e}(t) + [\underline{A}_m - \underline{A}_p(t)] \underline{x}_p(t) + [\underline{B}_m - \underline{B}_p(t)] \underline{u}(t)$$

$$\dot{\underline{e}}(t) = \underline{A}_m \underline{e}(t) + A(t) \underline{x}_p(t) + B(t) \underline{u}(t) \quad (\text{II-7.A})$$

where

$$A(t) = \underline{A}_m - \underline{A}_p(t), \quad (\text{II-8.A})$$

$$B(t) = \underline{B}_m - \underline{B}_p(t). \quad (\text{II-9.A})$$

The basic purpose in using a Lyapunov function in the design procedure of a model-reference adaptive control system is to guarantee that the system error is asymptotically stable. By constructing a Lyapunov function positive definite in \underline{e} , such that V evaluated along the state trajectory is negative definite in \underline{e} , the system error will asymptotically approach zero thus assuring that the plant is tracking the model. A number of appropriate Lyapunov functions have been proposed in the literature [2,3,4,5,6]. The Lyapunov functions in [3,5,6,16] are special cases of the one in [7] which is used here and is given in (II-10.A).

$$\begin{aligned} V = & \underline{e}^T Q \underline{e} + \sum_{i,j=1}^n \frac{1}{\alpha_{ij}} \left\{ a_{ij} + \beta_{ij} \sum_{k=1}^n e_{kq_{ki}} x_{pj} + \right. \\ & \left. \rho_{ij} \frac{d}{dt} \left[\sum_{k=1}^n e_{kq_{ki}} x_{pj} \right] \right\}^2 + \sum_{i,j=1}^n \rho_{ij} \left[\sum_{k=1}^n e_{kq_{ki}} x_{pj} \right]^2 \\ & + \sum_{i=1}^n \sum_{j=1}^r \frac{1}{\gamma_{ij}} \left\{ b_{ij} + \delta_{ij} \sum_{k=1}^n e_{kq_{ki}} u_j \right. \\ & \left. + \sigma_{ij} \frac{d}{dt} \left[\sum_{k=1}^n e_{kq_{ki}} u_j \right] \right\}^2 + \sum_{i=1}^n \sum_{j=1}^r \sigma_{ij} \left[\sum_{k=1}^n e_{kq_{ki}} u_j \right]^2. \end{aligned} \quad (\text{II-10.A})$$

In the above equation, Q is a symmetric positive definite matrix, a_{ij} and b_{ij} are elements of the A and B matrices, α_{ij} and γ_{ij} are constants greater than zero, and β_{ij} , ρ_{ij} , δ_{ij} , and σ_{ij} are constants greater than or equal to zero.

Taking the time derivative of V in (II-10.A) and evaluating along the error trajectory given in (II-7.A) results in a sign indefinite

V . If the a_{ij} and b_{ij} terms are chosen to be of the form

$$\begin{aligned} \dot{a}_{ij} = & -\alpha_{ij} \sum_{k=1}^n e_k q_{ki} x_{pj} - \beta_{ij} \frac{d}{dt} \left[\sum_{k=1}^n e_k q_{ki} x_{pj} \right] \\ & - \rho_{ij} \frac{d^2}{dt^2} \left[\sum_{k=1}^n e_k q_{ki} x_{pj} \right], \quad i, j = 1, 2, \dots, n \end{aligned} \quad (\text{II-11.A})$$

$$\begin{aligned} \dot{b}_{ij} = & -\gamma_{ij} \sum_{k=1}^n e_k q_{ki} u_j - \delta_{ij} \frac{d}{dt} \left[\sum_{k=1}^n e_k q_{ki} u_j \right] \\ & - \sigma_{ij} \frac{d^2}{dt^2} \left[\sum_{k=1}^n e_k q_{ki} u_j \right], \quad i=1, 2, \dots, n \text{ and } j=1, 2, \dots, r \end{aligned} \quad (\text{II-12.A})$$

then the resulting V expression reduces to

$$\begin{aligned} \dot{V} = & \underline{e}^T (A_m^T Q + Q A_m) \underline{e} - 2 \sum_{i,j=1}^n \beta_{ij} \left[\sum_{k=1}^n e_k q_{ki} x_{pj} \right]^2 \\ & - 2 \sum_{i=1}^n \sum_{j=1}^r \delta_{ij} \left[\sum_{k=1}^n e_k q_{ki} u_j \right]^2. \end{aligned} \quad (\text{II-13.A})$$

The complete derivation is given in [7]. The last two terms in (II-13.A) are at least negative semi-definite since the β_{ij} and δ_{ij} are constants greater than or equal to zero. It is well known [1] that if the A matrix is stable, there exists a symmetric positive definite

matrix Q which satisfies the equation $A_m^T Q + Q A_m = -C$, where C is a symmetric positive definite matrix. Therefore, if A_m is stable, the first term in (II-13.A) is negative definite in \underline{e} thereby making V negative definite in \underline{e} . With V positive definite in \underline{e} and V negative definite in \underline{e} , the error $\underline{e} = \underline{x}_m - \underline{x}_p$ is guaranteed to be asymptotically stable.

The adaptive gain rates, K_{ij}^a , K_{ij}^b are determined from (II-3.A), (II-4.A), (II-8.A), and (II-9.A) as follows

$$a_{ij} = a_{ij}^m - a_{ij}^p = a_{ij}^m - c_{ij}^a(t) - K_{ij}^a(t), \quad (\text{II-14.A})$$

$$b_{ij} = b_{ij}^m - b_{ij}^p = b_{ij}^m - c_{ij}^b(t) - K_{ij}^b(t). \quad (\text{II-15.A})$$

Taking the time derivative of (II-14.A) and (II-15.A) and using the restriction that $c_{ij}^a(t)$ and $c_{ij}^b(t)$ are negligible compared to K_{ij}^a and K_{ij}^b , the adaptive gain rates become

$$a_{ij}(t) = -K_{ij}^a(t) \quad (\text{II-16.A})$$

$$b_{ij}(t) = -K_{ij}^b(t) \quad (\text{II-17.A})$$

Integrating (II-16.A) and (II-17.A), the resulting $K_{ij}^a(t)$ and $K_{ij}^b(t)$ adaptive gain expressions become

$$K_{ij}^a = \alpha_{ij} \int_{t_0}^t \left[\sum_{k=1}^n e_k q_{ki} x_{pj} \right] dt + \beta_{ij} \sum_{k=1}^n e_k q_{ki} x_{pj} + \rho_{ij} \frac{d}{dt} \left[\sum_{k=1}^n e_k q_{ki} x_{pj} \right] + K_{ij}^a(t_0), \quad (\text{II-18.A})$$

$$K_{ij}^b = \gamma_{ij} \int_{t_0}^t \left[\sum_{k=1}^n e_k q_{ki} u_j \right] dt + \delta_{ij} \sum_{k=1}^n e_k q_{ki} u_j + \sigma_{ij} \frac{d}{dt} \left[\sum_{k=1}^n e_k q_{ki} u_j \right] + K_{ij}^b(t_0). \quad (\text{II-19.A})$$

The q_{ki} are elements of Q and must satisfy the relation $A_m^T Q + Q A_m = -C$. Adaptation is implemented by means of these equations so as to cause the plant to track the model.

In order to implement the adaptive controller, some criteria for selecting the $\alpha, \beta, \rho, \gamma, \delta, \sigma$ adaptive gain parameters other than by trial and error simulation is needed. In addition, some means of determining the $[q_{ij}]$ elements is desired, inasmuch as the requirements that

- (1) Q be positive definite
- (2) $A_m^T Q + Q A_m =$ negative definite matrix

will offer, in an indirect way, only bounds for the values of the individual elements of Q . The following section addresses this problem.

B. Development of the Linearized Error Equation

In this section, a technique for obtaining an approximate solution to the adaptive error dynamic state equation is given. This method is based on a linearization of the error dynamics about a set of plant operating conditions at the instant that a perturbation in plant parameters occur. The linearization is necessary because, although the plant and model described by (II-1.A), (II-2.A) are linear, the resulting adaptive controller is non-linear. This comes about from the gains given in (II-18.A) and (II-19.A). To show this expand (II-18.A) for the particular case $i = 2, j = 1$,

$$K_{21}^a(t) = \alpha_{21} \int_{t_0}^t S \, dt + \beta_{21}[S] + \rho_{21} \frac{d}{dt} [S] \quad (\text{II-1.B})$$

where

$$S = (e_1 q_{21} + e_2 q_{22}) x_{1p}(t)$$

Substituting $e_1 = x_{1m} - x_{1p}$ and $e_2 = x_{2m} - x_{2p}$ into (II-1.B) yields

$$S = [x_{1m} x_{1p}(t) - x_{1p}(t)^2] q_{21} + [x_{1p}(t) x_{2m} - x_{1p}(t) x_{2p}(t)] q_{22}$$

Similar results can be obtained for the general case for both $K_{ij}^a(t)$ and $K_{ij}^b(t)$. It is clear that the gains involve both squares and cross products of the plant states, resulting in a non-linear feedback law.

Because of the large amount of work involved, the technique is first presented for a second order system with a scalar input. The results for an n^{th} order system with r -inputs are presented at the end of the section.

Consider a second order plant with the linear, time-invariant transfer function

$$\frac{x_p(s)}{u(s)} = G(s) = \frac{b_2^p}{s^2 - a_{22}^p s - a_{21}^p} \quad (\text{II-2.B})$$

The plant equations in phase variable form are

$$\begin{bmatrix} \dot{x}_{1p} \\ \dot{x}_{2p} \end{bmatrix} = \begin{bmatrix} 0 & 1 \\ (c_{21}^a + K_{21}^a) & (c_{22}^a + K_{22}^a) \end{bmatrix} \begin{bmatrix} x_{1p} \\ x_{2p} \end{bmatrix} + \begin{bmatrix} 0 \\ c_2^b + K_2^b \end{bmatrix} U. \quad (\text{II-3.B})$$

The model is described in phase variable form by

$$\begin{bmatrix} \dot{x}_{1m} \\ \dot{x}_{2m} \end{bmatrix} = \begin{bmatrix} 0 & 1 & x_{1m} \\ a_{21}^m & a_{22}^m & x_{2m} \end{bmatrix} \begin{bmatrix} 0 \\ b_m \end{bmatrix} U. \quad (\text{II-4.B})$$

Substituting (II-3.B) and (II-4.B) into (II-7.A) yields the error differential equation

$$\begin{bmatrix} \dot{e}_1 \\ \dot{e}_2 \end{bmatrix} = \begin{bmatrix} 0 & 1 & e_1 \\ a_{21}^m & a_{22}^m & e_2 \end{bmatrix} + \begin{bmatrix} 0 & 0 \\ a_{21} & a_{22} \end{bmatrix} \begin{bmatrix} x_{1p} \\ x_{2p} \end{bmatrix} + \begin{bmatrix} 0 \\ b_2 \end{bmatrix} U, \quad (\text{II-5.B})$$

where

$$a_{21} = a_{21}^m - c_{21}^m - k_{21}^m, \quad a_{22} = a_{22}^m - c_{22}^a - k_{22}^a$$

and

$$b_2 = b_m - c_2^b - k_2^b.$$

represent the plant parameter errors.

The equations for the three adaptive parameter rates may be obtained from (II-11.A), (II-12.A), (II-16.A) and (II-17.A)

$$K_{2i}^a = \alpha_{2i}(Y) + \beta_{21} \frac{d}{dt}(Y) + \rho_{21} \frac{d^2}{dt^2}(Y), \quad i = 1, 2, \quad (\text{II-6.B})$$

where

$$Y = \sum_{k=1}^2 e_k q_{k2} x_{pi}$$

and

$$K_2^b = \gamma_2(Z) + \delta_2 \frac{d}{dt}(Z) + \sigma_2 \frac{d^2}{dt^2}(Z), \quad (\text{II-7.B})$$

where

$$Z = \sum_{k=1}^2 e_k q_{k2} u.$$

Assume that a constant input U^0 has been applied for a long time and that the plant is tracking the model. The system parameters in this equilibrium state are given by $\underline{x}_p = \underline{x}_m^0$, $U = U^0$, $\underline{e} = \underline{e} = 0$, $K_{21}^a = K_{21}^{a0}$, $K_{22}^a = K_{22}^{a0}$, and $K_2^b = K_2^{b0}$. We shall derive the characteristic equation for the error $e_1(t)$ assuming that a small disturbance occurs in any or all of the adaptive parameters, thereby causing a resulting disturbance in the plant states. Expanding (II-5.B), (II-6.B), and (II-7.B) in a Taylor's series about the equilibrium point and truncating all second and higher order terms yields

$$\begin{aligned} \Delta \dot{e}_1 &= \Delta e_2 \\ \Delta \dot{e}_2 &= (c_{21}^a + K_{21}^{a0}) \Delta e_1 + (c_{22}^a + K_{22}^{a0}) \Delta e_2 - x_{1m}^0 \Delta K_{21}^a - x_{2m}^0 \Delta K_{22}^a - U^0 \Delta K_2^b \\ \Delta \dot{K}_{2i}^a &= (\alpha_{2i} q_{12} x_{ip}^0 + \beta_{2i} q_{12} \dot{x}_{ip}^0 + \rho_{2i} q_{12} \ddot{x}_{ip}^0) \Delta e_1 \quad (\text{II-8.B}) \\ &\quad + (\alpha_{2i} q_{22} x_{ip}^0 + \beta_{2i} q_{22} \dot{x}_{ip}^0 + \rho_{2i} q_{22} \ddot{x}_{ip}^0) \Delta e_2 \\ &\quad + (\beta_{2i} q_{12} x_{ip}^0 + 2\rho_{2i} q_{12} \dot{x}_{ip}^0) \Delta \dot{e}_1 + (\beta_{2i} q_{22} x_{ip}^0 + 2\rho_{2i} q_{22} \dot{x}_{ip}^0) \Delta \dot{e}_2 \\ &\quad + \rho_{2i} q_{12} x_{ip}^0 \Delta \ddot{e}_1 + \rho_{2i} q_{22} x_{ip}^0 \Delta \ddot{e}_2, \quad i=1,2 \\ \Delta \dot{K}_2^b &= \gamma_2 q_{12} U^0 \Delta e_1 + \gamma_2 q_{22} U^0 \Delta e_2 + \delta_2 q_{12} U^0 \Delta \dot{e}_1 + \delta_2 q_{22} U^0 \Delta \dot{e}_2 \\ &\quad + \sigma_2 q_{12} U^0 \Delta \ddot{e}_1 + \sigma_2 q_{22} U^0 \Delta \ddot{e}_2. \quad (\text{II-9.B}) \end{aligned}$$

Taking the Laplace transform of (II-8.B) and (II-9.B) using the relationships $x_{1m}^0 = x_{2m}^0 = x_{1m}^0 = x_{2m}^0 = x_{2m}^0 = 0$ and $\Delta E_2(s) = s\Delta E_1(s)$ and substituting the resulting expressions for $\Delta K_{21}^a(s)$, $\Delta K_{22}^a(s)$, and $\Delta K_2^b(s)$ into (II-8.B) yields

$$\begin{aligned} & \{s[s^2 - s(c_{22}^a + K_{22}^{ao}) - (c_{21}^a + K_{21}^{ao})] + [(\alpha_{21}x_{1m}^{o2} + \gamma_2 U^{o2}) \\ & + s(\beta_{21}x_{1m}^{o2} + \delta_2 U^{o2}) + s(\rho_{21}x_{1m}^{o2} + \sigma_2 U^{o2})]q_{12} + \\ & s[(\alpha_{21}x_{1m}^{o2} + \gamma_2 U^{o2}) + s(\beta_{21}x_{1m}^{o2} + \delta_2 U^{o2}) \\ & + s^2(\rho_{21}x_{1m}^{o2} + \sigma_2 U^{o2})]q_{22}\} \Delta E_1(s) = -(x_{1m}^0 K_{21}^{ao} + U^{o2} K_2^{bo}). \end{aligned} \quad (II-10.B)$$

In (II-10.B) let

$$K_1 = \alpha_{21}x_{1m}^{o2} + \gamma_2 U^{o2}, \quad K_2 = \beta_{21}x_{1m}^{o2} + \delta_2 U^{o2}, \quad (II-11.B)$$

and

$$K_3 = \rho_{21}x_{1m}^{o2} + \sigma_2 U^{o2}.$$

The characteristic equation for the error $e(t)$ can be obtained by setting the coefficient of $\Delta E_1(s)$ in (II-10.B) equal to zero and dividing by the first term in order to place in the standard form for plotting root loci (i.e., $1 + KG(s) = 0$).

$$1 + \frac{q_{22} K_1 (s + q_{12}/q_{22}) (1 + K_2/K_1 s + K_3/K_1 s^2)}{s[s^2 - (c_{22}^a + K_{22}^{ao})s - (c_{21}^a + K_{21}^{ao})]} = 0 \quad (II-12.B)$$

This is of the form

$$1 + \frac{K(s+a)(1+bs+cs^2)}{s[s^2 - (c_{22}^a + K_{22}^{a0})s - (c_{21}^a + K_{21}^{a0})]} = 0 \quad (\text{II/13.B})$$

where $K = q_{22}K_1$, $a = q_{12}/q_{22}$, $b = K_2/K_1$, and $c = K_3/K_1$. The compensator thus looks like a proportional plus integral plus derivative (P-I-D) controller with an added zero at $s = -a = -q_{12}/q_{22}$. In the adaptive scheme proposed by Gilbert, Monopoli and Price [6], K_3 is zero since ρ_{21} and σ_2 do not appear in the adaptive rate equations. Their equations. Their compensator, therefore, is a proportional plus integral controller with an added zero at $s = -a$. In the adaptive control scheme proposed by Winsor and Roy [5], K_2 and K_3 are zero since β_{21} , δ_2 , ρ_{21} and σ_2 do not appear in the adaptive rate equations. Their compensator behaves as an integral controller with an added zero at $s = -a$.

The above procedure is easily extended to include the general case of an n^{th} order plant with r inputs. In general there will be nr transfer functions between the r inputs and n outputs. The transfer function between the i^{th} input and the j^{th} output is of the form

$$G_{ij}(s) = \frac{b_{0j}^{ij} s^{\ell-1} + b_1^{ij} s^{\ell-2} + \dots + b_{\ell-1}^{ij} s + b_{\ell}^{ij}}{s^n + a_1 s^{n-1} + a_2 s^{n-2} + \dots + a_{n-1} s + a_n}, \text{ for } \ell \leq n,$$

and for $i = 1, 2, \dots, r$; $j = 1, 2, \dots, n$. (II-14.B)

If the system can be put in the form

$$\dot{\underline{x}} = \hat{A}\underline{x} + \hat{B}\underline{u} \text{ where}$$

$$\hat{A} = \begin{bmatrix} 0 & 1 & 0 & 0 & \dots & 0 \\ 0 & 0 & 1 & 0 & \dots & 0 \\ \vdots & \vdots & \vdots & \vdots & \ddots & \vdots \\ \vdots & \vdots & \vdots & \vdots & \vdots & \vdots \\ -a_n & -a_{n-1} & & \dots & & -a_1 \end{bmatrix} \quad \hat{B} = \begin{bmatrix} b_{11} & b_{12} & \dots & b_{1r} \\ b_{21} & b_{22} & \dots & b_{2r} \\ \vdots & \vdots & \ddots & \vdots \\ \vdots & \vdots & \vdots & \vdots \\ b_{n1} & b_{n2} & & b_{nr} \end{bmatrix},$$

(II-15.B)

then the results of (II-12.B) can be extended to the case of multivariable systems. The general conditions under which such a transformation can be made are discussed in Appendix B. Using equations (II-2.B) through (II-12.B) for the cases of $n = 1, 2, \dots$ and $r = 1, 2, \dots$, by mathematical induction a general expression for the linearized adaptive error characteristic equation was developed. The general form for this equation then becomes

$$1 + \frac{\left[\sum_{k=1}^n q_{kn} s^{k-1} \right] \left[\sum_{i=1}^p K_i s^{i-1} \right]}{s \Delta_m(s)} = 0, \quad \text{(II-16.B)}$$

where p is the type of controller defined by

$$p = \begin{cases} 1, & \text{Winsor and Roy, } \beta = \rho = \delta = \sigma = 0 \\ 2, & \text{Gilbart, Monopoli, and Price, } \rho = \sigma = 0 \\ 3, & \text{Boland and Sutherland} \end{cases}$$

and

$$K_1 = \alpha_{n1} x_{1m}^{\circ 2} + (\gamma_{11} + \gamma_{21} + \dots + \gamma_{n1}) U_1^{\circ 2} \\ + (\gamma_{12} + \gamma_{22} + \dots + \gamma_{n2}) U_2^{\circ 2} + \dots$$

$$(\gamma_{1r} + \gamma_{2r} + \dots + \gamma_{nr})U_r^{02} \quad (\text{II-17.B})$$

$$\begin{aligned} K_2 = & \beta_{n1}x_{1m}^{02} + (\delta_{11} + \delta_{21} + \dots + \delta_{n1})U_r^{02} \\ & + (\delta_{12} + \delta_{22} + \dots + \delta_{n2})U_2^{02} \\ & + \dots + (\delta_{1r} + \delta_{2r} + \dots + \delta_{nr})U_r^{02} \end{aligned} \quad (\text{II-18.B})$$

$$\begin{aligned} K_3 = & \rho_{n1}x_{1m}^{02} + (\sigma_{11} + \sigma_{21} + \dots + \sigma_{n1})U_1^{02} \\ & + (\sigma_{12} + \sigma_{22} + \dots + \sigma_{n2})U_2^{02} \\ & + \dots + (\sigma_{1r} + \sigma_{2r} + \dots + \sigma_{nr})U_r^{02}. \end{aligned} \quad (\text{II-19.B})$$

Note that for $n = 2$, (II-16.B) reduces to

$$1 + \frac{(q_{22} + q_{22}s)(K_1 + K_2s + K_3s^2)}{s\Delta_m(s)} \quad (\text{II-20.B})$$

which agrees with (II-12.B) if one assumes that the plant and model dynamics are identical before the small perturbation occurred.

C. Decoupling the Input From The Linearized Error Dynamics

The general expression for the linearized adaptive error equation in the form of the characteristic equation of a single loop negative feedback system $1 + GH(s) = 0$. The locus of the error roots as a multiplicative parameter gain in $GH(s)$ is varied can be sketched using the well known root-locus techniques. These error loci begin at the zeroes of

$$s\Delta_m(s) = 0 \quad (\text{II-1.C})$$

representing the model poles $\Delta_m(s)$ and a zero at the origin due to the integration in the adaptive gain expressions, and end at the zeroes of the polynomials

$$\left[\sum_{i=1}^p K_i s^{i-1} \right] \left[\sum_{k=1}^n q_{kn} s^{k-1} \right] \quad (\text{II-2.C})$$

The zeroes of the second factor depend on the values of the elements of the Q matrix which are chosen to satisfy

$$A_m^T Q + Q A_m = -C \quad (\text{II-3.C})$$

in order to guarantee asymptotic stability. The zeroes of the first factor depend on the relative values of K_1 , K_2 , and K_3 , all greater than zero, as given in (II-17.B), (II-18.B), and (II-19.B). Factoring K_1 out of this polynomial results in

$$k_1 (s^2 + bs + c), \text{ where } b = K_2/K_3, \text{ } c = K_1/K_3 \quad (\text{II-4.C})$$

The roots of (II-4.C) are

$$s = \left(-b \pm \sqrt{b^2 - 4c} \right) / 2 \quad (\text{II-5.C})$$

The dependence of these roots on the various input magnitudes as well as x_{1m}^0 is evident in (II-17.B), (II-18.B), and (II-19.B). Unless this dependence is eliminated, the ending points of the root loci, determined by the zeroes of (II-16.B), will be a function of the inputs and x_{1m}^0 . This would mean the entire character of the root loci would change as the inputs and x_{1m}^0 changed.

Consider the second order system error characteristic equation

$$1 + \frac{q_{22}K_3(s + q_{12}/q_{22})(s^2 + K_2/K_3s + K_1/K_3)}{s\Delta_m(s)} = 0$$

where K_1 , K_2 , and K_3 are as given in (II-11.B). In (II-6.C) the gain ratios are given by

$$K_2/K_3 = \frac{\beta_{21}x_{1m}^{o2} + \delta_2U^{o2}}{\rho_{21}x_{1m}^{o2} + \sigma_2U^{o2}} \quad \text{and}$$

$$K_1/K_3 = \frac{\alpha_{21}x_{1m}^{o2} + \gamma_2U^{o2}}{\rho_{21}x_{1m}^{o2} + \sigma_2U^{o2}} \quad (\text{II-7.C})$$

If the adaptive gain parameters are chosen such that

$$\gamma_2/\alpha_{21} = \delta_2/\beta_{21} = \sigma_2/\rho_{21} = d = \text{constant} \quad (\text{II-8.C})$$

then (II-7.C) reduces to

$$K_2/K_3 = \frac{\beta_{21}(x_{1m}^{o2} + d U^{o2})}{\rho_{21}(x_{1m}^{o2} + d U^{o2})} = \frac{\beta_{21}}{\rho_{21}} = b \quad (\text{II-9.C})$$

and

$$K_1/K_3 = \frac{\alpha_{21}(x_{1m}^{o2} + d U^{o2})}{\rho_{21}(x_{1m}^{o2} + d U^{o2})} = \frac{\alpha_{21}}{\rho_{21}} = c \quad (\text{II-10.C})$$

In this manner, the zeroes of $(s^2 + K_2/K_3 s + K_1/K_3)$ are made independent of the magnitudes of the input U^o and x_{1m}^o and the shape of the root locus became a function of the a-priori fixed α , β , ρ , γ , δ , σ adaptive gain parameters, with the actual root location on the loci being a function

only of the gain factor $q_{22} K_1$. Comparing (II-8.C) with (II-18.A) and (II-19.A) indicates that this choice simply places a weighted emphasis on the three terms in the K_{ij}^a and K_{ij}^b adaptive gain expressions. This is a logical choice since it would not be uncommon to place more emphasis on the adaptation of certain parameters than on others. This is done through the proper choice of the constant d . The constants b and c in (II-9.C) and (II-10.C) establish the weighted importance of the proportional and derivative terms to the integral term in the adaptive gain expressions. These ratios are the same for all adaptive gains.

The above results for the second order case with scalar input can be extended to the n th order case with r inputs. By doing so, (II-17-18-19 .B) result. In order to insure that the ratios K_1/K_3 , K_2/K_3 , K_1/K_2 are independent of variations in input magnitude and state values, if the expressions

$$\begin{aligned} & (\gamma_{11} + \gamma_{21} + \dots + \gamma_{n1}) \\ & (\gamma_{12} + \gamma_{22} + \dots + \gamma_{n2}) \\ & \quad \vdots \\ & (\gamma_{1r} + \gamma_{2r} + \dots + \gamma_{nr}) \end{aligned}$$

are related to α_{n1} and similarly with the δ 's and β 's in K_2 and σ 's and ρ 's of K_3 in (II-17-18-19 .B), then if the adaptive gain constants are chosen to satisfy the following relationships, decoupling of zero placement from input magnitudes results:

$$\begin{aligned}
\frac{\gamma_{11} + \gamma_{21} + \dots + \gamma_{n1}}{\alpha_{n1}} &= \frac{\delta_{11} + \delta_{21} + \dots + \delta_{n1}}{\beta_{n1}} = \frac{\sigma_{11} + \sigma_{21} + \dots + \sigma_{n1}}{\rho_{n1}} = C_1 \\
\frac{\gamma_{12} + \gamma_{22} + \dots + \gamma_{n2}}{\alpha_{n1}} &= \frac{\delta_{12} + \delta_{22} + \dots + \delta_{n2}}{\beta_{n1}} = \frac{\sigma_{12} + \sigma_{22} + \dots + \sigma_{n2}}{\rho_{n1}} = C_2 \\
&\vdots \\
&\vdots \\
&\vdots \\
\frac{\gamma_{1r} + \gamma_{2r} + \dots + \gamma_{nr}}{\alpha_{n1}} &= \frac{\delta_{1r} + \delta_{2r} + \dots + \delta_{nr}}{\beta_{n1}} = \frac{\sigma_{1r} + \sigma_{2r} + \dots + \sigma_{nr}}{\rho_{n1}} = C_r
\end{aligned}$$

(II-11.C)

where C_1, C_2, \dots, C_r are positive constants. Substituting (II-11.C) into (II-17.B), (II-18.B), and (II-19.B) one obtains

$$\begin{aligned}
K_1 &= \alpha_{n1} (x_{1m}^o{}^2 + C_1 U_1^o{}^2 + C_2 U_2^o{}^2 + \dots + C_r U_r^o{}^2) \\
K_2 &= \beta_{n1} (x_{1m}^o{}^2 + C_1 U_1^o{}^2 + C_2 U_2^o{}^2 + \dots + C_r U_r^o{}^2) \\
K_3 &= \rho_{n1} (x_{1m}^o{}^2 + C_1 U_1^o{}^2 + C_2 U_2^o{}^2 + \dots + C_r U_r^o{}^2).
\end{aligned} \tag{II-12.C}$$

Using (II-12.D)

$$K_2/K_3 = \beta_{n1}/\rho_{n1} = b \quad \text{and} \quad K_1/K_3 = \alpha_{n1}/\rho_{n1} = c \tag{II-13.C}$$

and the roots of $K_3 (s^2 + bs + c)$ are independent of $x_{1m}^o, U_1^o, U_2^o, \dots, U_r^o$.

Such a "decoupling" scheme would have practical implications in terms of the control of aerospace vehicles, wherein, a well defined error response would be highly desirable over a wide range of inputs. Such conditions could occur in a space shuttle vehicle in regards to varying

RCJ thrust levels and varying roll-pitch-yaw commands (given by elevon motions) required to stabilize the vehicle. The following is an example which shows pole-zero movement with and without the decoupling procedure being used.

Example

2nd order, 2 inputs

$$G_{m1}(s) = G_{m2}(s) = \frac{1}{s^2 + 2s + 2} \quad (\text{II-14.C})$$

$$G_{p1}(s) = \frac{\alpha_1}{s^2 + 2s + a_{21}^p} \quad G_{p2}(s) = \frac{\alpha_2}{s^2 + 2s + a_{21}^p} \quad (\text{II-15.C})$$

$\alpha_1, \alpha_2, a_{21}^p$ adapting

With two inputs and $p = 3$, (II-16.B) becomes

$$1 + \frac{K_3 q_{22} (s + q_{12}/q_{22}) (s^2 + K_2/K_3 s + K_1/K_3)}{s(s^2 + 2s + 2)} = 0 \quad (\text{II-16.C})$$

Selecting as suitable parameters

$$\alpha_{21} = 40 \quad \beta_{21} = 40 \quad \rho_{21} = 10 \quad q_{12} = 2 \quad q_{22} = 1$$

$$(s^2 + K_2/K_3 s + K_1/K_3) = s^2 + 4s + 4 = (s + 2)^2$$

$$K_1 = 40 x_{1m}^2 + \gamma_{21} U_1^2 + \gamma_{22} U_2^2$$

$$K_2 = 40 x_{1m}^2 + \delta_{21} U_1^2 + \delta_{22} U_2^2 \quad (\text{II-17.C})$$

$$K_3 = 10 x_{1m}^2 + \sigma_{21} U_1^2 + \sigma_{22} U_2^2$$

DECOUPLED CASE

In order to "decouple" the error dynamics of α_1 and α_2 as compared with a_{21}^P in (II-15.C), it is necessary to employ (II-11.C)

$$\frac{\gamma_{21}}{\alpha_{21}} = \frac{\delta_{21}}{\beta_{21}} = \frac{\sigma_{21}}{\rho_{21}} = C_1 = 1.0 \quad (\text{II-18a.C})$$

$$\frac{\gamma_{22}}{\alpha_{21}} = \frac{\delta_{22}}{\beta_{21}} = \frac{\sigma_{22}}{\rho_{21}} = C_2 = 2.0 \quad (\text{II-18b.C})$$

Using (II-18a,b.C), the K_1 in (II-17.C) became

$$K_1 = 40 (x_{1m}^{o2} + 1.0 U_1^{o2} + 2.0 U_2^{o2})$$

$$K_2 = 40 (x_{1m}^{o2} + 1.0 U_1^{o2} + 2.0 U_2^{o2})$$

$$K_3 = 10 (x_{1m}^{o2} + 1.0 U_1^{o2} + 2.0 U_2^{o2})$$

and (II-16.C) reduces to

$$1 + \frac{10(x_{1m}^{o2} + 1.0 U_1^{o2} + 2.0 U_2^{o2})(s+2)(s^2+4s+4)}{s(s^2+2s+2)} = 0 \quad (\text{II-19.C})$$

For the particular cases of

$$(a) \quad U_1^o = 3, U_2^o = 0, x_{1m}^o = 3/2 \quad (\text{II-19.C) becomes}$$

$$1 + \frac{(112.5) (s+2)^3}{s(s^2+2s+2)} = 0 \quad (\text{II-20a.C})$$

$$(b) \quad U_1^o = 3, U_2^o = 6, x_{1m}^o = 9/2 \quad (\text{II-19.C) becomes}$$

$$1 + \frac{(1012.5) (s+2)^3}{s(s^2+2s+2)} = 0 \quad (\text{II-20b.C})$$

The root loci and location of the closed loop poles for (II-20a,b.C) are shown in Figure II-1a.C. Note that the "shape" of the root locus is input magnitude invariant, although the root locations are a function of the input magnitude.

COUPLED CASE

Now consider the same example without using (II-11.C). Such a case would be

$$\begin{aligned} \frac{\gamma_{21}}{\alpha_{21}} = K_1 = 1 & & \frac{\delta_{21}}{\beta_{21}} = K_2 = 2 & & \frac{\sigma_{21}}{\rho_{21}} = K_3 = 3 \\ \frac{\gamma_{22}}{\alpha_{21}} = K_4 = 4 & & \frac{\delta_{22}}{\beta_{21}} = K_5 = 5 & & \frac{\sigma_{22}}{\rho_{21}} = K_6 = 6 \end{aligned}$$

Using these numbers in (II-17.C) results in the zeroes of (II-16.C) being a function of x_{1m}^{o2} , U_1^{o2} , U_2^{o2} . For the same conditions as the "decoupled" case

$$\begin{aligned} \text{(a) } U_1^o = 3, U_2^o = 0, x_{1m}^o = 3/2 & \quad \text{(II-16.C) becomes} \\ 1 + \frac{(29.25)(s+2)(s^2+2.778s+1.538)}{s(s^2+2s+2)} = 0 & \quad \text{(II-21a.C)} \end{aligned}$$

$$\text{(b) } 1 + \frac{(263.25)(s+2)(s^2+3.32s+2.64)}{s(s^2+2s+2)} = 0 \quad \text{(II-21b.C)}$$

Figures II-1b.C and II-1c.C show the root loci and position of the closed loop error roots for (II-21a,b.C). Note that as the inputs change, the entire shape and character of the root loci changes. From the standpoint of well-behaved error dynamics, this is a highly undesirable

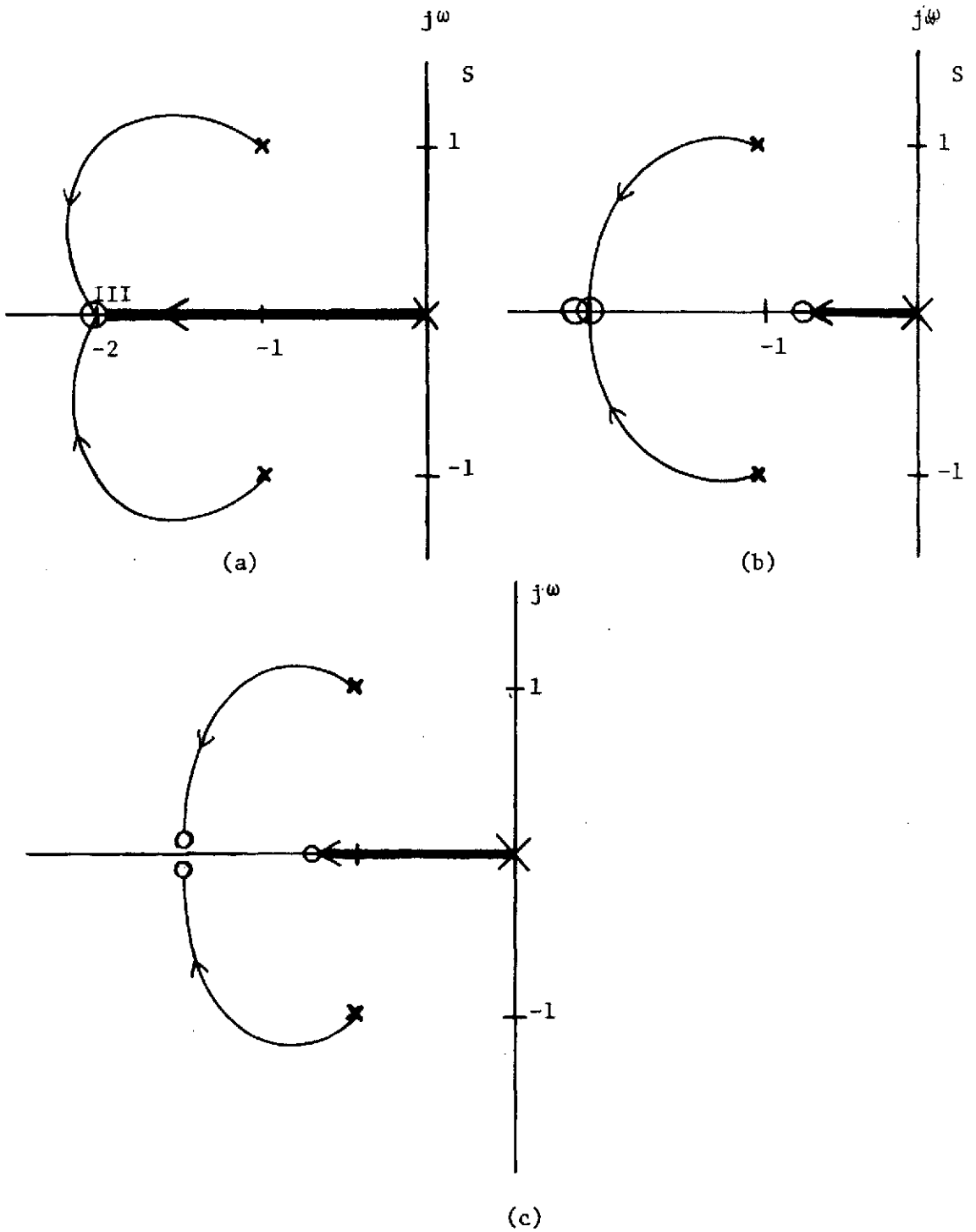


Figure II-1.C. Various Root Loci Configurations Comparing "Coupled" and Decoupled Design Techniques.

situation. Hence, in order to obtain a good design, with well defined error dynamics, the decoupling scheme in (II-11.C) should be used, it requires no additional computational difficulties and the degree of control that results is well worth it.

D. Application of the Error Equation

The design of an adaptive controller using the class of model-reference schemes discussed consists of determining the best combination of values for the adaptive gain parameters α , β , ρ , γ , δ , σ and the q_{ij} elements. At best this is a trial and error process unless some systematic technique is utilized. The basic error equation in (II-16.B) will now be used to develop a design method based on the location of root loci as the adaptive gain parameters are adjusted. The location of the roots of the linearized error characteristic equation in the s-plane will, to a first order approximation, completely characterize the nature of the transient response of the system error. By going to a linear system description of the error, the familiar figures of merit from classical controls such as rate of convergence, settling time, per cent overshoot, etc. can be used.

That the design method is based on the small-signal approach is of no concern, because completely independent of the design technique the plant has been guaranteed to be asymptotically stable using Lyapunov theory. In this way, if an error perturbation occurs, even if it is very large, the adaptive system will force the error towards zero, and the closer the error gets to zero the better the small signal approximation.

By designing for a very fast transient response the error will be forced to be near zero. This is a noticeable departure from the usual analysis of systems by small-signal approximations. At no time is (II-16.B) implemented as part of a control system. It represents only an analytical tool to aid in design of an efficient, practical MRAS controller.

Example: Application of the Error Equation to a Space Shuttle Vehicle

This example clarifies the design method applied to the pitch-axis attitude control system of a space shuttle vehicle using aerodynamic control surfaces during re-entry. Because of the extreme variations in altitude and velocity encountered, the plant dynamics are time varying with order of magnitude changes of as much as 200 occurring.

The basic vehicle configuration is shown in Figure (II-1.D). It is assumed that the pitch axis is decoupled from the roll and yaw axes.

The linear time-varying plant dynamics are obtained as follows:

$$M_{\text{pitch}} = I_{\text{pitch}} \ddot{\theta} = f_m(\alpha, \dot{\theta}, \delta_e) \quad (\text{II-1.D})$$

where α = angle of attack (radians)

$\dot{\theta}$ = pitch rate (radian|sec)

δ_e = elevator deflection (radians)

I_{pitch} = moment of inertia of the pitch axis of vehicle

Expanding f_m in a Taylor series about α_0 , $\dot{\theta}_0$ and δ_{e0} yields

$$f_m(\alpha, \dot{\theta}, \delta_e) = f_m(\alpha_0, \dot{\theta}_0, \delta_{e0}) + \frac{\partial f_m}{\partial \alpha} (\alpha - \alpha_0) + \frac{\partial f_m}{\partial \dot{\theta}} (\dot{\theta} - \dot{\theta}_0) + \frac{\partial f_m}{\partial \delta_e} (\delta_e - \delta_{e0}) + \text{higher order terms (HOT)} \quad (\text{II-2.D})$$

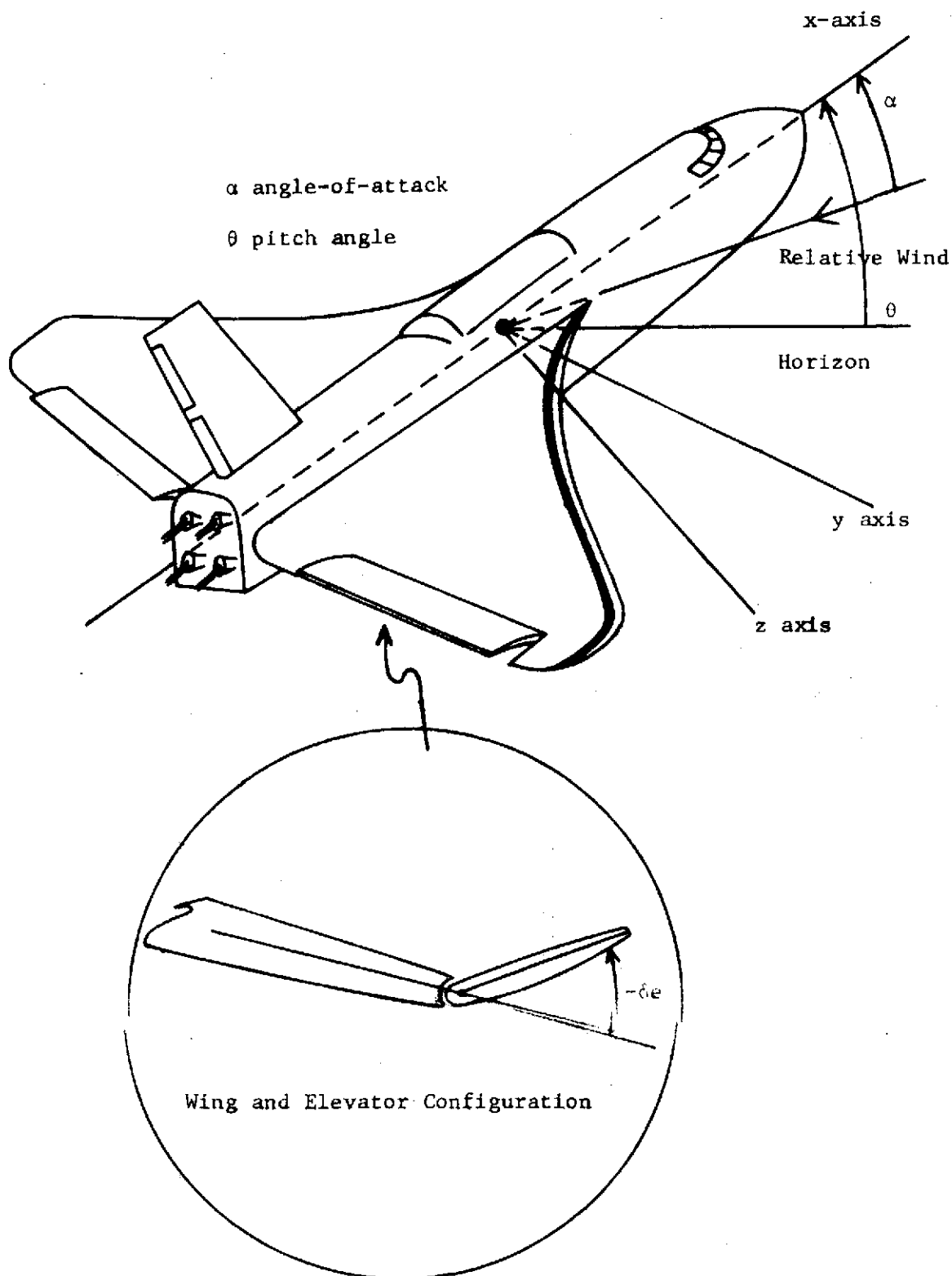


Figure II-1.D Re-Entering Space-Shuttle Vehicle

By selection of appropriate axes,

$$I_{pitch} \ddot{\theta} + f_{m\alpha} \alpha + f_{m\dot{\theta}} \dot{\theta} + f_{m\delta_e} \delta_e \quad (II-3.D)$$

where $f_{m\alpha}$, $f_{m\dot{\theta}}$, $f_{m\delta_e}$ represent moment stability derivatives. Through some involved calculations, these moment derivatives can be related to the well known aircraft stability derivatives $C_{m\alpha}$, $C_{m\dot{\theta}}$, $C_{m\delta_e}$ as follows

$$\begin{aligned} f_{m\alpha} &= c\rho V_r^2 S_{ref} / 2I_p \cdot C_{m\alpha} = C_1 C_{m\alpha} \\ f_{m\dot{\theta}} &= c^2 \rho V_r S_{ref} / 4I_p \cdot C_{m\dot{\theta}} = C_2 C_{m\dot{\theta}} \\ f_{m\delta_e} &= c\rho V_r^2 S_{ref} / 2I_p \cdot C_{m\delta_e} = C_3 C_{m\delta_e} \end{aligned} \quad (II-4.D)$$

where

ρ = air density (time varying due to altitude changes)

S_{ref} = vehicle reference cross sectional effective lift area

c = vehicle characteristic length (used to normalize stability derivatives)

V_r = vehicle relative velocity

C_{m_x} = aerodynamic stability partial derivative taken with respect to x .

Because ρ and V_r vary with time in an indeterminate manner (dependent upon re-entry trajectory which is controlled "on-line" by the pilot) the vehicle dynamics are time-varying.

Defining

$$x_1 = \theta \quad x_2 = \dot{\theta} \quad U_1 = \alpha \quad U_2 = \delta_e$$

the unadapted vehicle dynamics can be written as

$$\dot{\underline{x}}_p = \begin{bmatrix} 0 & 1 \\ 0 & C_2 C_{m\dot{\theta}} \end{bmatrix} \underline{x}_p + \begin{bmatrix} 0 & 0 \\ C_1 C_{m_{u_1}} & C_1 C_{m_{u_2}} \end{bmatrix} \underline{U} \quad (\text{II-5.D})$$

Plots of typical mission profile data for ρ and V_T are shown in Figure (II-2.D). Using nominal values for C_{m_α} , $C_{m\dot{\theta}}$, $C_{m\delta_e}$, the actual time varying plant coefficients are shown in Figure (II-3.D). With the dynamics of the form $\dot{\underline{x}}_p = A_p \underline{x}_p + B_p \underline{U}$ it is clear that the zero in the a_{21}^p position implies a pure integration; hence the unadapted vehicle is unstable. The basic attitude controller with the adaptive gains included is shown in Figure (II-4.D). The equations of the plant with adaptation are

$$\dot{\underline{x}}_p = \begin{bmatrix} 0 & 1 \\ K_{21}^a(t) & (C_2 C_{m\dot{\theta}} + K_{22}^a(t)) \end{bmatrix} \underline{x}_p(t) + \begin{bmatrix} 0 & 0 \\ (C_1 C_{m_{u_1}} + K_{21}^b(t)) & (C_1 C_{m_{u_2}} + K_{22}^b(t)) \end{bmatrix} \underline{U} \quad (\text{II-6.D})$$

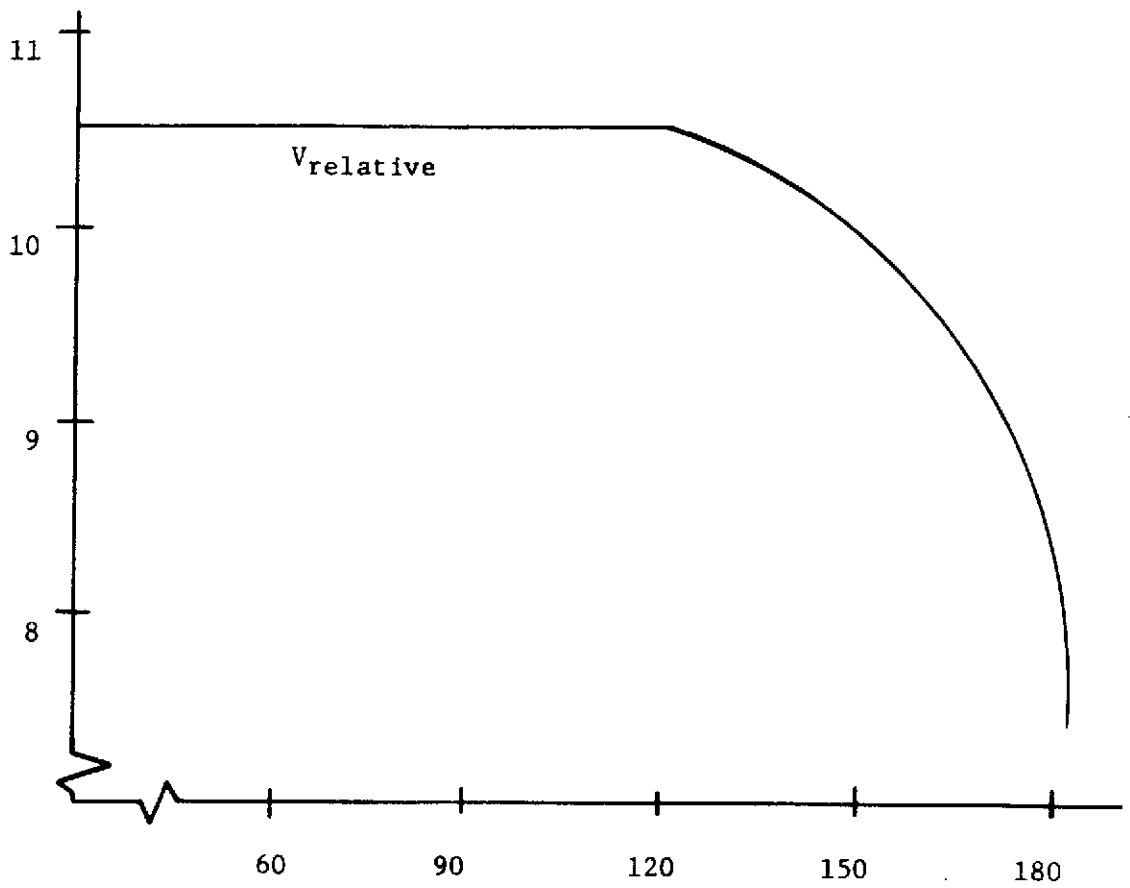
where $K_{ij}^a(t)$ and $K_{ij}^b(t)$ are the adaptive gains.

A model based on the two assumptions that (1) no complex roots are desired and (2) a fast, over damped response is desired, was chosen to be

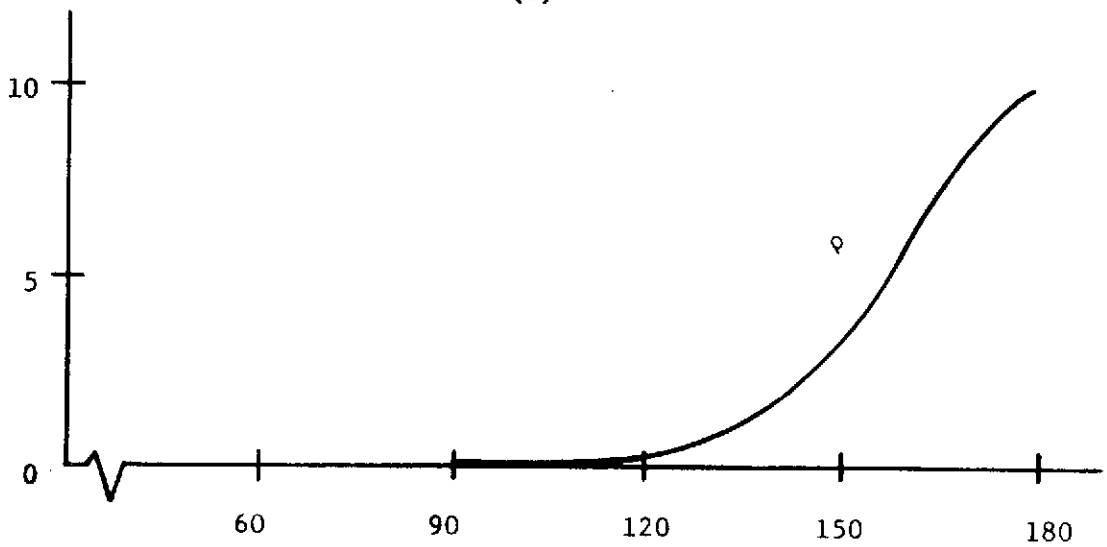
$$\frac{\theta}{U_1}(s) = \frac{\theta}{U_2}(s) = \frac{-0.05}{s^2 + 3s + 2} = \frac{-0.05}{(s+1)(s+2)} \quad (\text{II-7.D})$$

For the plant chosen, specific parameter values used were $U_1 = 1.047$ ($\alpha=60^\circ$), $U_2 = 1.13438$ ($\delta e=65^\circ$), and $x_{1m}^0 = -0.0545$ (attitude = -0.0545 radians).

The general adaptive gain parameter equations are



(a)



Time From Booster Separation (seconds)

Figure II-2.D Typical Time-Varying Physical Data Causing Time-Varying Plant Parameters.

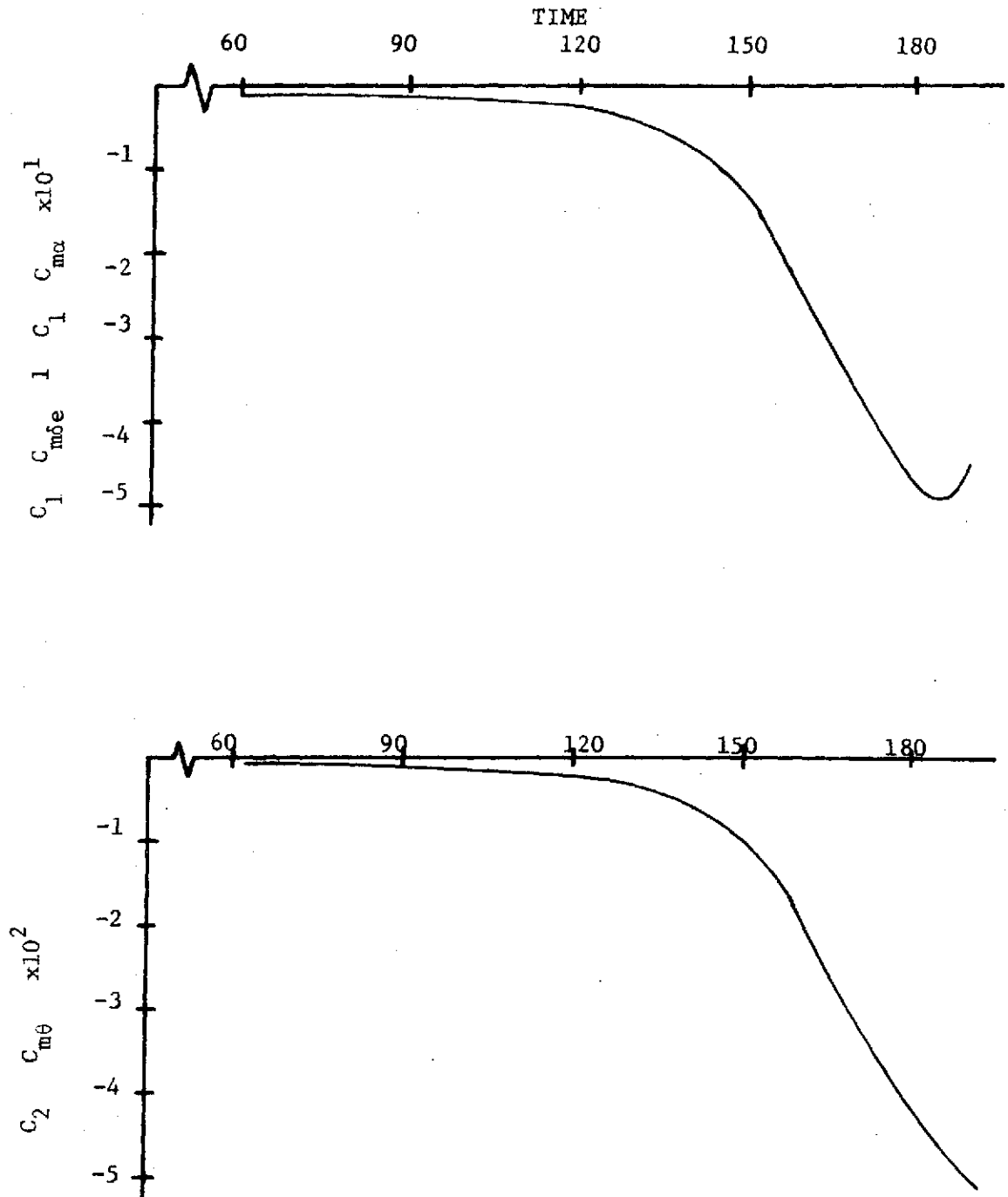
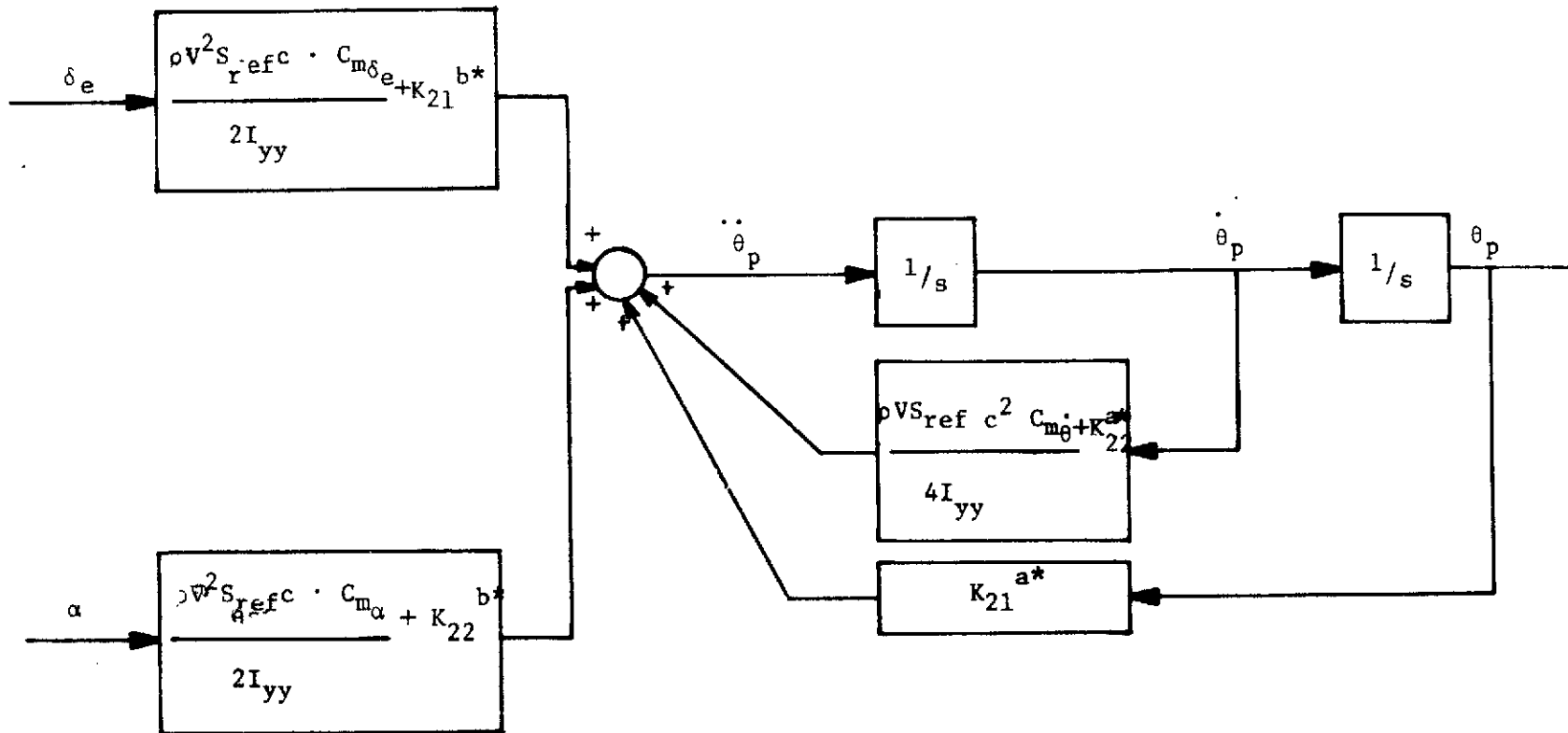


Figure II-3.D Typical Time Variation of Plant Parameters During Re-Entry (adaptation must compensate for the changes)



* Denotes adaptive gain

$$\dot{\underline{x}} = \begin{bmatrix} 0 & 1 \\ K_{21}^a & K_2 C_{m\theta} + K_{22}^a \end{bmatrix} \underline{x} + \begin{bmatrix} 0 & 0 \\ (K_1 C_{m\alpha} + K_{21}^b) & (K_1 C_{m\delta e} + K_{22}^b) \end{bmatrix} \underline{u}$$

Figure II-4.D Simulation Diagram of Adapted Attitude Controller

$$K_{21}^a = \alpha_{21} \int_{t_0}^t W dt + \beta_{21} W + \rho_{21} \frac{d}{dt} [W], \quad K_{22}^a = \alpha_{22} \int_{t_0}^t Y dt + \beta_{22} Y + \rho_{22} \frac{d}{dt} [Y], \quad (\text{II-8.D})$$

$$K_{21}^b = \gamma_{21} \int_{t_0}^t Z dt + \delta_{21} Z + \sigma_{21} \frac{d}{dt} [Z], \quad K_{22}^b = \gamma_{22} \int_{t_0}^t S dt + \delta_{22} S + \sigma_{22} \frac{d}{dt} [S]$$

where $W = e_1 q_{12} x_{1p} + e_2 q_{22} x_{1p}$, $Y = e_1 q_{12} x_{2p} + e_2 q_{22} x_{2p}$ and (II-9.D)

$$Z = e_1 q_{12} U_1 + e_2 q_{22} U_1, \quad S = e_1 q_{12} U_2 + e_2 q_{22} U_2$$

and the α , β , ρ , γ , δ , σ , q_{12} , q_{22} values are yet to be determined.

In order to choose appropriate values for the adaptive gains α , β , ρ , γ , δ , and σ the root loci for the three model reference adaptive control schemes in references [3, 5, 6] are plotted in Figure (II-5.D). The loci begin in all three cases at the zeroes of the model characteristic equation plus an additional locus beginning at the origin. The loci end at the zeroes of $(1 + q_{12}/q_{22})(1 + K_2/K_1 s + K_3/K_1 s^2)$. In all three cases the zero at $-q_{12}/q_{22}$ was chosen to be -3 with $q_{12}=1.26$ and $q_{22}=0.42$. It is desired to locate this zero as far in the left half plane as possible. However, this ratio is limited to three in this example in order for the Q matrix to be positive definite.

Using the above values the characteristic equation for the Winsor and Roy method is

$$1 + \frac{k(s+3)}{s(s^2 + 3s + 2)} = 0, \quad \text{where } k = q_{22} K_1 \quad (\text{II-10.D})$$

The root loci for $0 \leq k \leq \infty$ are shown in Figure (II-5.D(a))

The Gilbert, Monopoli, and Price method has an additional zero at $s = -K_1/K_2$. It is clear that this zero should be as far to the right as possible in order to pull the root loci to the left. This zero should

not be to the right of $s = -3$, however, since for high gains the root on the real axis is the dominant root and determines the speed of response. The additional zero is placed at $s = 4.5$ and the error characteristic equation becomes

$$1 + \frac{k(s+3)(s+4.5)}{s(s^2+3s+2)} = 0, \text{ where } k = q_{22}K_2 \quad (\text{II-11.D})$$

The resulting root loci are shown in Figure (II-5.D(b)).

The additional zero in the Boland and Sutherlin method is placed at $s = -4.5$ which yields an error characteristic equation of

$$1 + \frac{k(s+3)(s+4.5)^2}{s(s^2+3s+2)} = 0, \text{ where } k = q_{22}K_3 \quad (\text{II-12.D})$$

The resulting root loci are shown in Figure (II-5.D(c)).

In order to verify the results of the linearization procedure the time response of the error for each of the three model-reference schemes was computed. A gain of $k = 10$ was used in each case. The location of the roots of the linearization error equation for this value of gain are shown on the root loci in Figure (II-5.D).

In each of the three methods the conditions of (II-11.C) are satisfied with $C_1 = C_2 = 10$. Using these values of C_1 and C_2 , the gain $k = 10$, and combination of zero locations given in (II-10.D), (II-11.D), and (II-12.D), the adaptive gain constants can be computed and are given in Table 1.

(a) Winsor and Roy

$-.15 + j3.4$

(b) Gilbert, Monopoli, and Price

$-5.4 + j4.7$

-2.7

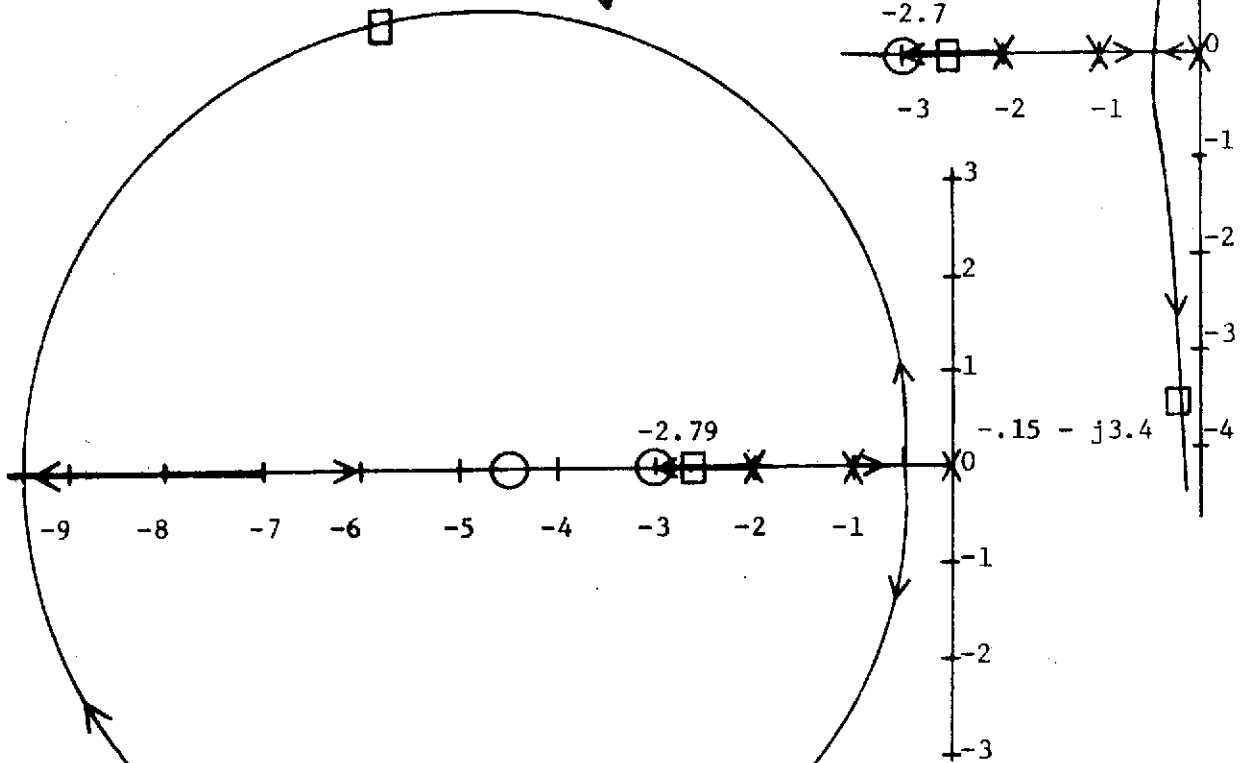
-3

-2

-1

-2.79

$-.15 - j3.4$



(c) Boland and Sutherlin

$-4.2 + j1.4$

-2.85

-5

-4

-3

-2

-1

$-4.2 - j1.4$

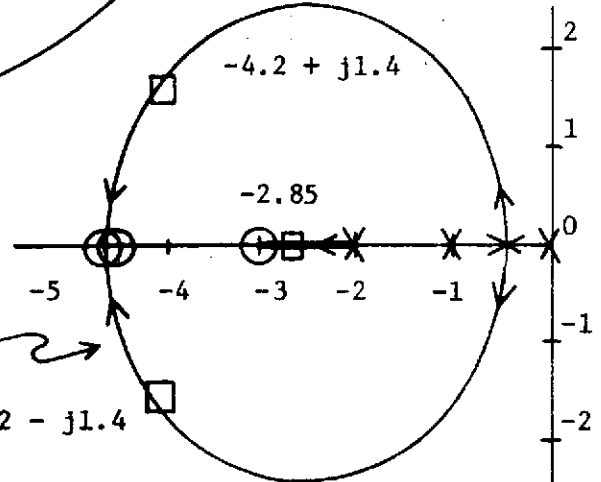


Figure II-5.D. Root Loci of the Linearized Error Characteristic Equation.

Method in Reference	α_{21}	α_{22}	β_{21}	β_{22}	ρ_{21}	ρ_{22}	γ_{21}	γ_{22}	δ_{21}	δ_{22}	σ_{21}	σ_{22}
[5]	100	100	0	0	0	0	100	100	0	0	0	0
[6]	450	450	100	100	0	0	45	45	10	10	0	0
[7]	2025	2025	900	900	100	100	202.5	202.5	90	90	10	10

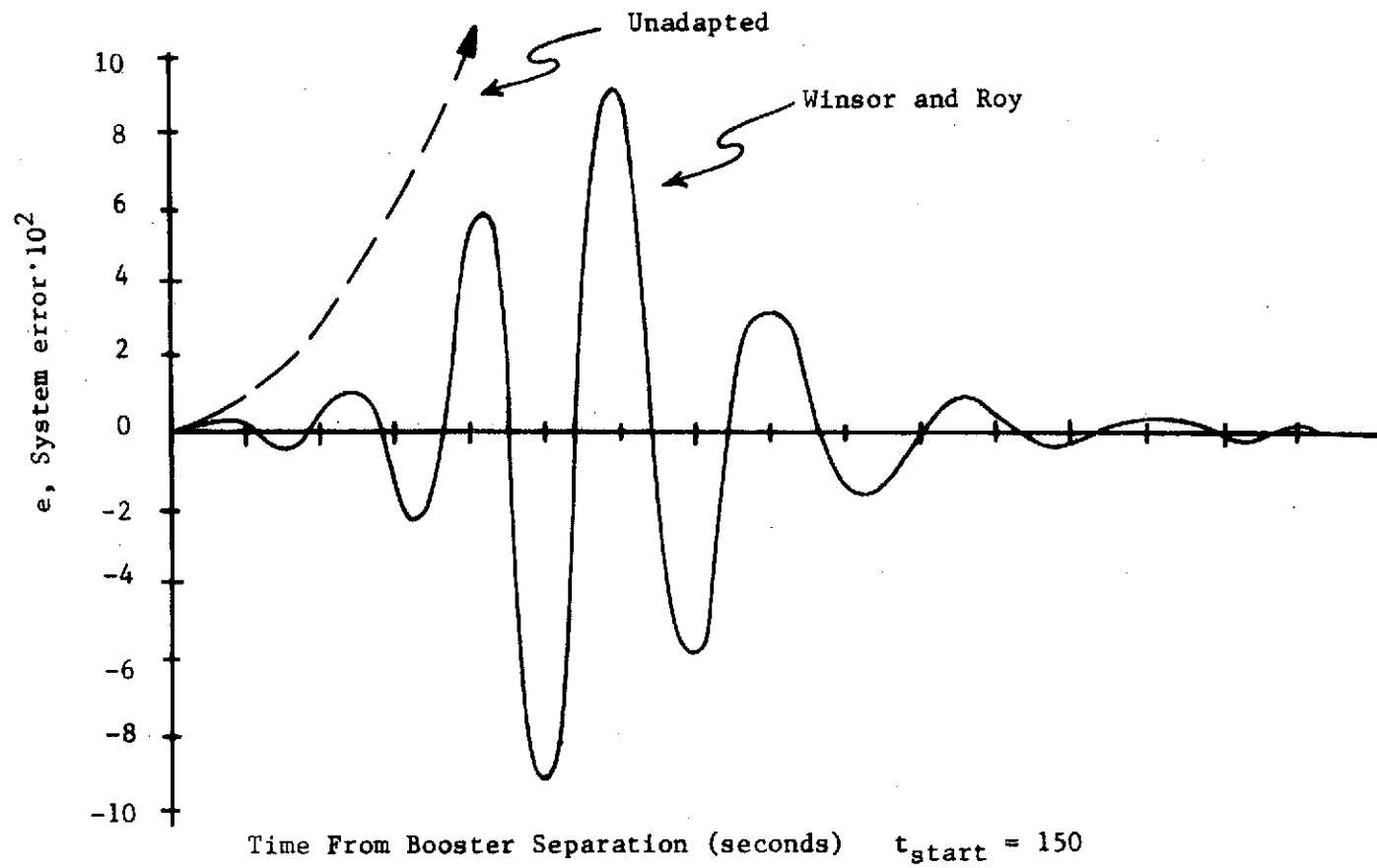
Table II-1. Adaptive Gain Values

The time response of the error $e_1(t)$ for the Winsor and Roy method is shown in Figure (II-6.D(a)), where the model and plant states are identical at time $t_0 = 150$ seconds. At t_0^+ a step disturbance is given to all of the adaptable parameters in (II-6.D). The disturbances are such that at $t = t_0^+$ the plant transfer functions are

$$\frac{\theta(s)}{U_1(s)} = \frac{.073}{(s+0)(s+.009)}, \text{ and } \frac{\theta(s)}{U_2(s)} = \frac{-.073}{(s+0)(s+.009)} \quad (\text{II-13.D})$$

The model transfer functions are as given in (II-7.D). The response in Figure (II-6.D(a)) is highly oscillatory as predicted by the root locations in Figure (II-5.D(a)). The dotted line in Figure (II-6.D(a)) is the unstable error response for the system with no adaptation.

The time responses of $e_1(t)$ for the Gilbert, Monopoli, and Price method and for the Boland and Sutherlin method are shown in Figure (II-6.D(b)). These two responses plot as one curve since the real root is the dominant one at this value of gain k . Again the time response agrees with the response as predicted from the root locations in the s -plane. In all three of the adaptive control methods the error approached zero asymptotically although the plant parameters are time varying.



(a)

Figure II-6.D. Time Response of the System Error Due to a Plant Disturbance at $t = 150$ seconds (a) Winsor and Roy

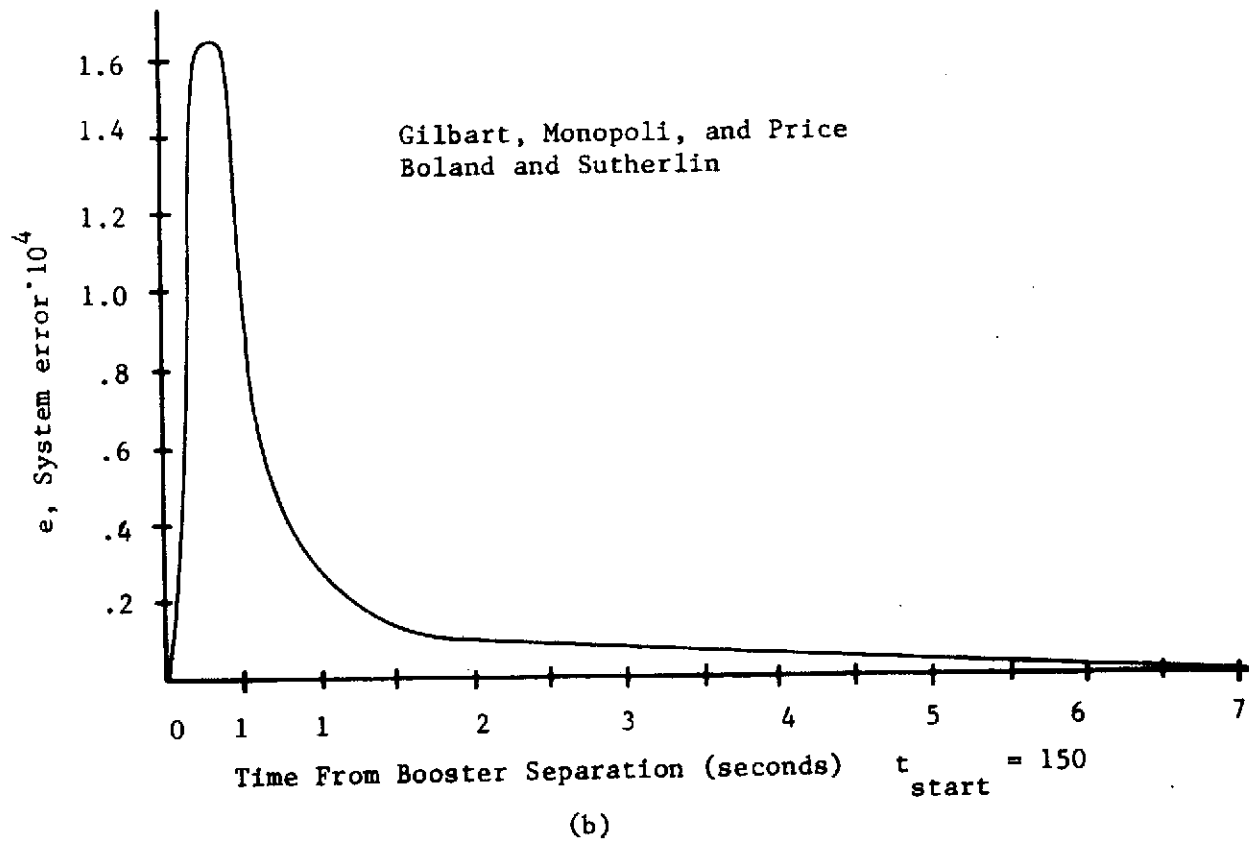


Figure II-6.D. Time Response of the System Error Due to a Plant Disturbance at $t = 150$ seconds (b) Gilbart, Monopoli, and Price; Boland and Sutherlin.

E. Adaptive Error Determination

As an extension of (II-16.B), representing an approximate characteristic equation of the adaptive error, a technique for approximating the magnitude of the maximum error and the time interval from application of a disturbance until maximum error is reached is presented. Advantages of the proposed error estimation scheme include:

- (1) prediction of the maximum error and its time of occurrence
- (2) saturation non-linearities can be avoided, or at least designed around
- (3) simple solution of the error dynamics is available
- (4) insight into the relationship between adjustable adaptive gain coefficient selection and the error magnitudes is available. A simulation example is given demonstrating the utility of the proposed method.

Referring to the basic second order derivation of the error equation, it can be seen that (II-10.B) is in the form

$$\Delta E_1(s) (1+GH(s)) = - \left[x_{10}^o K_{21}^{ao} + U^o K_2^{bo} \right] \quad (\text{II-1.E})$$

where (1) $1+GH(s)$ - represents the error characteristic equation (2)

K_{21}^{ao} , K_2^{bo} - represent steady state adaptive gain values at the instant

a perturbation occurs. Following along the lines of the previous error derivation, (II-10.B) can be generalized to

$$\Delta E_1(s) \left\{ s\Delta_m(s) + \left[\sum_{i=1}^p K_i s^{i-1} \right] \left[\sum_{j=1}^n q_{jn} s^{(j-1)} \right] \right\} \\ = - \left[K_{ni}^{ao} X_{1m}^o + \sum_i^v \sum_j^l U_j^o K_{ij}^{bo} \right] \quad (\text{II-2.E})$$

where

$$v \leq n$$

$$l \leq r$$

(II-3.E)

$$x_{1m}^o = \sum_{j=1}^r G_{mj}^o U_j^o$$

\sum_i^m represents a sum of m terms not necessarily in consecutive order

Rearranging (II-3.E) and using the fact that

$$\Delta e(t) = e(t) - e(o) = e(t) - 0 = e(t) \quad (\text{II-4.E})$$

$$\Delta E_1(s) = E_1(s) = \frac{K_{i.c.}}{s\Delta_m(s) + \left[\sum_{i=1}^p K_i s^{(i-1)} \right] \left[\sum_{j=1}^n q_{jn} s^{(j-1)} \right]} \quad (\text{II-5.E})$$

where

$K_{i.c.}$ represents an "initial condition" gain

$$K_{i.c.} = - \left[K_{ni}^{ao} X_{1m}^o + \sum_i^v \sum_j^l U_j^o K_{ij}^{bo} \right] \quad (\text{II-6.E})$$

The denominator of (II-5.E) represents the error roots which determine the error convergence rate; i.e.

$$s\Delta_m(s) + \left[\sum_{i=1}^p K_i s^{(i-1)} \right] \left[\sum_{j=1}^n q_{jn} s^{(j-1)} \right] = \sum_{k=1}^y (s+p_k) = 0 \quad (\text{II-7.E})$$

where

p_k = closed loop error roots

$$y = n - 2 + p$$

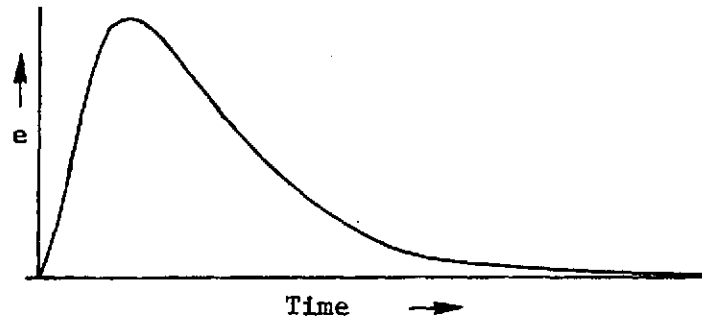


Figure II-1.E. Typical Error Versus Time Trajectory

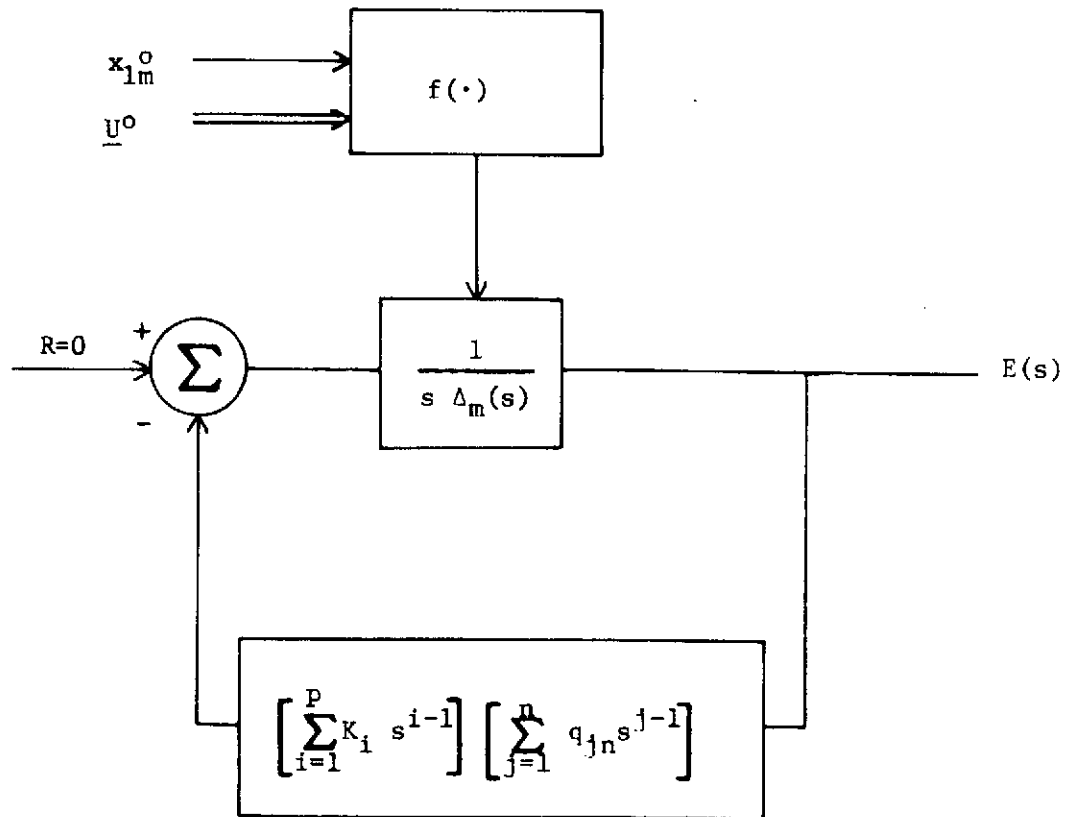
Shown in Figure (II-1.E) is a typical error versus time trajectory for an adaptive system with real dominant roots. Dividing the numerator and denominator of (II-5.E) by the factor $s\Delta_m(s)$, $E(s)$ can be modeled as

$$E(s) = K_{1.c.} \frac{G(s)}{1 + G(s) H(s)} \quad (\text{II-8.E})$$

where $G(s) = \frac{1}{s\Delta_m(s)}$ represent the open loop poles of the error dynamics and

$$H(s) = \left[\sum_{i=1}^p K_i s^{(i-1)} \right] \left[\sum_{j=1}^n q_{jn} s^{(j-1)} \right]$$

which is shown in Figure (II-2.E) as a single-loop feedback control system with no input and output $E(s)$. With no forcing function present the error response is due solely to the initial conditions. That this is so should have been expected since the MRAS error is asymptotically



$f(\cdot)$ is a non-linear operator which transforms x_{1m}^0 and \underline{U}^0 into initial conditions for the error equation

Figure II-2.E Error Magnitude Simulation Model

stable and therefore must tend to zero independent of any forcing function. Consequently, the only "driving function" on $E(s)$ is the initial condition gain $K_{i.c.}$.

Because the MRAS scheme is not an identification technique, best results for magnitude prediction are obtained only if either (1) all the adaptive terms are numerator coefficients of (II-14.B) or (2) all adapting terms are denominator coefficients. The actual adaptation process works equally well with all terms adapting; it is simply that no unique values for K_{ni}^{ao} and the K_{ij}^{bo} are then available. This is because the adaptive controller identifies output state values (the error goes to zero) but does not necessarily identify plant parameters. This means

$$G_m(\Delta) = \frac{2}{s+2}$$

α, β adapting

$$G_p(s) = \frac{\alpha}{s+\beta}$$

then any $\frac{\alpha}{\beta} = 2$ might result, depending on initial conditions. If α is fixed, then β would correctly identify the plant parameter.

It should be noted that the numerical magnitude of

$$|K_{i.c.}| = K_{n1}^{ao} x_{1m}^o + \sum_i \sum_j^v \sum_j^l U_j^o K_{ij}^{bo} \quad (\text{II-9.E})$$

in no way effects the small perturbation linearization analysis. The magnitude of x_{1m}^o depends only on the input and model and the K_{ij} only on the cumulative total plant parameter misalignments. The linearization analysis presumes only that small changes K_{ij}^a, K_{ij}^b occur at any given instant.

Using partial fraction expansion and (II-6.E), the inverse transform of (II-5.E) becomes

$$e(t) = A_1 e^{-p_1 t} + A_2 e^{-p_2 t} + \dots + A_y e^{-p_y t} \quad y \leq (n+1). \quad (\text{II-10.E})$$

The time at which maximum error occurs can be found by taking the time derivative of $e(t)$ and solving for the t at which $\dot{e}(t) = 0$.

In most work of practical and significant interest, e_{\max} could be taken to be

$$e_{\max} = \frac{\max}{h} \left\{ e(t_h) \right\} \quad (\text{II-11.E})$$

where there are h solutions obtained from $\dot{e}(t)=0$. Two of the most likely types of responses would be (1) a pure exponential decay or (2) a damped sinusoid. Either one of these responses would result in $\dot{e}(t)=0$, implying a relative maximum or minimum of $e(t)$.

Under the assumption that $E(s)$ can be approximated by a second-order plant with real poles

$$e(t) \approx \mathcal{L}^{-1} \left\{ \frac{K_{i.c.}/P}{(s+p_1)(s+p_2)} \right\} \quad (\text{II-12.E})$$

where

$$P = \begin{cases} \sum_{i=1}^{n-1} p_k & \text{if } n=1 \\ 1 & \text{if } n=1 \end{cases}$$

$$e(t) = \frac{K_{i.c.}}{P(p_2 - p_1)} \left[e^{-p_1 t} - e^{-p_2 t} \right] \quad p_1 < p_2 \quad (\text{II-13.E})$$

To obtain an estimate of e_{\max} , set

$$\frac{de(t)}{dt} = 0$$

or

$$-p_1 e^{-p_1 t} + p_2 e^{-p_2 t} = 0 \quad (\text{II-14.E})$$

from which the time interval t_m , representing the elapsed time from occurrence of a perturbation to the occurrence of maximum error can be found.

$$t_m = \frac{\ln(p_1/p_2)}{p_1 - p_2} \quad (\text{II-15.E})$$

Substituting (II-15.E) into (II-13.E) results in a simple expression for estimating the maximum magnitude of the error,

$$e_{\max} \approx \frac{K_{i.c.}}{P(p_2 - p_1)} \left[e^{-p_1 \frac{\ln(p_1 p_2)}{p_1 - p_2}} - e^{-p_2 \frac{\ln p_1/p_2}{p_1 - p_2}} \right] \quad (\text{II-16.E})$$

An unusual happening with (II-16.E) is that $|K_{i.c.}|$, the initial condition gain given in (II-9.E), is a function of the magnitudes of the plant parameter disturbances occurring at the previous disturbance time. If at time t_0 adaptation starts and at time $t_1 > t_0$ error steady state has been reached and a set of plant parameter perturbations occur, and by time $t_2 > t_1$ error steady state has occurred again

then

$$|e(\tau)|_{\max} = f(|\underline{e}(T)|_{\max}) \quad \tau \in (t_0, t_1] \quad (\text{II-17.E})$$

$$\tau \in (t_1, t_2]$$

Following along similar lines, an estimate of the error bounds for the case of a pair of complex poles and a dominant real root can be developed. The error can now be related to the dominant root locations as

$$e(t) = \mathcal{L}^{-1} \left\{ \frac{K_{i.c.}/p}{(s+\alpha+j\omega_d)(s+\alpha-j\omega_d)(s+p)} \right\} \quad (\text{II-18.E})$$

where $s = -\alpha \pm j\omega$, $-p$ represent dominant roots of $E(s)$. Using (II-18.E), it can be shown that

$$e(t) = \left[\frac{K_{i.c.}/p}{\omega_d^2 \sqrt{1 + \left(\frac{p-\alpha}{\omega_d}\right)^2}} e^{-\alpha t} \cos \left(\omega_d t - 90^\circ - \tan^{-1} \left(\frac{\omega_d}{p-\alpha} \right) \right) \right. \quad (\text{II-19.E})$$

$$\left. + \frac{K_{i.c.}/p}{(\alpha-p)^2 + \omega_d^2} e^{-pt} \right]$$

Proceeding as in (II-14.E),

$$\frac{de(t)}{dt} = -2C_1 e^{-\alpha t} \left[\alpha \cos \omega_d t - 90^\circ - \tan^{-1} \left(\frac{\omega_d}{p-\alpha} \right) \right.$$

$$\left. + \omega_d \sin \left(\omega_d t - 90^\circ - \tan^{-1} \left(\frac{\omega_d}{p-\alpha} \right) \right) \right] - C_2 p e^{-pt} = 0 \quad (\text{II-20.E})$$

where

$$C_1 = \frac{K_{i.c.}/P}{2\omega_d^2 \sqrt{1 + \left(\frac{p-\alpha}{\omega_d}\right)^2}}, \quad C_2 = \frac{K_{i.c.}/P}{(\alpha-p)^2 + \omega_d^2}$$

(II-20.E) is of the form

$$a_1 \cos(\omega_d t + \theta) + a_2 \sin(\omega_d t + \theta) + a_3 e^{-pt} = 0 \quad (\text{II-21.E})$$

which is a transcendental equation in t , the variable to be solved for. Since a_1 , a_2 , and a_3 are known constants, (II-21.E) may be graphically solved for those points, t_i , which satisfy the equation. Substituting the t_i into (II-19.E) and determining

$$e_{\max} = \max_{i,t} \left\{ e(t_i) \right\} \quad (\text{II-22.E})$$

yields a "best estimate" of the maximum value of the error.

Unfortunately, due to the uncertainty in the plant parameter perturbations, the "direction" of the error time trajectory above or below zero when a disturbance occurs cannot be predicted beforehand. To demonstrate this, consider the following n^{th} order linear plant

$$\frac{Y_p(s)}{U} = \frac{1}{s^n + a_{n-1}^p s^{n-1} + a_{n-2}^p s^{n-2} + \dots + a_1^p s + a_0^p} \quad (\text{II-23a.E})$$

and the n^{th} order model

$$\frac{X_m}{U}(s) = \frac{1}{s^n + a_{n-1}^m s^{n-1} + a_{n-2}^m s^{n-2} + \dots + a_1^m s + a_0^m} \quad (\text{II-23b.E})$$

As before $e_1 = x_m - x_p$ it is assumed that at steady state

$$e_k(t) = 0, \quad a_k^m = a_k^p \quad k = 1, 2, \dots, n \quad (\text{II-24.E})$$

The sign of e_1 depends on the "direction" of plant perturbation, i.e. if a disturbance occurs at $t = t_0$

$$e(t_0^+) < 0 \quad \text{if} \quad a_0^p(t_0^+) < a_0^m \quad (\text{II-25.E})$$

$$e(t_0^+) > 0 \quad \text{if} \quad a_0^p(t_0^+) > a_0^m$$

Since the sign of e_1 depends on future conditions, nothing can be said about sign definiteness. Since the error is defined as $\underline{e} = \underline{x}_m - \underline{x}_p$, then if $e_k(t) < 0$, $k = 1, 2, \dots, n$ the plant state $x_{k_p}(t)$ lags the model state, and if $e_{k_p}(t) > 0$, the reverse is true.

The error magnitude estimation procedure can be of particular value in the case of linear plants with a saturation non-linearity of the type shown in Figure II-3.E. With a priori knowledge of the expected range of values of \underline{U} , a "worst case" design can be anticipated and the appropriate adaptive gain parameters adjusted so as to allow x_1^p to remain within the linear range of operation. Knowing a priori a range of values of \underline{U} and the plant parameter variation, an estimate of K_{ni}^{a0} and K_{ij}^{b0} can be performed; these values coupled with (II-9.E), (II-16.E), and (II-19.E) allow estimates of maximum e_1 by maximizing $|K_{i.c.}|$.

Assuming the plant output saturation value is C_s , the maximum allowable error, e_a , is determined to be

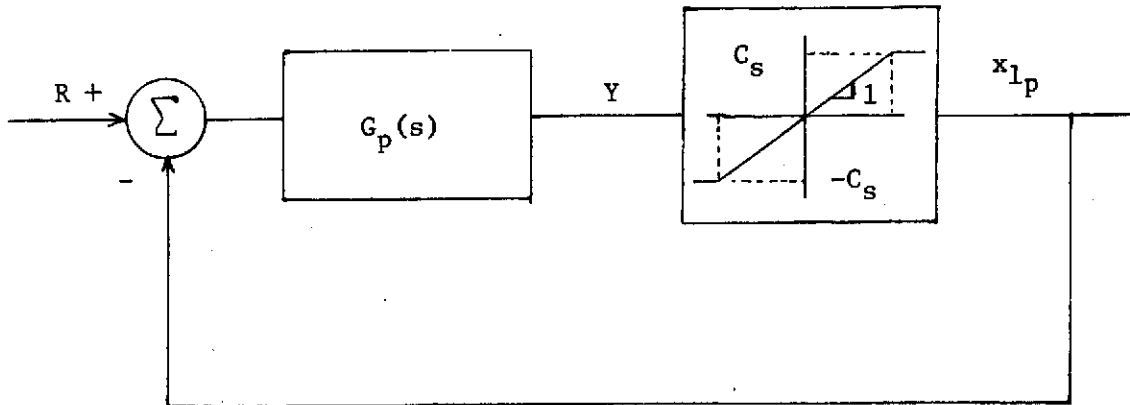


Figure II-3.E. Nonlinear Problem.

$$|e_a| = C_s - x_{1m}(\text{max}) \quad (\text{II-26.E})$$

where $x_{1m}(\text{max})$ is strictly a function of the input(s), since the model has been fixed a-priori. If $|e_1| > |e_a|$, then the model and/or adaptive gain parameters must be modified and $|e_1|$ recomputed if plant saturation is to be avoided.

EXAMPLE:

Consider the MRAS system with model

$$\frac{x_{1p}(s)}{U} = G_m(s) = \frac{2}{s^2 + 2s + 2} \quad n = 2$$

and plant

$$G_p(s) = \frac{2}{s^2 + 2s + a_{21}^p}$$

where a_{21}^p is an unknown and (possibly) slowly time-varying plant parameter. For the case of $U = 4\mu(t)$, the steady state output of the

plant becomes

$$x_{1p}(s.s.) = x_{1m} = \lim_{s \rightarrow 0} \frac{4}{s} \cdot \frac{2}{s^2 + 2s + 2} = 4 \cdot G(0) = 4$$

Using the development in [7], the root locus equation from (II-16.B) becomes

$$1 + \frac{K_1 + K_2 s}{s} \frac{q_{12} + q_{22} s}{s^2 + 2s + 2} = 0$$

where $K_1 = \alpha_{21} x_{1m}^o$

$$K_2 = \beta_{21} x_{1m}^o$$

and it is desired to determine q_{12} , q_{22} , q_{21} , β_{21} such that the error roots are real. An acceptable compensation scheme is

$$1 + \frac{K_2 q_{22} (s + 2)^2}{s(s^2 + 2s + 2)} = 0 \quad (\text{II-27.E})$$

which is in the familiar form

$$1 + k P(s) = 0$$

with $K = q_{22}(\beta_{21} x_{1m}^o)$

A plot of (II-27.E) is shown in Figure (II-4.E). From an investigation of this figure, a desirable set of error roots exists if k is chosen to be 800. From this information a compatible set of parameters is

$$\alpha_{21} = 10 \quad \beta_{21} = 5 \quad q_{12} = 20 \quad q_{22} = 10$$

The closed loop error roots for $k = 800$ are marked in Figure II-4.E and are found to be

$$s_1 = -2.075 \quad s_2 = -1.935 \quad s_3 = -798$$

Using the approximation in (II-12.E)

$$|e(t)| = |K_{21}^{a0} x_{1m}^o| (.00879) \begin{bmatrix} -1.9325t & -2.075t \\ e & -e \end{bmatrix} \quad (\text{II-28.E})$$

Initial conditions were placed on K_{21}^a in order to force $a_{21}^p = 2$ at $t = 0$. At $t = 0^+$ a step disturbance was applied to a_{21}^p . Figure II-5.E compares normalized values (with respect to the predicted error response) of $e(t)$ versus time for various initial conditions on K_{21}^{a0} . Note the excellent correlation between predicted and actual results.

F. Design Implementation

Assuming the plant-model dynamics are expressible in the form of (II-15.B), the first step in the design procedure is the selection of appropriate, linear, time-invariant models. To date, little design criteria, insofar as relating to MRAS controllers is available. Hence, a-priori knowledge of physical conditions and overall performance criteria must be used to select the models. At present, this is an art more than a science.

Secondly, using $\Delta_m(s)$ from $G(s)$, determine the error characteristic equation as given in (II-16.B). It is recommended that (II-11.C) be

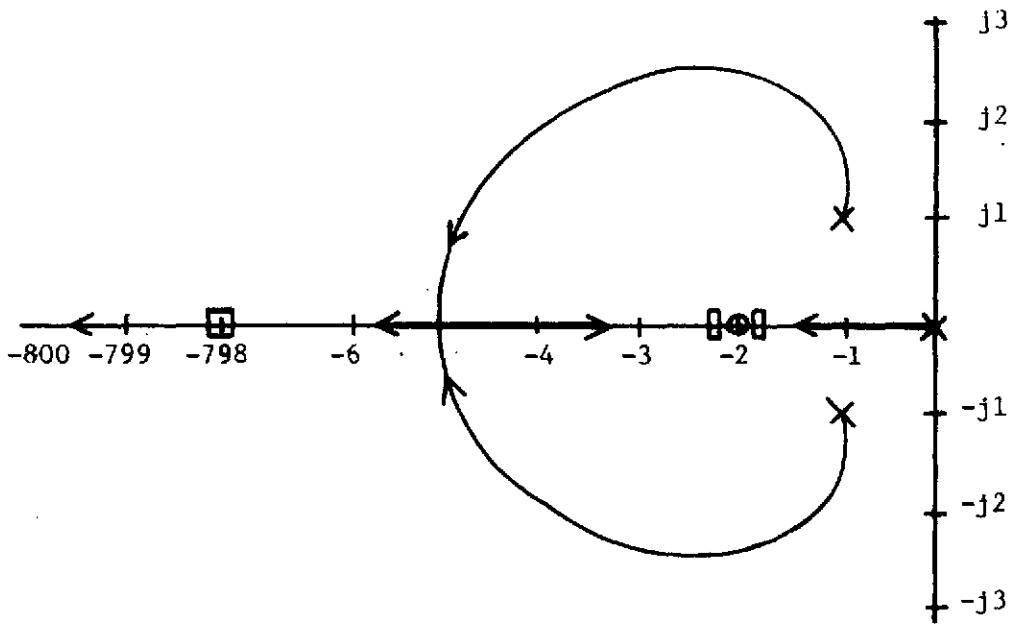


Figure II-4.E. Error Characteristic Equation Root Locus

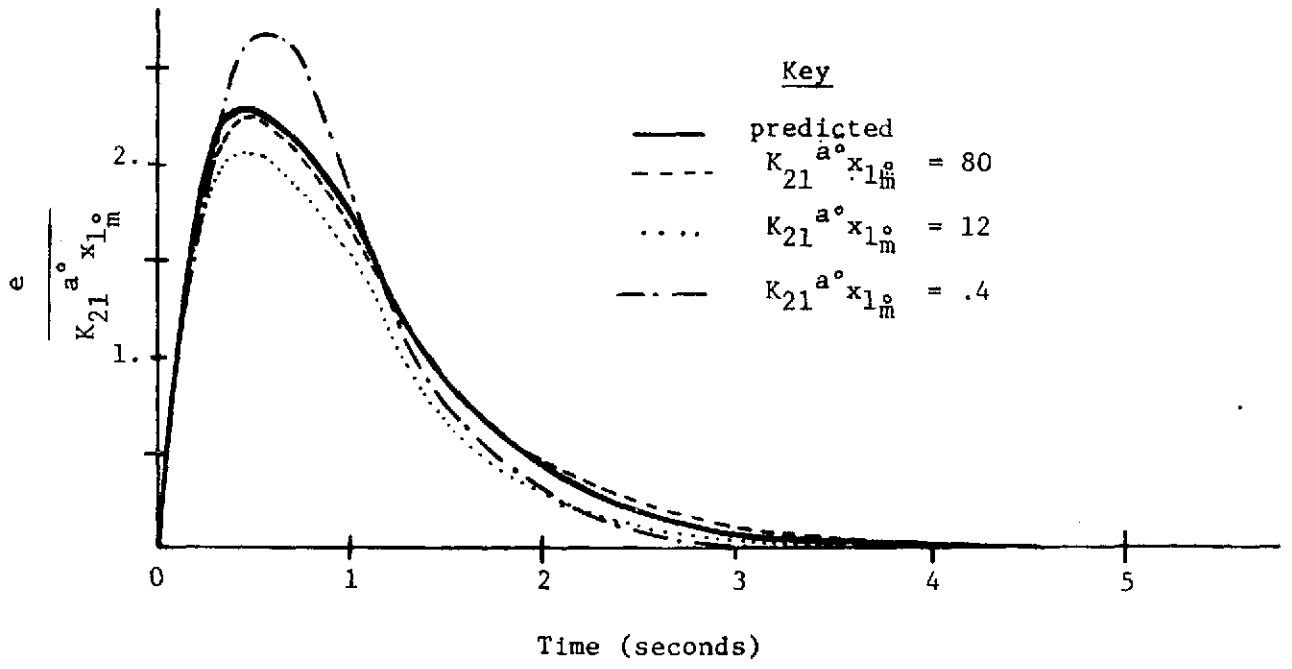


Figure II-5.E. Error Time Response

employed also to "decouple" numerator and denominator dynamics of $G_{ij}^P(s)$. With these equations values for n of the q_{ij} values, plus the $\alpha, \beta, \rho, \gamma, \delta, \sigma$ adaptive gain coefficients can be determined so as to obtain a desired transient response. Since this portion of the design involves linear frequency methods, the well-known tools of linear systems analysis can be utilized to define a "best" response. Since Q is a positive definite symmetric matrix there are $\frac{n(n+1)}{2}$ distinct terms. However, the aforementioned design method only supplies numbers for n of the entries; hence $\frac{n(n-1)}{2}$ terms are left unknown. It is necessary to insure that for the n elements of Q selected that the $\frac{n(n-1)}{2}$ remaining elements form a compatible set such that

- (1) Q is positive definite
- (2) $A_m^T Q + QA_m = -C$ when C is any positive definite matrix

If A_m is a stable matrix, a positive definite Q exists which satisfies (2) [1]. Unfortunately, this method does not take into consideration the transient error response. The inverse statement, given a Q a p.d. C exists, is not necessarily true. Consequently, selection of the remaining $\frac{n(n-1)}{2}$ Q elements is an iterative procedure; all that is necessary is to show that there exists elements satisfying (1) and (2).

It should be pointed out that until now, one of the shortcomings of using Lyapunov designed controllers was that no clear-cut technique existed for relating the Q elements and the $\alpha, \beta, \rho, \gamma, \delta, \sigma$ terms. Consequently, a common procedure was to select the Q matrix by using

an a-priori fixed C (usually the identity matrix I_n) and solving for the q_{ij} terms; the adaptive gain coefficients were then chosen by trial and error methods. As with the error equation linearization, there is no unique set of q_{ij} obtained from (2).

Although the linearized error equation in (II-16.B) is valid only for small errors, the design method outlined can also be used in the case of large errors. Since the adaptive error is guaranteed to be globally asymptotically stable from Lyapunov theory, no matter what the order of magnitude of the errors they will eventually tend to zero. Once the errors become "small" the linearized error approximation is valid. Estimates of transient performance of the system error for large disturbances may not be valid, although simulation results for a large number of cases tend to show strong correlation between predicted response and large error disturbances.

G. Error Transient Response Determination With Lyapunov Functions

Under certain conditions, knowing the form of a Lyapunov function V and its time derivative \dot{V} , it is possible to determine the transient behavior of the MRAS error dynamics. However, to be useful, it is generally necessary that \dot{V} be obtained as a function of time without having to integrate the system equations. This requirement, plus the need for the resulting V and \dot{V} expressions to be simple have generally not made it possible for the following method to be practical.

Noting that

$$\dot{V} = \left(\frac{\dot{V}}{V} \right) V, \quad (\text{II-G.1})$$

if it can be established that the quantity $\left(\frac{\dot{V}}{V} \right)$ is never greater in magnitude than some constant $-k$, $k > 0$, then

$$\dot{V} \leq -kV, \quad (\text{II-G.2})$$

and by integration

$$V(\underline{x}_p, t) \leq V(\underline{x}_p^o, t_0) e^{-k(t-t_0)} \quad (\text{II-G.3})$$

If it is known that

$$V \leq -a(\|\underline{x}_p\|)$$

$$\text{and } \dot{V} \leq b(\|\underline{x}_p\|) \quad (\text{II-G.4})$$

then k is simply

$$k = \min_{\underline{x}_p, t} \frac{a(\|\underline{x}_p\|)}{b(\|\underline{x}_p\|)} \quad (\text{II-G.5})$$

Such a k value yields a lower bound on the speed of response. Known results in this direction, however, are rare [17,18].

As an application of this technique, consider the Winsor and Roy Lyapunov function [5],

$$v = \sum_{i=1}^n \sum_{j=1}^n \frac{1}{\alpha_{ij}} a_{ij}^2 + \sum_{i=1}^n \sum_{j=1}^n \frac{1}{\beta_{ij}} b_{ij}^2 + \underline{e}^T Q \underline{e}$$

By appropriate choice of the adaptive gains,

$$\dot{v} = \underline{e}^T (A_m^T Q + Q A_m) \underline{e} \quad (\text{II-G.6})$$

from which

$$\dot{v} = \frac{-\|c\| \underline{e}}{\|Q\| \underline{e} + \sum_{i=1}^n \sum_{j=1}^n \frac{1}{\alpha_{ij}} a_{ij}^2 + \sum_{i=1}^n \sum_{j=1}^n \frac{1}{\beta_{ij}} b_{ij}^2} v \quad (\text{II-G.7})$$

where

$$-C = A_m^T Q + Q A_m.$$

If information on upper and lower bounds of the excursions of the model and plant parameters is known a priori, then bounds on the last two terms in the denominator of (II-G.6) can be obtained. In general, such information will not be available, in which case approximations are needed. An estimate of the transient behavior of the error using [5] will now be performed in order to illustrate the difficulty of using the procedure.

(II-G.7) is in the form

$$\frac{3}{A+B+C} \quad A, B, C > 0 \quad (\text{II-G.8})$$

where

$$\frac{3}{A+B+C} < \frac{1}{A} + \frac{1}{B} + \frac{1}{C}$$

or

$$\frac{1}{A+B+C} < \frac{1/3}{A} + \frac{1/3}{B} + \frac{1/3}{C} \quad (\text{II-G.9})$$

Using (II-G.9) on (II-G.7) $(\|\underline{e}\|_Q^2 = 1, C \text{ defined in (II-3.C)})$

$$\dot{v} \leq \left\{ -1/3 \left[\lambda_{\min} (CQ^{-1}) \right] -1/3 \frac{\|\underline{e}\|_C^2}{\sum_{i=1}^n \sum_{j=1}^n \frac{1}{\alpha_{ij}} a_{ij}^2} + \right. \\ \left. -1/3 \frac{\|\underline{e}\|_e^2}{\sum_{i=1}^n \sum_{j=1}^n \frac{1}{\beta_{ij}} b_{ij}^2} \right\} v \quad (\text{II-G.10})$$

Defining

$$k_1 = \max \left\{ \frac{\|\underline{e}\|_C^2}{\sum_{i=1}^n \sum_{j=1}^n \frac{1}{\alpha_{ij}} a_{ij}^2} \right\} \quad (\text{II-G.11})$$

$$k_2 = \max \left\{ \frac{\|\underline{e}\|_C^2}{\sum_{i=1}^n \sum_{j=1}^n \frac{1}{\beta_{ij}} b_{ij}^2} \right\}$$

The difficulty with using (II-G.10) is that k_1 and k_2 of (II-G.11) require a knowledge of the error \underline{e} , and unknown quantity. As an estimate of the error decay rate, it might be possible to disregard the parameter misalignments a_{ij} , b_{ij} and only be concerned with $\lambda_{\min}(CQ^{-1})$. However, results would be only approximate and would need to be interpreted with care. Under certain conditions,

then

$$\dot{V} \lesssim \left[-1/3 \lambda_{\min}(CQ^{-1}) \right] V \quad (\text{II-G.12})$$

In the cases of [6] and [7], no results thus far are available using the Lyapunov function decay rate approach. This is because in both methods, the ratios $\frac{\dot{V}}{V}$ are complicated functions of the error and thus far no reasonable approximations have been found to simplify the resulting ratios as was done in (II-G.6) to (II-G.12).

III. DETERMINATION OF STABILITY CRITERIA PROVIDED BY LYAPUNOV THEORY

The adaptive gains given in Chapter II were derived using Lyapunov theory. Using this method sufficient conditions for asymptotic stability of the error were obtained. Unfortunately, one of the shortcomings of the Lyapunov design approach is that sufficient but not necessary conditions result, making it possible to "overdesign" a system. Discussed in this chapter are various techniques for simple determination of elements of the Q matrix such that asymptotic stability is assured. Also a method is proposed to relax the Lyapunov sufficiency conditions on the Q matrix and still have an asymptotically stable adaptive system error.

A. Conventional Technique for Selection of the Q matrix

In conventional Lyapunov-designed MRAS control theory, it is necessary for the designer to select, a priori, a p.d. Q matrix such that $A_m^T Q + QA_m$ is n.d. In practice determination of such a Q matrix is difficult. In Chapter II, methods for relating the adaptive error response to the selection of the Q elements were presented, however it was still necessary to insure independently that $A_m^T Q + QA_m$ was indeed n.d. It has been shown [15] that if C is a p.d. matrix, for a given A_m matrix there exists a p.d. Q matrix such that

$$A_m^T Q + QA_m = -C \quad \text{(III-1.A)}$$

However, as will be discussed later in this chapter, the converse is not necessarily true.

By selecting a C matrix at random it is possible to obtain a Q matrix satisfying the Lyapunov stability conditions for MRAS controllers. In most published reports this is the technique used. However, as has been clearly demonstrated in Chapter II, selection of certain elements of the Q matrix is desired first. Other sections of this chapter will investigate the problem of finding acceptable bounds on the elements of the Q matrix such that easy use of the design processes discussed is insured.

B. An Extended Stability Bounding Criteria

In Chapter II, the particular V function used for deriving the adaptive gains is given by (II-10.A) and the resulting \dot{V} function by (II-13.A), repeated here for easy reference:

$$\begin{aligned} \dot{V} = \underline{e}^T (A_m^T Q + Q A_m) \underline{e} & - 2 \sum_{i=1}^n \sum_{j=1}^n \beta_{ij} \left[\sum_{k=1}^n e_k q_{ki} x_{pj} \right]^2 \\ & - 2 \sum_{i=1}^n \sum_{j=1}^r \delta_{ij} \left[\sum_{k=1}^n e_k q_{ki} u_j \right]^2 \end{aligned} \quad (\text{III-1.B})$$

Since it is required that $A_m^T Q + Q A_m$ be negative definite, and $\delta_{ij}, \beta_{ij} > 0$, then it can be seen that \dot{V} is n.d. This V is the most general one and

is applicable to the case of the Boland and Sutherlin as well as the Gilbert, Monopoli, and Price methods. By combining terms (1) and (3) of \dot{V} it is possible, under certain conditions, to relax the requirement that $A_m^T Q + Q A_m$ is n.d. By relaxing this requirement it is possible to obtain a wider choice of q_{ij} values. In terms of the linearized error equation design method, this means that a larger "stability region" for compensating zero placement is possible and still insure asymptotic stability of the system error.

There are five major restrictions involved in the following procedure

1. A_m is in phase variable form
2. At least one non-zero input is present
3. There is at least one time-varying numerator gain term, i.e.

$$G_m(s) = \frac{s + \alpha}{\Delta_m(s)} \quad \text{or} \quad \frac{\alpha}{\Delta_m(s)} \quad , \quad \begin{array}{l} \alpha \text{ time varying} \\ \text{or unknown} \end{array}$$

4. The Gilbert, Monopoli, and Price/or Boland and Sutherlin type adaptive controller is used
5. B_m contains all zero entries except for the nth row

Under these conditions, term (3) of (III-1.B) may be written as

$$\begin{aligned} (3) = & 2 \left\{ \left[\delta_{n1} (e_1 q_{1n} + e_2 q_{2n} + \dots + e_n q_{nn}) u_1 \right]^2 \right. \\ & + \delta_{n2} \left[(e_1 q_{1n} + e_2 q_{2n} + \dots + e_n q_{nn}) u_2 \right]^2 + \dots \\ & \left. + \delta_{nr} \left[(e_1 q_{1n} + e_2 q_{2n} + \dots + e_n q_{nn}) u_r \right]^2 \right\} \end{aligned} \quad (\text{III-2.B})$$

which reduces to

$$= 2 \left[\delta_{n1} U_1^2 + \delta_{n2} U_2^2 + \dots + \delta_{nr} U_r^2 \right] \left[e_1 q_{1n} + e_2 q_{2n} + \dots + e_n q_{nn} \right]^2 \quad (\text{III-3.B})$$

The squared factor in (III-3.B.) may be expanded as follows:

$$\begin{aligned} & (e_1 q_{1n} + e_2 q_{2n} + \dots + e_n q_{nn}) (e_1 q_{1n} + e_2 q_{2n} + \dots + e_n q_{nn}) = \\ & e_1^2 q_{1n}^2 + 2e_1 e_2 q_{1n} q_{2n} + 2e_1 e_3 q_{1n} q_{3n} + \dots \\ & + 2e_1 e_n q_{1n} q_{nn} + e_2^2 q_{2n}^2 + 2e_2 e_3 q_{2n} q_{3n} + 2e_2 e_4 q_{2n} q_{4n} \\ & + \dots + 2e_2 e_n q_{2n} q_{nn} + \dots + \dots + e_n^2 q_{nn}^2 \end{aligned}$$

which may be put in matrix form as

$$= \underline{e}^T \begin{bmatrix} 2 & & & & \\ q_{1n} & q_{1n} q_{2n} & q_{1n} q_{3n} & \dots & q_{1n} q_{nn} \\ & 2 & & & \\ q_{2n} q_{1n} & q_{2n} & q_{2n} q_{3n} & \dots & q_{2n} q_{nn} \\ \cdot & \cdot & \cdot & & \cdot \\ \cdot & \cdot & \cdot & & \cdot \\ & & & 2 & \\ q_{nn} q_{1n} & q_{nn} q_{2n} & q_{nn} q_{3n} & \dots & q_{nn} \end{bmatrix} \underline{e} \quad (\text{III-4.B})$$

Defining

$$\Omega = 2(\delta_{n1} U_1^2 + \delta_{n2} U_2^2 + \dots + \delta_{nr} U_r^2)$$

and

$$\hat{\underline{q}} = \begin{bmatrix} q_{1n} \\ q_{2n} \\ \vdots \\ \vdots \\ q_{nn} \end{bmatrix},$$

(III-3.B) may be written in the compact form

$$\underline{\Omega} \underline{e}^T (\hat{\underline{q}} \hat{\underline{q}}^T) \underline{e} \quad (\text{III-5.B})$$

Using (III-5.B), (III-1.B) may be rewritten

$$\begin{aligned} \dot{\underline{V}} &= \underline{e}^T (A_m^T Q + Q A_m) \underline{e} - \underline{\Omega} \underline{e}^T (\hat{\underline{q}} \hat{\underline{q}}^T) \underline{e} \\ &\quad - 2 \sum_{i=1}^n \sum_{j=1}^n \left[\sum_{k=1}^n e_k q_{ki} x_{pj} \right]^2 \end{aligned}$$

which finally simplifies to

$$\dot{\underline{V}} = \underline{e}^T (W) \underline{e} - 2 \sum_{i=1}^n \sum_{j=1}^n \left[\sum_{k=1}^n e_k q_{ki} x_{pj} \right]^2 \quad (\text{III-6.B})$$

where

$$W = A_m^T Q + Q A_m - \underline{\Omega} \hat{\underline{q}} \hat{\underline{q}}^T$$

is a n.d. matrix. Under the constraint of the five conditions mentioned earlier, (III-6.B) may be used as a criterion for insuring asymptotic stability of the adaptation error. Using (III-6.B), the condition

$$A_m^T Q + Q A_m = -C$$

is relaxed and replaced with the overall condition

$$A_m^T Q + QA_m - \hat{\Omega} \hat{q} \hat{q}^T = -C \quad (\text{III-7.B})$$

Using (III-7.B) allows a wider choice of q_{ij} values. When compared with the design procedure in Chapter II, (III-7.B) allows the choice of q_{ij} values to more closely match with values allowed by linear systems (i.e. root locus) theory. The reason that the allowable regions for the zeroes of (II-16.B) may not be as wide as those allowed by linear methods is as has been mentioned previously, namely that sufficient but not necessary conditions are obtained from Lyapunov theory. By using the fixed criteria that $A_m^T Q + QA_m = -C$, C p.d., the capability of using other information from the Lyapunov \dot{V} function is ignored. (III-6.B) allows for a varying stability criterion which accounts for additional stability information when inputs are present. This amounts to a coupling effect between the choice of the Q elements and knowledge of the range of values of inputs present. Instead of fixing the zeroes of (II-16.B) using $p = 1$ and then adding additional zero compensators due to the type ($p = 2, 3$) of system, a whole new set of zeroes all together may be determined.

Some of the benefits of employing this extended stability criterion include

- (1) allows a wider choice of response characteristic of the adaptive error
- (2) the calculations involved are straightfoward and involve merely an extension of previously stated Lyapunov design techniques

(3) asymptotic stability of the error is guaranteed

The shortcoming of this method is that knowledge of the range of values of those inputs which pass through adapted feedforward gains (i.e. inputs corresponding to terms of B in $\dot{\underline{x}} = A\underline{x} + B\underline{U}$ which are adapted. However, in many practical cases, such a range is available.

Example

$$G_m(s) = \frac{2}{s^2+2s+2} \quad ; \quad \Delta_m(s) = s^2+2s+2$$

$$G_p(s) = \frac{\alpha_1}{s^2+2s+2} \quad (\text{III-8.B})$$

$$U(t)_{\min} = 10$$

Using (II-16.B) with $p = 1$ (in order to obtain the stability limits), the error characteristic equation becomes

$$1 + \frac{K(s+a)}{s(s^2+2s+2)} = 0 \quad (\text{III-9.B})$$

where

$$a = q_{12}/q_{22}$$

$$K = q_{22}(\alpha_{21}x_{1m}^{o2} + \gamma_{21}U_1^{o2})$$

With the center of gravity of the loci of the roots of (II-9.B) at the origin in the s -plane, the zero compensator denoted by "a" can not be

any further to the left of the origin on the real axis than two (this will be shown to be true by two independent methods in the next section). Since (from a knowledge of linear systems) it is desired to have the real root as far out in the L.H. s-plane as possible, $a = 2$ is chosen. Using $p = 2$ (the Gilbert, Monopoli, and Price method) as the control scheme, a second zero at $s = -4$ is selected. This results in the root locus expression

$$1 + \frac{K_2 q_{22} (s+2) (s+4)}{s(s^2+2s+2)} = 0 \quad (\text{III-10.B})$$

where

$$K_2 = (\beta_{21} x_{1m}^{o2} + \delta_{21} U_1^{o2})$$

$$q_{12}/q_{22} = 2$$

$$K_1/K_2 = 4.$$

Using the stability extension scheme, it is only necessary for (III-7.B) to be negative definite. Expanding $\hat{\Omega} \hat{q} \hat{q}^T - A_m^T Q - Q A_m = p.d.$ function, for the second order case, $\Delta_m(s) = s^2 - a_{22}^m s - a_{21}^m s$,

$$2\delta U_1^{o2} \begin{bmatrix} q_{12}^2 & q_{12} q_{22} \\ q_{22} q_{12} & q_{22}^2 \end{bmatrix} - \begin{bmatrix} 0 & a_{21}^m \\ 1 & a_{22}^m \end{bmatrix} \begin{bmatrix} q_{11} & q_{12} \\ q_{12} & q_{22} \end{bmatrix} - \begin{bmatrix} q_{11} & q_{12} \\ q_{12} & q_{22} \end{bmatrix} \begin{bmatrix} 0 & 1 \\ a_{21}^m & a_{22}^m \end{bmatrix} > 0 \quad (\text{p.d.}) \quad (\text{III-11.B})$$

which can be rewritten as

$$\begin{bmatrix} A & B \\ B & C \end{bmatrix} > 0 \quad (\text{III-12.B})$$

where

$$A = 2\delta_{12} U_1^2 q_{12}^2 - 2q_{12} a_{21}^m$$

$$B = 2\delta_{12} U_1^2 q_{22} - a_{21}^m q_{22} - a_{22}^m q_{12} - q_{11}$$

$$C = 2\delta_{12} U_1^2 q_{22}^2 - 2q_{12} - 2q_{22} q_{22}^m$$

If

$$(1) \quad A > 0$$

$$(2) \quad AC - B^2 > 0$$

then \dot{V} will be negative definite. In order to use (III-12.B), select a desired (q_{12}/q_{22}) ratio (preferably larger than that allowed by the $A_m^T Q + Q A_m = -C$ requirement). Select q_{22} so as to set the root locus gain ($= K_2 q_{22}$) and this then fixes q_{12} ; then determine if there exists a $q_{11} > 0$ value such that (2) above is met. If such a q_{11} exists, then the q_{12}/q_{22} ratio may be used. If none can be found, a smaller ratio of q_{12}/q_{22} should be chosen and the procedure repeated.

Selecting $q_{12} = 4$, $q_{22} = 1$

$$(1) \quad \text{is met}$$

$$(2) \quad AC - B^2 = 156 - (50 - q_{11})^2 > 0 \\ \text{if } q_{11} > 37.52$$

use $q_{11} = 40$

$$\therefore Q = \begin{bmatrix} 40 & 4 \\ 4 & 1 \end{bmatrix} \text{ and}$$

$$A_m^T Q + Q A_m = \begin{bmatrix} -16 & 30 \\ 30 & 4 \end{bmatrix} \text{ is not n.d., but (III-7.B) is}$$

Interpretation of results for higher order systems is more complex than for a second order case, but the basic procedure is the same.

C. An Exact Stability Bounding Technique Employing An Algebraic Equation

As has been emphasized previously, one of the shortcomings of Lyapunov-designed controllers is the "overdesign" capability. This comes from the sufficiency conditions of the Lyapunov theorems. Using (III-1.A), where it is desired that C and Q be p.d. $n \times n$ matrixes, a technique will now be given for obtaining numerical bounds on the elements of the Q matrix. This is important because, for any other than a second-order system, the relationship between the q_{ij} elements is very difficult to determine analytically because of the complex relationships relating negative and positive definiteness. As an example, consider the case of $n = 3$,

$$Q = \begin{bmatrix} q_{11} & q_{12} & q_{13} \\ q_{12} & q_{22} & q_{23} \\ q_{13} & q_{23} & q_{33} \end{bmatrix}$$

To be positive definite, the conditions on Q are

$$\begin{aligned} q_{11} &> 0 \\ q_{11}q_{22} - q_{12}^2 &> 0 \\ q_{11}(q_{22}q_{33} - q_{23}^2) - q_{12}(q_{12}q_{33} - q_{23}q_{13}) + q_{13}(q_{12}q_{23} - q_{22}q_{13}) &> 0 \end{aligned}$$

Simultaneously, the expression $(A_m^T Q + Q A_m)$ must be n.d., requiring an equally complex group of relationships. Fortunately, from a Lemma due to Kalman [15], if C is p.d. then there exists a p.d. Q matrix if A_m is a stable matrix. To obtain all combinations of Q, C would have to be ranged through all possible values.

That the converse to Kalman's Lemma is not necessarily true, and the reason for the algebraic method to be given, is easily seen by a counterexample. Using

$$A_m = \begin{bmatrix} 0 & 1 \\ -2 & -3 \end{bmatrix} \quad Q = \begin{bmatrix} 1 & 2 \\ 1 & 4 \end{bmatrix}$$

and (III-1.A), it is clear that

$$C = \begin{bmatrix} 6 & 13 \\ 10 & 21 \end{bmatrix}$$

which is not p.d.

Returning to Chapter II, the basic error characteristic equation (II-16.B) involves the q_{ij} ratios ($p = 1$),

$$1 + \frac{K(s^{n-1} + q_{(n-1)n}/q_{nn} s^{n-2} + \dots + q_{2n}/q_{nn} s + q_{1n}/q_{nn})}{s\Delta_m(s)} = 0 \quad (\text{III-1.C})$$

where $K = q_{nn} K_1$ q_{ij} = elements of Q n = system order

By knowing the combination of q_{ij}/q_{nn} values possible, an adaptive system design can be effected.

Using

$$A_m^T Q + Q A_m = \begin{bmatrix} 2c_{11} & & & \phi \\ & 2c_{22} & & \\ & & \ddots & \\ \phi & & & 2c_{nn} \end{bmatrix} \quad (\text{III-2.C})$$

a technique is developed in Appendix A for computing Q given C by an algebraic technique. The C matrix in (III-2.C) overconstrains the problem inasmuch as it is possible for many of the zero terms of (III-2.C) to be non-zero and still guarantee that the right hand side of (III-2.C) is n.d., but the particular form given simplifies the analytical derivation considerably and then allows for a straightforward computational technique.

As shown in Appendix A, (III-2.C) may be expanded into $\frac{n(n+1)}{2}$ independent equations in the $\frac{n(n+1)}{2} q_{ij}$ variables of the form

$$\sum_{i=1}^n \sum_{j=1}^{(n-i+1)} a_{ij} q_{ij} = f_{ij}$$

where a_{ij} , f_{ij} are constants q_{ij} elements of Q

which can be generalized into the algebraic matrix form

$$A \underline{x} = \underline{b} \quad (\text{III-3.C})$$

where

$$\begin{aligned} \underline{A} &= \frac{n(n+1)}{2} \times \frac{n(n+1)}{2} \text{ constant matrix} \\ \underline{x} &= \left[q_{11} \quad q_{12} \quad \cdots \quad q_{1n} \quad q_{22} \quad q_{23} \quad \cdots \quad q_{2n} \quad \cdots \quad q_{nn} \right]^T \frac{n(n+1)}{2} \text{ xl vector} \\ \underline{b} &= \frac{n(n+1)}{2} \text{ xl vector of 0's and } c_{ij} \text{'s} \end{aligned}$$

(III-3.C) defines a set of $\frac{n(n+1)}{2}$ linearly independent equations so $|A| \neq 0$ and A^{-1} is guaranteed to exist. Solving

$$\underline{x} = A^{-1} \underline{b} = \underline{f}(c_{ij}) \quad (\text{III-4.C})$$

by iteratively "sweeping" through the ranges of values of the c_{ij} from 0^+ to ∞^- it is possible to obtain numerical data on the range of values of q_{jn}/q_{nn} which, through (III-1.C) have been shown to help determine the zero compensator locations. For the general case, numerical solutions instead of general analytical results are much easier to find, although for low-order problems general results may be found.

The "sweeping" of the c_{ij} is performed as follows:

Let ϵ_i be a small positive number and $2c_{ii}$ the diagonal elements of C. Initially let $c_{ii} = \epsilon_i = \epsilon$ and then iteratively increase c_{nn} to some arbitrarily large value c_{\max} , then increment $c_{(n-1)(n-1)}$ and sweep through all c_{nn} 's. This could be performed by a sequence of nested DO loops of the form

```

DO      10      I = 1, MAXCOUNT
      :
      :
DO      10      J = 1, MAXCOUNT
      :
      :
DO      10      K = 1, MAXCOUNT
      :
      :
10 CONTINUE.

```

It is possible, for $n=2$, to obtain exact analytical results relating the c_{ii} and A_m elements to the q_{ij}/q_{nn} ratios, as will be pointed out in a later section of this chapter. However, for the general case, the analytical computations involved are unwieldy, and are best by numerical methods.

A computer program, QRANGE, has been written to numerically obtain allowable root location combinations so that the dynamic error response can be easily designed. The program is made up of a series of sub-routines which order the data so that a series of root-locus like curves are plotted by the computer showing the location of variation of each of $(N-1)$ roots, where N is the system order. This is accomplished by using a subroutine titled ARRAYR to order the roots in groups of $(N-1)$ from largest to smallest (most positive to most negative) and then plotting all first terms, second terms, etc. of each group together. To see this, consider that there are a large number of groups of $(N-1)$ data points, each group of which is arrayed largest to smallest:

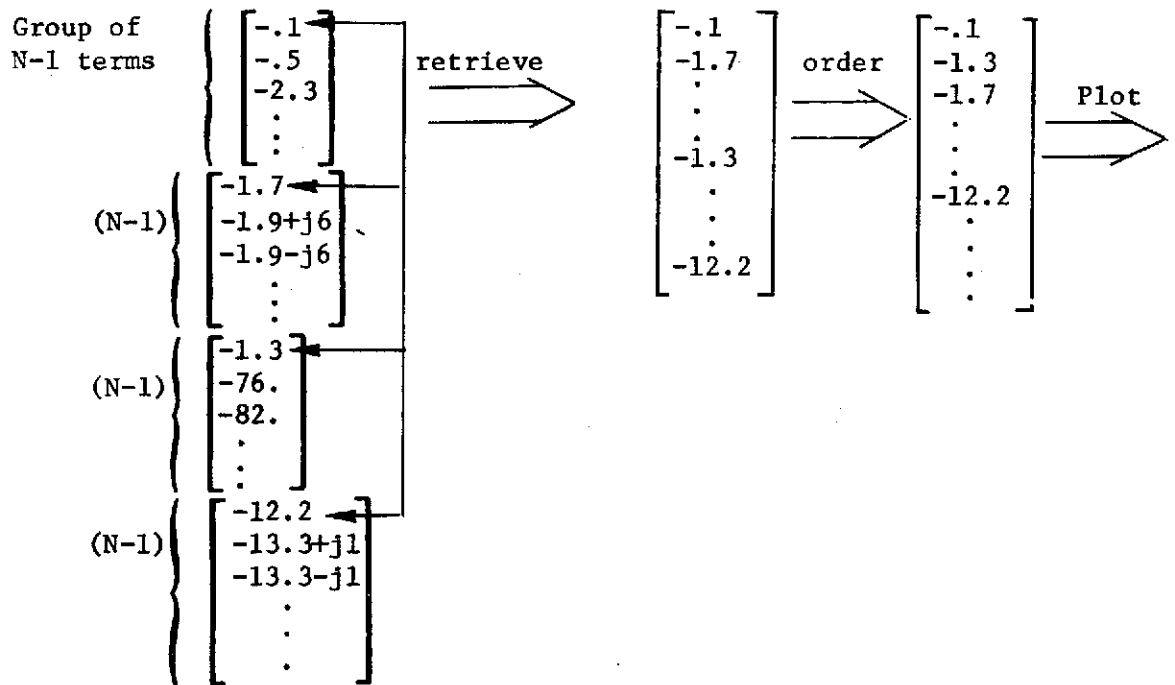


Figure III-1.C. Root Ordering By Groups.

This operation is performed repeatedly until $(N-1)$ sets of roots have been plotted. Then a listing of all groups of coefficients, the groups ordered so the first term of group 1 \geq first term of group 2 \geq first term of group 3 \dots , is given.

It is felt that by displaying a representative sample of root locations that guarantee asymptotic adaptive error stability, the designer can make a judicious choice of some root combination which is close to what he desires. Overall error transient response can then be improved beyond this by using the methods in [7,11].

A brief discussion of the special form of the C matrix used is in order. For the Q-ratio determination technique presented, it has been assumed that the C matrix is a diagonal of positive numbers with all

off diagonal elements zero. This is a sufficient but not necessary condition for C to be p.d. However, the alternative is that, to cover all combinations of the C elements for which C is p.d., all off diagonal elements must be swept through their ranges of values. This would require complete knowledge of all the non-linear relationships guaranteeing C be p.d. a situation that is difficult for low (i.e. 2nd) order systems and completely unwieldy for higher (i.e. ≥ 3) order systems. Therefore, the range of values of the Q ratios obtained with the sweeping techniques are a subset of a larger, unknown set. This is not of any real consequence because it simply means the designer is forced to select his zero compensators from a smaller choice set. Whatever combination he does choose will insure an asymptotically stable error response.

A second point to consider is that of sensitivity of the delta increments used in sweeping the c_{ii} terms through in a priori fixed range of values. By using discrete step increments the possibility of "missing" that particular (unknown) combination of c_{ii} values where the changes in Q -ratio roots is largest may occur. This is where a bit of insight on the part of the designer is needed. A first "guess-run" can be performed using estimated limits on the c_{ii} and a delta value to give a reasonable number of data points. After a cursory examination of the preliminary data a second run with appropriately modified data could be determined.

Such a computer design program is ideal for use on an on-line, time-sharing computer terminal system. In a relatively short time the

designer has a written and graphical record of results which he can later use in a full design study.

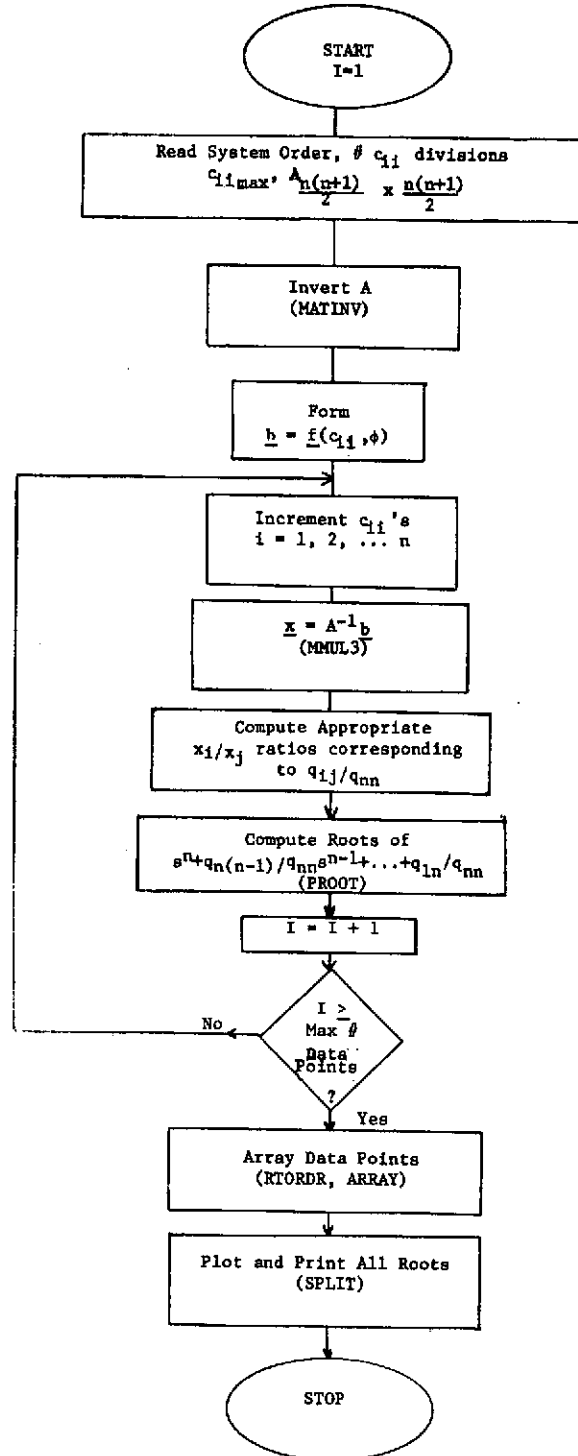
Shown in Figure III-2.C. is a flowchart of the program QRANGE, a copy of which is available from the Auburn University Electrical Engineering Department. This main program ties in with a number of subroutines. QRANGE, the main control program uses MATINV to obtain A^{-1} from A as in (III-2.C) and (III-3.C), then obtains feasible q_{ij}/q_{nn} ratios using MMUL. These coefficients are then transferred to PROOT where all of the (N-1) roots of the numerator expression in (III-1.C) are obtained. These roots are stored in two large arrays, for real and imaginary root parts. RTORDR arrays the roots in groups of (N-1) terms, from largest to smallest (smallest negative real part to largest negative real part). Using ARRAY, the jth ($j=1,2,\dots,N-1$) term of each of these groups is retrieved and plotted, real part vs. imaginary, using SPLIT. When all groupings of each of the (N-1) roots of the q_{ij}/q_{nn} ratios have been plotted, the entire set of data points is plotted.

D. Kleinman's Iterative Method For Determination of Bounds on Q Matrix Elements

As discussed in Chapter IV of the Third Technical Report, Kleinman's Iterative method [19] includes a subroutine that is a numerical technique for solving the equation

$$A_m^T Q + Q A_m = -C$$

for Q, given A_m and C. This is an iterative method whose results compare



III-2.C. Flowchart of GRANGE

with the method discussed in section C. By using this method in a loop and varying the C matrix a range of values on the Q matrix elements can be obtained. These results then help the designer define regions in the s-plane where zero compensators of the error characteristic equation in Chapter II may be placed.

Whereas the other numerical methods discussed thus far were exact, the Kleinman iterative method supplies answers which are only accurate to within some tolerance. Therefore, any zero compensator placement based on results from this technique would have to be verified to insure that Q was p.d. and that $A_m^T Q + QA_m$ was n.d. However, this need not negate the use of this method, for it would be expected that only near the boundary of a stability region would the approximate iterative results differ from exact results.

Computationally, it solves

$$A_m^T Q + QA_m + C = 0$$

by starting with an a priori input initial guess and then iteratively homing in on Q to within a tolerance. The tolerance is based on the requirement that

$$\frac{q_{ij}(k+1) - q_{ij}(k)}{q_{ij}(k+1)} < \text{TOL} \quad i = j$$

where (k+1) is the (k+1)st iteration. In this way TOL represents a per cent error ($0 \leq \text{TOL} \leq 1$). However, if it is desired to insure that all

elements meet precisely the TOL requirement, the program in [19] may be easily altered to check all the elements.

E. Comparison Between Stability Bounds Obtained From Lyapunov Theory and Linear Methods

In actual design work with model-reference adaptive systems it is necessary to use only those combinations of q_{ij}/q_{nn} in (II-16.B) such that the necessary stability conditions are maintained. However, the whole purpose of the linearization technique performed in Chapter II was to reduce all the Lyapunov stability considerations to classical control techniques, especially root locus methods. It is therefore instructive to compare stability predictions between linear methods and the exact Lyapunov methods to see just how well the small-signal technique works as a design tool. Through some examples, then, it may be possible to develop some "rules of thumb" for various order systems as to determining how one can be a bit conservative on the stability bounds for the roots of

$$\sum_{j=1}^n \left[q_{jn} s^{j-1} \right] = 0 \quad (\text{III-1.E})$$

as predicted by linear methods and still meet Lyapunov requirements.

The first example compares the two methods for the special case $n = 2$.

Example 1.

Consider the general second-order case of

$$G_m(s) = \frac{\omega_n^2}{s^2 + 2\zeta\omega_n s + \omega_n^2} \quad (\text{III-2.E})$$

$$\Delta_m(s) = s^2 + 2\zeta\omega_n s + \omega_n^2$$

It is desired to find bounds on the zero "-a" using (II-16.B) for the case $p=1, n=2$;

$$1 + \frac{k(s+a)}{s(s^2 + 2\zeta\omega_n s + \omega_n^2)} = 0 \quad (\text{III-3.E})$$

A_m is

$$\begin{bmatrix} 0 & 1 \\ -\omega_n^2 & -2\zeta\omega_n \end{bmatrix} = \begin{bmatrix} 0 & 1 \\ -a_{21}^m & -a_{22}^m \end{bmatrix}$$

With

$$C = \begin{bmatrix} 2c_{11} & 0 \\ 0 & 2c_{22} \end{bmatrix} \quad c_{11}, c_{22} > 0$$

solving $A_m^T Q + QA_m = -C$ for the q_{ij} element,

$$q_{11} = \frac{c_{11}(a_{22}^m)^2 + c_{11}a_{21}^m + c_{22}(a_{21}^m)^2}{a_{21}^m a_{22}^m}$$

$$q_{12} = \frac{c_{11}}{a_{21}^m}$$

$$q_{22} = \frac{c_{11} + c_{22}a_{21}^m}{a_{21}^m a_{22}^m} \quad (\text{III-4.E})$$

Defining $a = q_{12}/q_{22}$

and substituting (III-4.E) results in

$$a = \frac{c_{11}a_{22}^m}{c_{11} + c_{22}a_{21}^m} \quad (\text{III-5.E})$$

Letting c_{11} , c_{22} take on all values between 0^+ and ∞ , note that "a" varies between 0 and a_{22}^m . For the second order example this is equivalent to

$$0 < a \leq 2\zeta\omega_n \quad (\text{III-6.E})$$

It should be noted that (III-4.E) was obtained by taking the general inverse of A in (III-3.C). Since A is of size $\frac{n(n+1)}{2} \times \frac{n(n+1)}{2}$, results become unwieldy for 3rd (A is 6 x 6) and higher order system, and this is when a numerical optimization is proposed.

Using Routh-Hurwitz methods, (III-3.E) becomes

$$s^3 + s^2(2\zeta\omega_n) + s(\omega_n^2 + k) + ka = 0 \quad (\text{III-7.E})$$

s^3	1	$(\omega_n^2 + k)$	0	
s^2	$2\zeta\omega_n$	ka	0	
s^1	$(2\zeta\omega_n)(\omega_n^2 + k) - ka$	0	0	(III-8.E)
	<hr/>	$2\zeta\omega_n$		
s^0	ka	0	0	

In order for (III-7.E) to be stable for all $k > 0$, it is necessary that

$$a < 2\zeta\omega_n \quad (\text{III-9.E})$$

From a knowledge of linear systems analysis, (III-3.E) requires that $a \geq 0$. Combining these two limits results in

$$0 < a \leq 2\zeta\omega_n \quad (\text{III-10.E})$$

which agrees with (III-6.E) obtained by the $A_m^T Q + QA_m = -C$ method.

In some sense this provides a check on the accuracy of the small signal error equation with exact Lyapunov methods, for it shows that for $n = 2$, results are identically the same.

A general third order problem will now be studied in order to compare linear vs. Lyapunov stability region predictions. As might be expected, results are much harder to interpret.

Assume the characteristic equation for $n = 3$ is

$$\Delta_m(s) = (s^2 + 2\zeta\omega_n s + \omega_n^2)(s + p) \quad (\text{III-11.E})$$

The linearized error equation from Chapter II is

$$1 + \frac{q_{33}K_1(s^2 + \frac{q_{23}}{q_{33}}s + \frac{q_{13}}{q_{33}})}{s \Delta_m(s)} = 0 \quad (\text{III-12.E})$$

where

$$K_1 = \alpha_{31}x_{1m}^2$$

Defining

$$\frac{q_{13}}{q_{33}} = d \quad \frac{q_{23}}{q_{33}} = c \quad (\text{III-13.E})$$

(III-12.E) may be rewritten as

$$1 + \frac{K(s+a)(s+b)}{s \Delta_m(s)} = 0 \quad (\text{III-14.E})$$

with

$$a = \frac{c + \sqrt{c^2 - 4d}}{2} \quad b = \frac{c - \sqrt{c^2 - 4d}}{2} \quad (\text{III-15.E})$$

and

$$(a+b) = \frac{q_{23}}{q_{33}} \quad (ab) = \frac{q_{13}}{q_{33}}$$

(III-14.E) represents the linear characteristic equation to be used in comparing stability prediction.

Using Lyapunov theory,

$$Q = \begin{bmatrix} q_{11} & q_{12} & q_{13} \\ q_{12} & q_{22} & q_{23} \\ q_{13} & q_{23} & q_{33} \end{bmatrix} \quad A_m = \begin{bmatrix} 0 & 1 & 0 \\ 0 & 0 & 1 \\ a_{31}^m & a_{32}^m & a_{33}^m \end{bmatrix}$$

$$a_{nj}^m < 0 \quad (\text{III-16.E})$$

$$A_m^T Q + Q A_m = -C$$

$$\begin{bmatrix} 0 & 0 & a_{31}^m \\ 1 & 0 & a_{32}^m \\ 0 & 1 & a_{33}^m \end{bmatrix} \begin{bmatrix} q_{11} & q_{12} & q_{13} \\ q_{12} & q_{22} & q_{23} \\ q_{13} & q_{23} & q_{33} \end{bmatrix} + \begin{bmatrix} q_{11} & q_{12} & q_{13} \\ q_{12} & q_{22} & q_{23} \\ q_{13} & q_{23} & q_{33} \end{bmatrix} \begin{bmatrix} 0 & 1 & 0 \\ 0 & 0 & 1 \\ a_{31}^m & a_{32}^m & a_{33}^m \end{bmatrix} \\ = \begin{bmatrix} -c_{11} & 0 & 0 \\ 0 & -c_{22} & 0 \\ 0 & 0 & -c_{33} \end{bmatrix}$$

$$(\text{III-17.E})$$

where a special form of C has been selected as discussed previously, $c_{ii} > 0$. Using (III-17.E), a set of $\frac{n(n+1)}{2}$ equations in the $\frac{n(n+1)}{2}$ variables q_{ij} is obtained

$$\left. \begin{aligned}
 a_{31} q_{13} + q_{13} a_{31} &= -c_{11} \\
 a_{31} q_{23} + q_{11} q_{13} a_{32} &= 0 \\
 a_{31} q_{33} + q_{12} + q_{13} a_{33} &= 0 \\
 q_{12} + a_{32} q_{23} + q_{12} + q_{23} a_{32} &= -c_{22} \\
 q_{13} + a_{32}^m q_{33} + q_{22} + q_{23} a_{33}^m &= 0 \\
 q_{23} + a_{33} q_{33} + q_{23} + a_{33} q_{33} &= -c_{33}
 \end{aligned} \right\} \text{(III-18.E)}$$

Solving for q_{jn} $j = 1, 2, 3$

$$\begin{aligned}
 q_{13} &= \frac{-c_{11}}{2a_{31}} \\
 &\quad \frac{-c_{22} a_{33} - c_{11} \frac{a_{33}^2}{a_{31}} + c_{33} a_{23} a_{33}}{a_{31}} \\
 q_{23} &= \frac{-c_{33}}{2} + \frac{-c_{22} a_{33} - c_{11} \frac{a_{33}^2}{a_{31}} + c_{33} a_{23} a_{33}}{4(a_{31} + a_{23} a_{33})} \quad \text{(III-19.E)} \\
 q_{33} &= \frac{c_{22} + c_{11} \frac{a_{33}}{a_{31}} - c_{33} a_{23}}{2(a_{31} + a_{23} a_{33})}
 \end{aligned}$$

Using the ratios q_{13}/q_{33} , q_{23}/q_{33} and the c_{ii} one can obtain combinations of q_{13}/q_{33} , q_{23}/q_{33} such that asymptotic stability of the error equation is maintained. The roots of

$$\left(s^2 + q_{23}/q_{33} s + q_{13}/q_{33} \right)$$

may then be obtained by using (III-15.E), and it is these roots which are to be compared with the zero placement from linear methods.

$$s^4(1) + s^3(2\zeta\omega_n+p) + s^2(\omega_n^2+2\zeta\omega_n p+K) + s(\omega_n^2 p+K(a+b)) + Kab = 0$$

s^4	1	$(\omega_n^2+2\zeta\omega_n p+K)$	(Kab)
s^3	$(2\zeta\omega_n+p)$	$\omega_n^2 p+K(a+b)$	0
s^2	$\frac{(2\zeta\omega_n+p)(\omega_n^2+2\zeta\omega_n p+K) - \omega_n^2 p+K(a+b)}{(2\zeta\omega_n+p)}$	(Kab)	0
s^1	$\frac{(2\zeta\omega_n+p)(\omega_n^2+2\zeta\omega_n p+K) - \omega_n^2 p+K(a+b)}{\omega_n^2 p+K(a+b) - (Kab)(2\zeta\omega_n+p)}$ $\frac{\omega_n^2 p+K(a+b) - (Kab)(2\zeta\omega_n+p)}{(2\zeta\omega_n+p)}$	0	0
s^0	Kab	0	0

$\zeta, \omega_n, p, a, b > 0$

Figure III-1.E. Routh Hurwitz Array for Third Order $G_m(s)$.

Using (III-12.E), the characteristic equation to be studied by Routh-Hurwitz array is

$$s(s+p)(s^2+2\zeta\omega_n s+\omega_n^2) + K(s+a)(s+b) = 0$$

or

$$s^4 + s^3(2\zeta\omega_n+p) + s^2(\omega_n^2+2\zeta\omega_n p+K) + s(\omega_n^2 p+Ka+Kb) + Kab = 0$$

(III-20.F)

The corresponding Routh-Hurwitz array is given in Figure III-1.E. From column 1 of this figure it is necessary that all entries be positive in order to insure stability, so

$$\zeta, \omega_n, p, a, b > 0 \quad (a)$$

$$(2\zeta\omega_n+p)(\omega_n^2+2\zeta\omega_n p+K) - (\omega_n^2 p+Ka+Kb) > 0 \quad (b)$$

$$K > 0 \quad (c)$$

$$(\omega_n^2 p+Ka+Kb) - \frac{(Kab)(2\zeta\omega_n+p)}{(2\zeta\omega_n+p)(\omega_n^2+2\zeta\omega_n p+K) - (\omega_n^2 p+Ka+Kb)} > 0 \quad (d)$$

(III-21.E)

Since ζ, ω_n, p are known, it is a, b and K which are variables to be related. Since K must be greater than 0, (b) and (d) of (III-21.E) can be combined as follows. From (b)

$$\text{if } 2\zeta\omega_n+p > a+b$$

$$\text{then } K > 0$$

$$\text{if } 2\zeta\omega_n+p < a+b$$

$$\text{then } K > \frac{2\zeta\omega_n(\omega_n^2+2\zeta\omega_n p+p^2)}{a+b-2\zeta\omega_n-p}$$

(d) is in the form of a quadratic in K , which can be seen by rewriting it in the form

$$AK^2 + BK + C > 0 \quad (\text{III-22.E})$$

where

$$A = 2\zeta\omega_n a + 2\zeta\omega_n b + a_p + b_p - a^2 - 2ab - b^2$$

$$B = p(\omega_n^2)(2\zeta\omega_n + p - (a+b)) - ab_p + 2\zeta\omega_n 2ab_p + \omega_n^2(a+b) + 2\zeta\omega_n p(a+b) + p^2(a+b)$$

$$C = 2\zeta\omega_n p\omega_n^2(\omega_n^2 + 2\zeta\omega_n p + p^2) - 2\zeta\omega_n ab$$

If either (a) the discriminant $B^2 - 4AC < 0$ or (b) all roots of (III-22.E) are negative then for K positive (III-22.E) is satisfied. Statement (a) can be seen by considering $f(K)$ versus K , where (III-22.E) can be written as

$$AK^2 + BK + C > 0 = f(K) \quad (\text{III-23.E})$$

If $B^2 - 4AC < 0$ then there are no real roots and (for $A > 0$ the parabolic function has a minimum greater than zero. Statement (b) allows for negative crossings of the K axis, such that for all $K > 0$, $f(K) > 0$. This is illustrated in Figure III-2.E.

In order to illustrate the types of stability bounds which can be expected from Lyapunov techniques versus linear methods using (II-16.B), a third order example will be given.

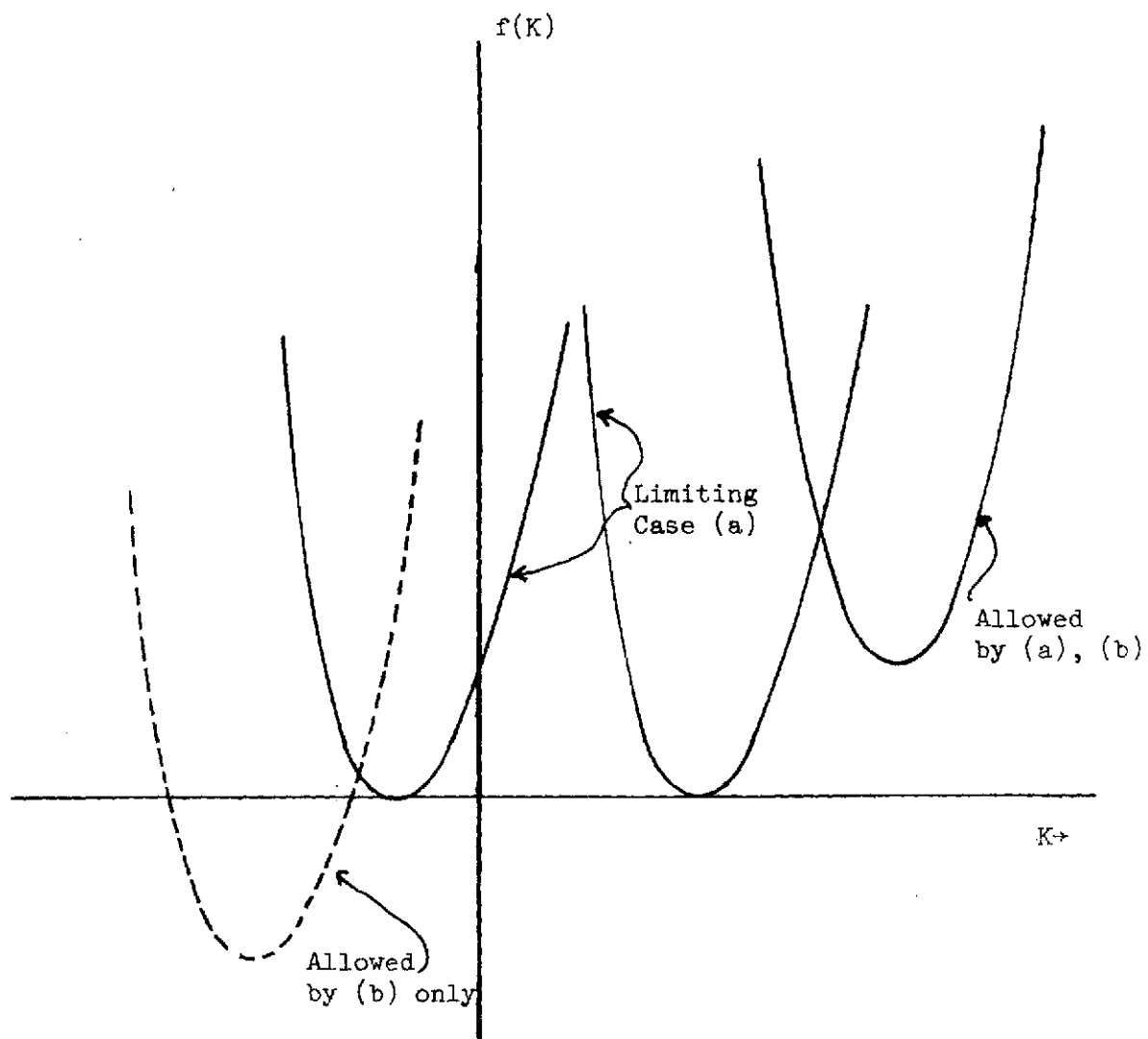


Figure III-2.E- Illustration of $f(K)$ vs. K Requirement for (III-23.F)

Example:

$$G_m(s) = \frac{6}{(s+1)(s+2)(s+3)}$$

Q and A_m of the form in (III-16.E)

$$1 + \frac{k(s+a)(s+b)}{s(s+1)(s+2)(s+3)} = 0$$

is the error characteristic equation of interest. Using Routh Hurwitz linear stability methods, a region of a, b zero placement can be determined. Using exact Lyapunov techniques, a stability region for a, b placement was determined using QRANGE. The results of both the linear and Lyapunov stability regions are shown in Figure III-3.E.

Some important points to note from Figure III-3.E are (1) as expected, Lyapunov-obtained results are more conservative than from the approximate linear methods, (2) the Lyapunov stable-region is clustered near the origin with respect to linear results, (3) no part of the Lyapunov predicted region is outside that obtained from linear methods, suggesting that the Lyapunov results are a subset of linear results. In addition, it appears from both second and third order examples that a "rule-of-thumb" might be that some fraction of the linear stability region would fit Lyapunov conditions. Results would have to be interpreted carefully, however in order to insure stability, but as a starting point for compensating design the rule-of-thumb might be used.

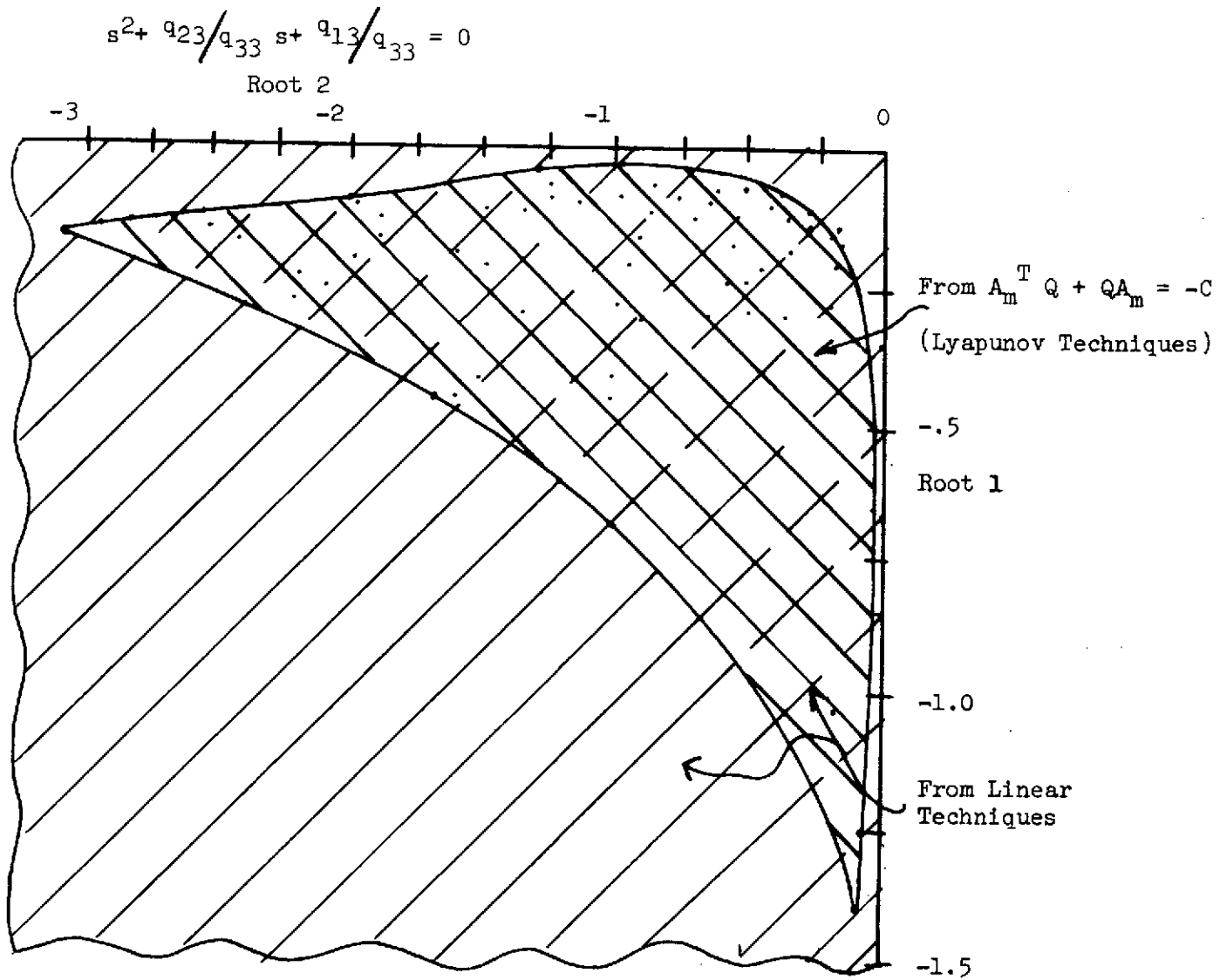


Figure III-3.E - Allowable "Zero" Root Locations Guaranteeing Asymptotic Error Stability

IV. PRACTICAL DIFFICULTIES IN IMPLEMENTING AN MRAS CONTROLLER

In Chapters II and III design criteria and stability analysis were discussed and a number of examples given to illustrate implementation. Up until now, the "ideal" case was assumed, i.e. no plant or input noise, all plant states measurable and available for feedback. In most practical situations one or more of these conditions will be violated to some extent and the purpose of this chapter is to study such effects on the performance of an MRAS controller. Analytical results will be presented when possible and examples given to illustrate discussion topics.

A. MRAS Controllers With Noise

Noise is an imprecise term which is often used in practice to account for modeling uncertainties, undetermined environmental disturbances, and linearization effects of non-linear system. Noise will be considered in this section in regard to its effect on stability of error in a model-reference control system.

In particular, a plant with input noise and state noise will be studied. The state noise could conceivably represent the effects of

- (a) electrical noise
- (b) vibration
- (c) measurement transducer misalignment

- (d) random wind gusts
- (e) bending moment effects on measurement transducers

Input noise could be represented by

- (a) mechanical play in control guides and surfaces
- (b) electrical noise in drive signal due to induction pickup
- (c) wind disturbances on control surfaces

Shown in Figure IV-1.A is a diagram of the plant of an MRAS controller subjected to input noise $\underline{v}(t)$ and state noise $\underline{\eta}(t)$. Using Lyapunov theory and the Lyapunov functions in [5, 6, 7] an analytical description of an upper bound on the norm of the error in steady-state will be found. Asymptotic stability no longer has meaning when noise is present; instead bounded stability is of concern. The dynamics given in Figure IV-1.A will now be discussed.

The disturbance inputs are

$$\begin{aligned} \dot{\underline{v}} &= \theta(t) \underline{v} + \Delta(t) \underline{\xi} & \underline{\xi}(t) &= \underline{f}(\cdot) \underline{1} \quad (\text{input}) & \text{(IV-1.A)} \\ \dot{\underline{\eta}} &= \Gamma(t) \underline{\eta} + \Psi(t) \underline{\omega} & \underline{\omega}(t) &= \underline{f}(\cdot) \underline{0} \quad (\text{state}) \end{aligned}$$

where

$\underline{\xi}, \underline{\omega}$ are nth order gaussian-white uncorrelated processes with zero mean

$\underline{v}(t), \underline{\eta}(t)$ are correlated noises

$\underline{f}(\cdot)$ is a saturation function which clamps at the $\pm 3\sigma$ values of the appropriate gaussian input

The plant dynamics are

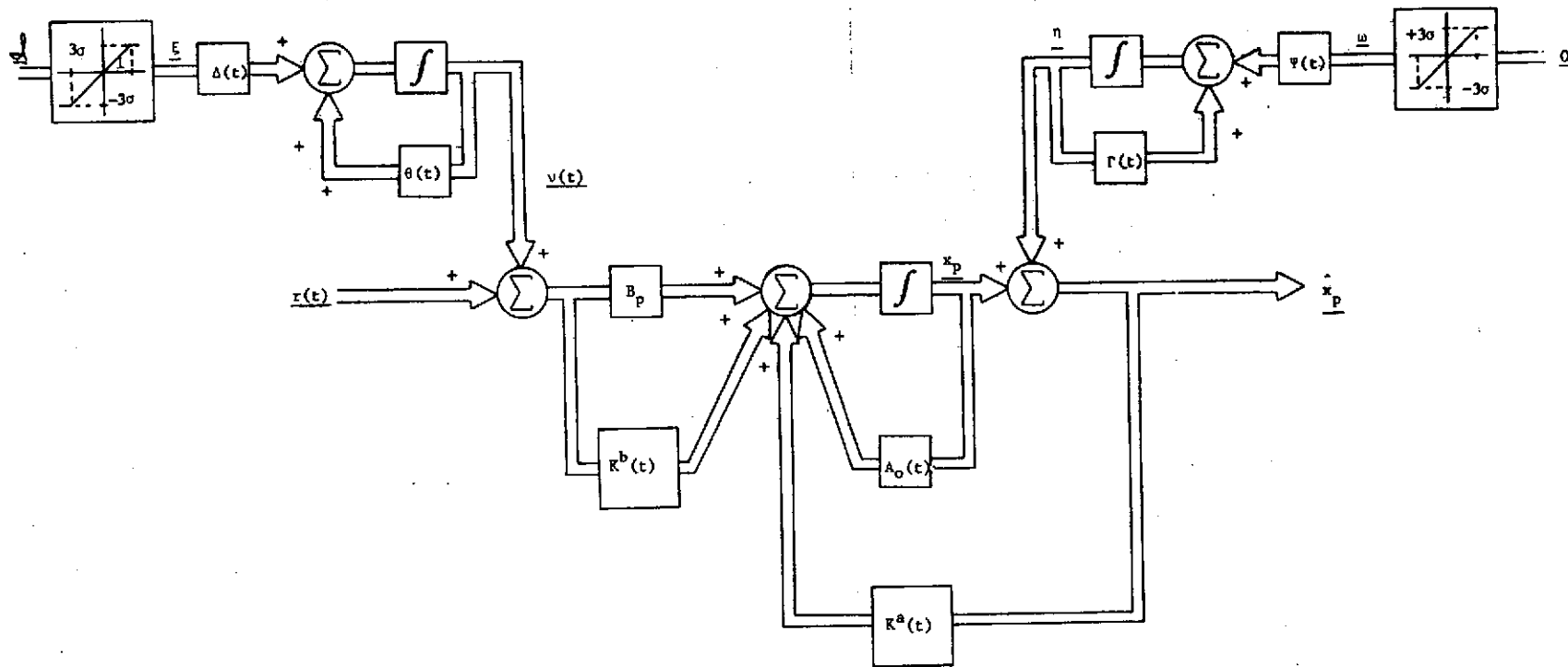


Figure IV-1.A. Adaptive Controller With Stochastic Input and State Noise Present.

$$\dot{\underline{x}}_p = A_p(t) \underline{x}_p + K(t) \left[\underline{x}_p + \underline{\eta}(t) \right] + B_p(t) \left[\underline{r} + \underline{v}(t) \right] \quad (\text{IV-2.A})$$

where

\underline{x}_p is an $n \times 1$ state vector

\underline{r} is an $r \times 1$ input vector

$K(t)$ is the adaptive gain matrix

$A_p(t)$, $B_p(t)$ are $n \times n$ and $n \times r$ unadapted state and input matrices

Defining

$$\hat{\underline{x}}_p(t) = \underline{x}_p + \underline{\eta}(t) \quad (\text{IV-3.A})$$

$$\underline{u}(t) = \underline{r}(t) + \underline{v}(t)$$

$\hat{\underline{x}}_p$, $\underline{u}(t)$ represent the available plant information. Substituting (IV-3.A) into (IV-2.A) results in

$$\dot{\underline{x}}_p = A_p(t) \underline{x}_p + K(t) \hat{\underline{x}}_p(t) + B_p(t) \underline{u}(t) \quad (\text{IV-4.A})$$

which is similar to (II-1.A) except that now the internal feedback $A(t) \underline{x}_p$ is separated from the external, physically available $K(t) \hat{\underline{x}}_p(t)$ which is corrupted by noise $\underline{\eta}(t)$. Since a control law must be implemented with available state information, a new error variable

$$\underline{\hat{e}} = \underline{x}_m - \hat{\underline{x}}_p(t) \quad (\text{IV-5.A})$$

is defined. Since the noises cannot be controlled but only identified by their statistical properties, the effects of them on the MRAS

controller performance are important considerations. In Appendix C is developed an analytical expression for determining the error bounds as a function of the input and state noise statistics, and certain adaptive gain parameters. Two such independent studies have been performed in recent times [9, 10].

Using the V function given in Chapter II, \dot{V} is determined in Appendix E for the case of additive noise. The results are that V is p.d. but \dot{V} is indefinite,

$$\begin{aligned} \dot{V} = & \hat{\underline{e}}^T (A_m^T Q + QA_m) \hat{\underline{e}} - 2 \sum_{i=1}^n \sum_{j=1}^n \beta_{ij} \left[\sum_{k=1}^n \hat{e}_k q_{ki} \hat{x}_{pj} \right]^2 \\ & - 2 \sum_{i=1}^n \sum_{j=1}^r \delta_{ij} \left[\sum_{k=1}^n \hat{e}_k q_{ki} u_j \right]^2 + 2 \hat{\underline{e}}^T Q \left[A_o \underline{\eta} - \dot{\underline{n}} - B_m \underline{v} \right] \end{aligned} \quad (\text{IV-6.A})$$

If the noises were not present, then \dot{V} would revert to a function n.d. in \underline{e} . For the case of noise assuming that \underline{v} , $\underline{\eta}$, and $\dot{\underline{n}}$ are bounded, the last term of (IV-6.A) can be written as

$$2 \left| \left| A_o \underline{\eta} - \dot{\underline{n}} - B_m \underline{v} \right| \right|_{\max} \leq \Gamma \quad (\text{IV-7.A})$$

Defining

$$\begin{aligned} \dot{V}_1 = & \hat{\underline{e}}^T (A_m^T Q + QA_m) \hat{\underline{e}} - 2 \sum_{i=1}^n \sum_{j=1}^n \beta_{ij} \left[\sum_{k=1}^n \hat{e}_k q_{ki} \hat{x}_{pj} \right]^2 \\ & - 2 \sum_{i=1}^n \sum_{j=1}^r \delta_{ij} \left[\sum_{k=1}^n \hat{e}_k q_{ki} u_j \right]^2 \end{aligned} \quad (\text{IV-8.A})$$

and using (IV-7.A),

$$\dot{V} \leq \dot{V}_1 + ||\hat{\underline{e}}^T Q||\Gamma \quad (\text{IV-9.A})$$

since the second term of (IV-9.A) is equal to or more positive than the last term of (IV-6.A). Using a procedure outlined in [9] an upper bound on the norm of the error is found to be

$$||\hat{\underline{e}}|| > \frac{\lambda(Q)_{\max}}{\lambda(-A_m^T Q - QA_m)_{\min}} \quad \Gamma = p \quad (\text{IV-10.A})$$

where

$\lambda(Q)_{\max}$ is the maximum eigenvalue of Q

$\lambda(-A_m^T Q - QA_m)_{\min}$ is the minimum eigenvalue of $(-A_m^T Q + QA_m)$

Γ is defined in (IV-7.A)

$p =$ radius of convergence of n -dimensional hypersphere in $\hat{\underline{e}}$ -space.

(IV-10.A) says that as long as the norm of the noisy error, $||\hat{\underline{e}}||$, is greater than the analytically derived number p , then \dot{V} will be n.d. in \underline{e} and the MRAS controller will guarantee bounded stability to at least an error region with norm p . It could be that the norm of the error is considerably smaller, and in fact may approach zero, but no concrete statements can be made for $||\hat{\underline{e}}|| < p$.

Using

$$\underline{e} = \hat{\underline{e}} - \underline{\eta} \quad (\text{IV-11.A})$$

an upper bound on the norm of the error \underline{e} ,

$$\underline{e} = \underline{x}_m - \underline{x}_p$$

can be found,

$$||\underline{e}|| \leq ||\hat{\underline{e}}|| + ||\underline{n}||_{\max} \quad (\text{IV-12.A})$$

$$||\underline{e}|| \leq p + ||\underline{n}||_{\max} = s \quad (\text{IV-13.A})$$

(IV-13.A) gives an upper bound on the "steady-state" error, i.e. what is the smallest difference between plant and model states in the presence of noise. This is illustrated graphically in Figure IV-2(a,b,c).A. In (a) C is a typical phase plane trajectory. As long as C is outside the circle with radius p , then \dot{V} is p.d., \hat{V} is n.d. and the error continues to decrease. It may be, as shown in (b) that C may enter the circular region of radius p ; it is simply that in general, using (IV-10.A), nothing more than bounded stability with $||\hat{\underline{e}}|| < p$ can be made. (c) shows how (IV-10.A) provides an error band on the state $\underline{x}_p(t)$. This is similar to the $\pm 1\sigma$ limits used to describe probability accuracy bands for various states for systems corrupted by Gaussian noises, except that the error bands shown in dotted lines give the best "steady-state" tracking results which can be expected between the model and plant after a plant disturbance has occurred.

The error region given by (IV-13.A) will represent an upper limit for the worst-case condition. In general, the actual errors involved would most likely be much less. The form of the error bound in (IV-13.A)

leaves much room for interpretation of its meaning. This is because the error bound is on the norm of the total error vector, not an error bound on any individual error state. Consequently, an inexact procedure of weighting the errors, based on simulation or other external information, might need to be used to obtain an estimate of the proportion of the normed error bound due to any one state error.

Example:

Third order system in phase variable form corrupted by noise

From a priori information, it is known that the errors are apportioned approximately on the basis

$$e_1 \approx \frac{1}{3} e_{\text{norm}}$$

$$e_2 \approx \frac{2}{3} e_{\text{norm}}$$

$$e_3 \approx 0$$

$$e_{\text{norm}} = \sqrt{e_1^2 + e_2^2 + e_3^2}$$

From design information it is known that

$$\lambda(Q)_{\text{max}} = 1$$

$$\lambda(-A_m^T Q - Q A_m)_{\text{min}} = 4$$

$$\Gamma = .4$$

$$\underline{n}_{\max} = \begin{bmatrix} n_{1\max} \\ n_{2\max} \\ n_{3\max} \end{bmatrix} = \begin{bmatrix} .3 \\ .4 \\ 0 \end{bmatrix} \rightarrow \|\underline{n}\|_{\max} = .5$$

Using (IV-10.A) and (IV-13.A)

$$\|\underline{e}\|_{\max} = \frac{(1)}{(4)} (.4) + (.5) = .6 = e_{\text{norm}}$$

$$e_{1\max} \approx \pm .2$$

$$e_{2\max} \approx \pm .4$$

This shows that an indeterminacy band of ± 2 could be expected in e_1 and $\pm .4$ in e_2 as shown in Figure IV-3.A.

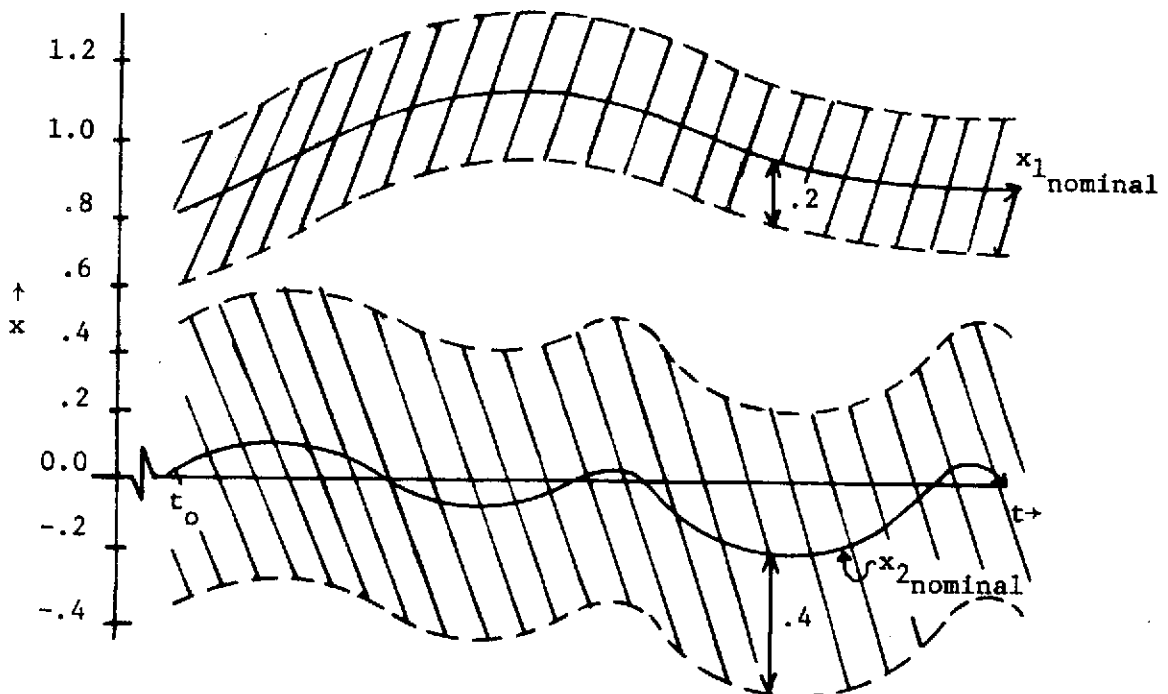


Figure IV-3.A. State Indeterminacy Due To Noise

Because the error bound with noise is given in terms of matrix related values, i.e. eigenvalues, no general relationship exists at present between a particular choice of a Q matrix for a given model and the resulting upper error bound given by (IV-10.A) and (IV-13.A). It is of course true that the largest eigenvalue of Q is a function of the magnitude of the elements of Q, but using small q_{ij} values to minimize $\lambda(Q)_{\max}$ in no way insures that $\lambda(-A_m^T Q - QA_m)_{\min}$ is large; it is the ratio which counts, not an individual term.

Although no general n^{th} order relationship exists for relating the choice of the Q elements to the resulting $\lambda(Q)_{\max}$ and $\lambda(-A_m^T Q - QA_m)_{\min}$ values, exact results for a 2^{nd} order case can be developed and will now be outlined.

Consider the general 2^{nd} order model

$$A_m = \begin{bmatrix} 0 & 1 \\ a_{21} & a_{22} \end{bmatrix} \quad \text{with } Q = \begin{bmatrix} q_{11} & q_{12} \\ q_{21} & q_{22} \end{bmatrix}$$

$a_{21}^m, a_{22}^m < 0$ for a stable model. It is desired to determine a relationship for expressing the ratio

$$\frac{\lambda(Q)_{\max}}{\lambda(-A_m^T Q - QA_m)} \quad (\text{IV-14.A})$$

as a function of model parameters and the adjustable q_{ij} elements.

To determine the eigenvalues of Q,

$$|\lambda I - Q| = \begin{vmatrix} \lambda - q_{11} & -q_{12} \\ -q_{21} & \lambda - q_{22} \end{vmatrix} = 0 \quad (\text{IV-15.A})$$

which reduces to the characteristic equation

$$\lambda^2 + \lambda(-q_{11} - q_{22}) + (q_{11}q_{22} - q_{12}^2) = 0$$

which has roots

$$\lambda_1, \lambda_2 = \frac{(q_{11} + q_{22}) \pm \sqrt{(q_{11} + q_{22})^2 - 4(q_{11}q_{22} - q_{12}^2)}}{2} \quad (\text{IV-16.A})$$

Dividing and multiplying by q_{22} , (IV-16.A) can be put in the form

$$\lambda_1, \lambda_2 = \frac{q_{22}}{2} \left[(1 + b) \pm \sqrt{(1 - b)^2 + 4a^2} \right] \quad (\text{IV-17.A})$$

where

$$a = \frac{q_{12}}{q_{22}} = \text{zero compensator location as given in (II-16.B)}$$

$$b = \frac{q_{11}}{q_{22}}$$

For Q to be p.d., both roots of (IV-17.A) must be positive, so the limiting case is for $\lambda_{\min} = 0$, or

$$(1 + b) = \sqrt{(1 - b)^2 + 4a^2} \quad (\text{IV-18.A})$$

which reduces to

$$b = a^2. \quad (\text{IV-19.A})$$

In general,

$$b > a^2 \quad (\text{IV-20.A})$$

Similarly, for $(A_m^T Q + QA_m)$,

$$A_m^T Q + QA_m = \begin{bmatrix} (2q_{12}a_{21}^m) & (q_{22}a_{21}^m + q_{11} + q_{12}a_{22}^m) \\ (q_{22}a_{21}^m + q_{11} + q_{12}a_{22}^m) & 2(q_{12} + q_{22}a_{22}^m) \end{bmatrix} \quad (\text{IV-21.A})$$

with the relation

$$A_m^T Q + QA_m = -C$$

where C is p.d., the eigenvalues of C are

$$|\lambda I - C| = \begin{vmatrix} (\lambda + 2q_{12}a_{21}^m) & (q_{22}a_{21}^m + q_{11} + q_{12}a_{22}^m) \\ (q_{22}a_{21}^m + q_{11} + q_{12}a_{22}^m) & \lambda + 2(q_{12} + q_{22}a_{22}^m) \end{vmatrix} \quad (\text{IV-22.A})$$

from which the characteristic equation is

$$\lambda^2 + \lambda(2q_{12} + 2q_{22}a_{22}^m + 2q_{12}a_{21}^m) + \left[4q_{12}^2a_{21}^m + 4q_{12}q_{22}a_{21}^ma_{22}^m - (q_{22}a_{21}^m + q_{11} + q_{12}a_{22}^m)^2 \right] = 0 \quad (\text{IV-23.A})$$

Solving for the roots of (IV-23.A) and rearranging terms,

$$\lambda_1, \lambda_2 = q_{22} \left\{ -(a + a_{22}^m + aa_{21}^m) \pm \left(\sqrt{(a + a_{22}^m + aa_{21}^m)^2} \dots \right. \right. \\ \left. \left. - \left[4a^2 a_{21}^m + 4aa_{21}^m a_{22}^m - (a_{21}^m + b + aa_{22}^m)^2 \right] \right) \right\} \quad (\text{IV-24.A})$$

Both (IV-17.A) and (IV-24.A) are similar in that the roots are a function of constants and ratio of q_{1j} elements, and the magnitude of q_{22} . It is the numerical value of q_{22} , then, that determines both sets of roots, given that an a and b have been picked.

From (IV-17.A),

$$\lambda(Q)_{\max} = \frac{q_{22}}{2} \left[(1 + b) + \sqrt{(1 - b)^2 + 4a^2} \right] \quad (\text{IV-25.A})$$

and from (IV-24.A)

$$\lambda(-A_m^T Q - QA_m)_{\min} = q_{22} \left\{ -(a + a_{22}^m + aa_{21}^m) - \right. \\ \left. \sqrt{(a + a_{22}^m + aa_{21}^m)^2} \dots \right. \\ \left. - \left[4a^2 a_{21}^m + 4aa_{21}^m a_{22}^m - (a_{21}^m + b + aa_{22}^m)^2 \right] \right\} \quad (\text{IV-26.A})$$

From (IV-25.A) and (IV-26.A), the desired ratio

$$\frac{\lambda(Q)_{\max}}{\lambda(-A_m^T Q - QA_m)_{\min}}$$

can now be formed,

$$\frac{\lambda(Q)_{\max}}{\lambda(-A_m^T Q - QA_m)_{\min}} = \frac{[(1+b) + \sqrt{(1-b)^2 + 4a^2}]}{2 \left\{ -(a + a_{22}^m + aa_{21}^m) + \sqrt{(a + a_{22}^m + aa_{21}^m)^2 - [4a^2 a_{21}^m + 4aa_{21}^m a_{22}^m - (a_{21}^m + b + aa_{22}^m)^2]} \right\}} \dots$$

$$\frac{\lambda(Q)_{\max}}{\lambda(-A_m^T Q - QA_m)_{\min}} = \frac{[(1+b) + \sqrt{(1-b)^2 + 4a^2}]}{2 \left\{ -(a + a_{22}^m + aa_{21}^m) + \sqrt{(a + a_{22}^m + aa_{21}^m)^2 - [4a^2 a_{21}^m + 4aa_{21}^m a_{22}^m - (a_{21}^m + b + aa_{22}^m)^2]} \right\}}$$

(IV-27.A)

For a given model, the ratio

$$\frac{\lambda(Q)_{\max}}{\lambda(-A_m^T Q - QA_m)}$$

may be plotted as a function of a with b as a parameter. Since for the case of the model in phase-variable form no information about q_{11} is available, in practice only a single curve with $b = \epsilon$, $\epsilon > 0$ is needed.

Lacking a general relationship for an n^{th} order system between the selection of the Q matrix and the error norm bound does not mean that nothing can be done. Using (IV-10.A) and (IV-13.A) for a particular choice of Q will supply a bound on the indeterminacy due to noisy states and inputs. If this bound is sufficiently small with respect to the range of values of states expected, then the given Q values should be sufficient. If not, a brief "trial-and-error" study of adjusting the Q matrix and determining the error bound from (IV-13.A) may provide an empirical relationship which may be used to home in on an acceptable Q matrix.

Example:

Given the 2nd order model

$$G_m(s) = \frac{2}{(s+1)(s+2)} \quad (\text{IV-28.A})$$

It is desired to determine the Q matrix in order to implement the adaptive gains for the plant

$$G_p(s) = \frac{2}{s^2 + a_{22}^p s + a_{21}^p} \quad (\text{IV-29.A})$$

Assuming there are large noises on the input and state measurements, a trade-off between the error transient response, as discussed in Chapter II, and the noise-present system, discussed in Chapter IV, is necessary. Placing the model in phase-variable form

$$A_m = \begin{bmatrix} 0 & 1 \\ -2 & -3 \end{bmatrix} \quad (\text{IV-30.A})$$

it is desired to determine

$$Q = \begin{bmatrix} q_{11} & q_{12} \\ q_{12} & q_{22} \end{bmatrix}$$

Using analysis and design procedures from Chapter II, the noise-free error transient response is determined by (using [6])

$$1 + k \frac{(s+a)(s+d)}{s(s^2 + 3s + 2)} = 0 \quad (\text{IV-31.A})$$

where

$$k = q_{22} K_2$$

$$a = \frac{q_{12}}{q_{22}}$$

$$d = \frac{K_1}{K_2}$$

and

$$0 < a < 3$$

Based on a noise-present design, given that the noise cannot be reduced it is important to minimize the effects of the noise. From (IV-10.A) and (IV-13.A), by minimizing the ratio

$$\frac{\lambda(Q)_{\max}}{\lambda(-A_m^T Q - QA_m)_{\min}} \quad (\text{IV-32.A})$$

the controllable effects of noise on the plant are optimized. Using (IV-27.A) with b as a parameter, Figure IV-4.A shows the relationship between (IV-32.A) and the choice of "a". As is evident from Figure IV-4.A, a trade-off between the desire for a large "a" for good transient response versus a small multiplier ratio as given in (IV-32.A). As a compromise, "a" = 1.5 was chosen. This results in the error root locus given in Figure IV-5.A.

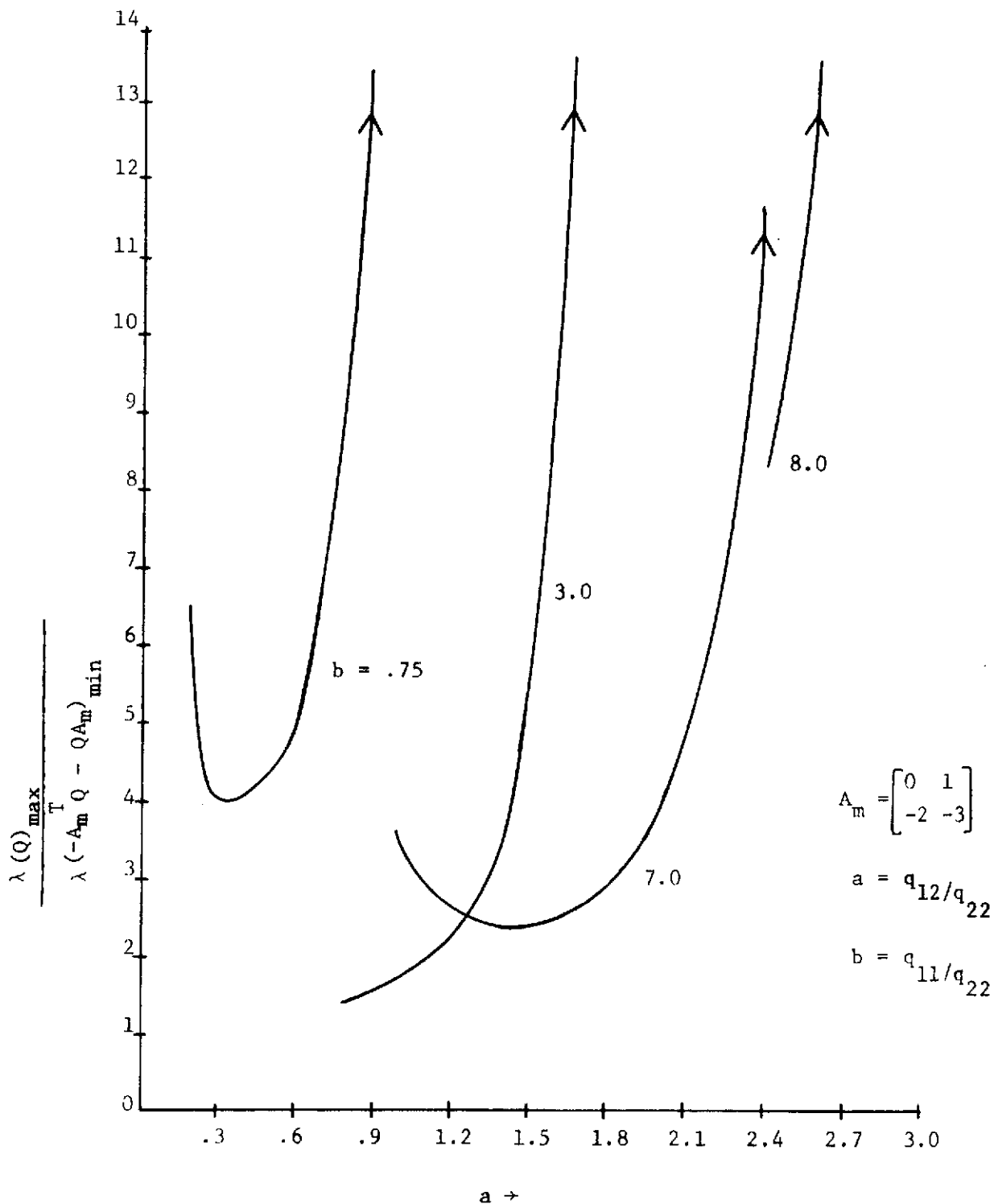


Figure IV-4.A. Relationship between $\frac{\lambda(Q)_{\max}}{\lambda(-A_m^T Q - QA_m)_{\min}}$ and "a" with "b" as a parameter.

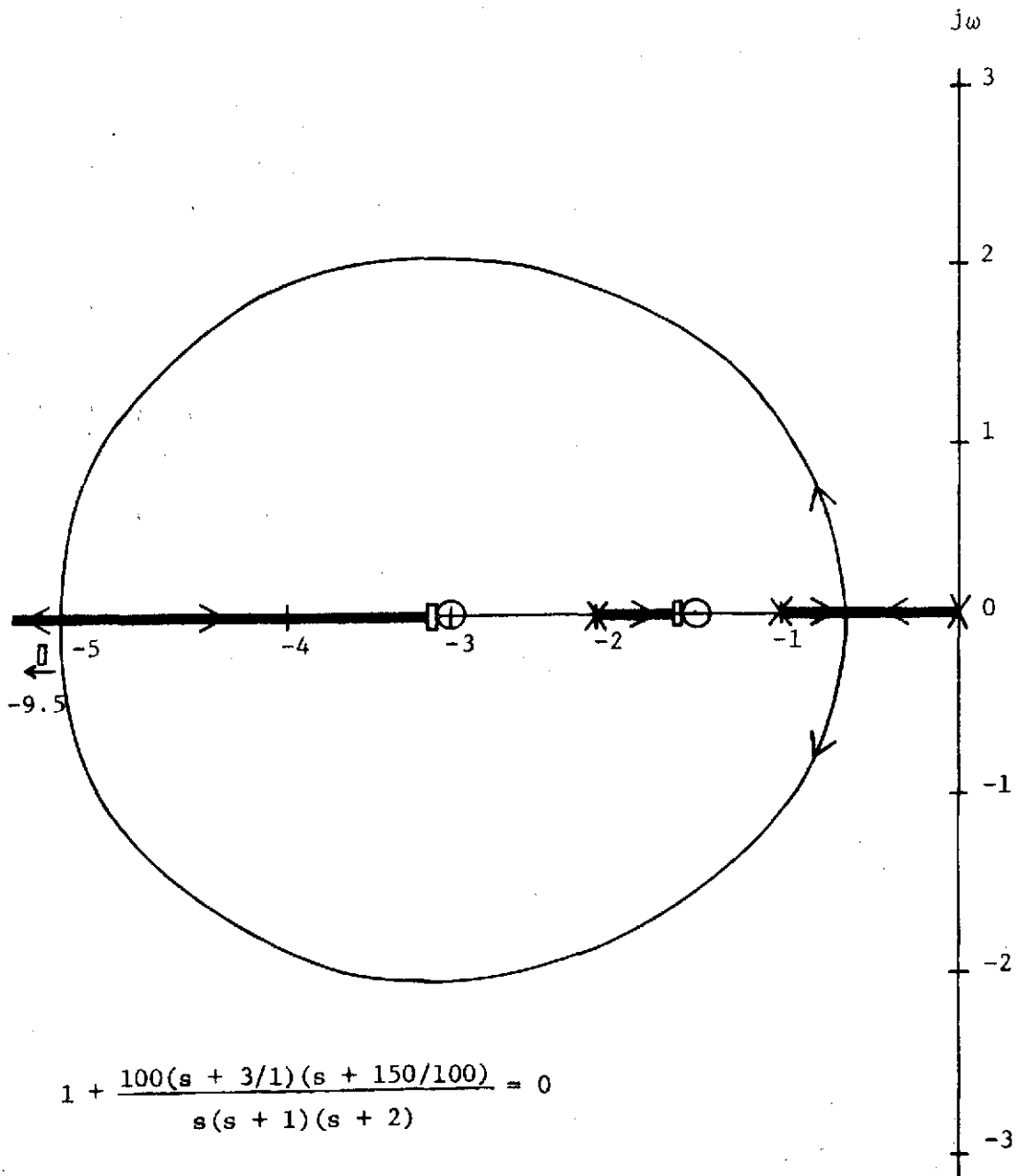


Figure IV-5.A Error Root Locus For Example With Stochastic Noise.

In Figure IV-6.A are shown the results for two runs with different noise combinations and these in turn are compared with a deterministic run. Using (IV-13.A) $||\underline{e}|| \approx .4$ assuming the error contributions are equal between e_1 and e_2 , the maximum error (e_1) should be less than .283, or about 5.6%. The actual results show the steady-state errors in two cases to be less than .025 with an input of $5\mu(t)$. The noises were correlated by passing Gaussian white signals through magnitude limited $\pm 3\sigma$, low-pass filters with 10 Hz bandwidths, where bandwidth is defined here to be the frequency range where $|G| > -60$ db (gain of 1/1000). This stringent requirement on the definition of bandwidth was chosen so that when some maximum value of the state noise rate, $\dot{\eta}$, was analytically determined then the resulting analytical bound would be accurately reflected in the actual error bound. $|\dot{\eta}_i|_{\max}$ is determined by

$$|\eta_i|_{\max} = 2\pi (\Delta f_i) |\eta_i|_{\max}, \quad i = 1, 2, \dots, n$$

where

Δf_i - bandwidth, Hz

$|\eta_i|_{\max}$ - maximum value

As would be expected, the actual error bounds were much less than the predicted ones.

B. Parametric Study of the Error Bound As a Function of the Noise Bounds

In this section, a form of sensitivity analysis will be performed in order to obtain relationships between changes in peak values in the

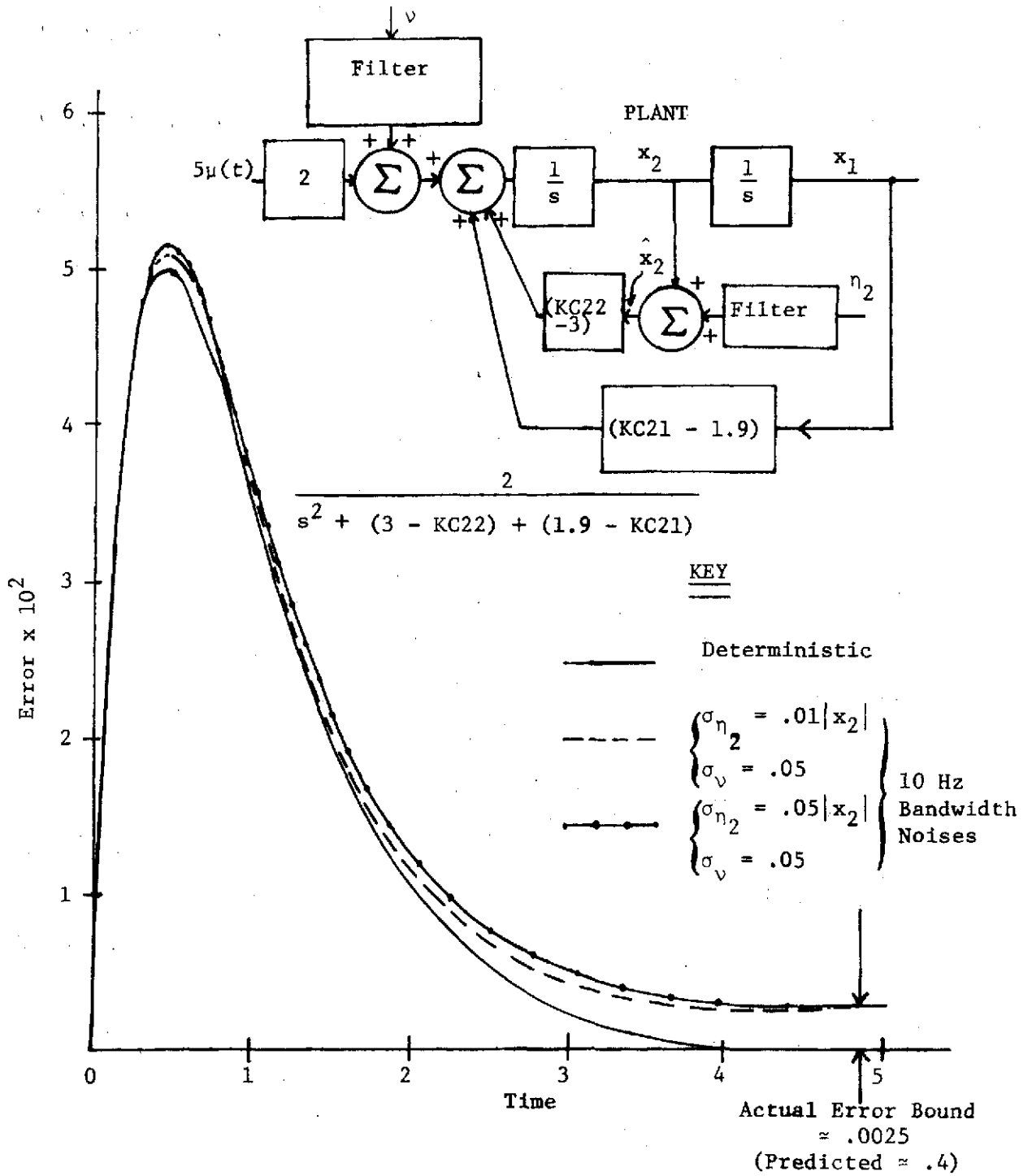


Figure IV-6. A. Adaptive Error Response With Stochastic Noise Present.

noise states, determined by the $\pm 3\sigma$ limits, to the normed error bound given in (IV-13.A),

$$\begin{aligned} \|\underline{e}\| \leq & \frac{\lambda(Q)_{\max}}{\lambda(-A_m^T Q - Q A_m)_{\min}} \left(2 \|\underline{A}_0 \underline{\eta} - \dot{\underline{\eta}} - B_m \underline{v}\|_{\max} \right) \\ & + \|\underline{\eta}\|_{\max} \end{aligned} \quad (\text{IV-1.B})$$

where the various terms are described in section A. The interest in this study comes from practical considerations wherein the noise statistics, i.e. mean and standard deviation, are often directly related to the type of hardware used in the controller. Such hardware would include type of measurement transducer, transducer mounting integrity, types of electrical shielding employed, amplifier linearities and drift (if analog hardware employed), number of bits and D/A, A/D accuracy (both time and magnitude) if digital implementation is used in the controller.

For purposes of this study, each noise source, either η_i or v_i may be depicted by a bound on its peak value, whether it be plus or minus. Thus if η_2 has a mean of 2 and σ of 1, its peak value could be considered to be 5 or -1, whichever maximizes (IV-1.B).

It is assumed that the Q matrix has been selected and is fixed and only changes in the noise statistics are to be considered. Consequently (IV-1.B) becomes

$$\|\underline{e}\|_{\max} = C y_1 + y_2 \quad (\text{IV-2.B})$$

where

$C = \text{constant}$

$$y_1 = 2 \left| \left| A_{o\underline{n}} - \dot{\underline{n}} - B_{\underline{m}\underline{v}} \right| \right|_{\max}$$

$$y_2 = \left| \left| \underline{n} \right| \right|_{\max}$$

$$\left| \left| \underline{a}_n \right| \right| = \sqrt{a_1^2 + a_2^2 + \dots + a_n^2}$$

Since A_o is in phase variable form, $A_{o\underline{n}}$ is in the particular form

$$A_{o\underline{n}} = \left[\eta_2, \eta_3, \dots, \eta_{n-1}, N \right]^T \quad (\text{IV-3.B})$$

where

$$N = (-a_n \eta_1 - a_{n-1} \eta_2, \dots, -a_1 \eta_n)$$

A_o in the form of \hat{A} in (II-15.B)

$\dot{\underline{n}}$ is determined by the band-limited nature of the noise, i.e.

$$\left| \dot{\eta}_{i_{\max}} \right| = 2\pi f_{\max} \left| \eta_{i_{\max}} \right| \quad (\text{IV-4.B})$$

where

$f_{\max} = \text{arbitrary frequency cut-off point}$

$\eta_{i_{\max}}$ determined by mean and 3σ limits

First, the case of no state noise, $\underline{\eta} = \underline{0}$ will be investigated.

With this restriction (IV-2.B) becomes

$$||\underline{e}||_{\max} = 2C ||\underline{B}_m \underline{v}||_{\max} \quad (\text{IV-5.B})$$

With \underline{B}_m in the form of \hat{B} given in (II-15.B),

$$||\underline{B}_m \underline{v}|| = \sqrt{(b_{11}v_1 + b_{12}v_2 + \dots + b_{1r}v_r)^2 + (b_{21}v_1 + b_{22}v_2 + \dots + b_{2r}v_r)^2 + \dots + (b_{n1}v_1 + b_{n2}v_2 + \dots + b_{nr}v_r)^2} \quad (\text{IV-6.B})$$

In order to determine the sensitivity of the error norm to any particular noise state, defining $||\underline{e}||_{\max} = e_{\text{norm}}$, the incremental change in the error norm is found as follows

$$\Delta e_{\text{norm}} = \left[\frac{\partial ||\underline{e}||_{\max}}{\partial v_1} \Delta v_{1\max} + \frac{\partial ||\underline{e}||_{\max}}{\partial v_2} \Delta v_{2\max} + \dots + \frac{\partial ||\underline{e}||_{\max}}{\partial v_r} \Delta v_{r\max} \right] \quad (\text{IV-7.B})$$

where

$$\frac{\partial ||\underline{e}||_{\max}}{\partial v_j} = \frac{C \sum_{i=1}^n b_{ij} (b_{i1}v_1 + b_{i2}v_2 + \dots + b_{ir}v_r)}{\sqrt{\sum_{i=1}^n (b_{i1}v_1 + b_{i2}v_2 + \dots + b_{ir}v_r)^2}} \quad (\text{IV-8.B})$$

$\Delta v_{j \max}$ - the incremental change in the peak value of the noise state v_j (determined by the mean and standard deviation)

Often the relative change, in %, of the error is important and this is determined as in (IV-7.B):

$$\frac{\Delta e_{\text{norm}}}{e_{\text{norm}}} = \sum_{j=1}^r \left[\frac{\partial ||e||_{\text{max}}}{\partial v_j} \cdot \frac{\Delta v_j}{e_{\text{norm}}} \right] \quad (\text{IV-9.B})$$

where e_{norm} is computed at the nominal noise state values.

Example:

An increase in σ of 1.0 for all noises is contemplated as it has been determined that by doing so electrical cable shielding costs can be reduced by 50%. It is desired to determine the maximum expected increase in error due to this change.

The existing conditions are as follows

$$B_m = \begin{bmatrix} 0 & 0 \\ 2 & 3 \end{bmatrix} = \begin{bmatrix} b_{11} & b_{12} \\ b_{21} & b_{22} \end{bmatrix}$$

$$\underline{v} = \begin{bmatrix} v_1 \\ v_2 \end{bmatrix}$$

$$v_1: \mu: \text{mean} = 0. \quad \sigma = 1.0$$

$$v_2: \text{mean} = 1.0 \quad \sigma = .5$$

$$C = .005$$

Using (IV-5.B), e_{norm} before the change is

$$e_{\text{norm}} = (2) (.005) \begin{bmatrix} 0 \\ (2v_1 + 3v_2) \end{bmatrix} \max \begin{bmatrix} v_{1\text{max}} \\ v_{2\text{max}} \end{bmatrix} = \begin{bmatrix} 3 (\mu_1 + 3\sigma_1) \\ 2.5 (\mu_2 + 3\sigma_2) \end{bmatrix}$$

$$e_{\text{norm}} = .135$$

Using (IV-7.B) the change in e_{norm} due to changes in σ_1 and σ_2 is

$$\Delta e_{\text{norm}} = (C) \frac{b_{21}(b_{21}v_1 + b_{22}v_2)\Delta v_1 + b_{22}(b_{21}v_1 + b_{22}v_2)\Delta v_2}{\sqrt{(b_{21}v_1 + b_{22}v_2)^2}} \quad (\text{IV-10.B})$$

$$\Delta e_{\text{norm}} = (.005) \frac{2(2(3) + 3(2.5))(3) + 3(2(3) + 3(2.5))(B)}{2(3) + 3(2.5)}$$

$$\Delta e_{\text{norm}} = \underline{.075}$$

Using (IV-9.B) the relative error increase is

$$\frac{\Delta e_{\text{norm}}}{e_{\text{norm}}} = \frac{.075}{.135} = \underline{55.5\% \text{ increase}}$$

This means that the new error bounds would be $\pm .21$. Assuming that the control system were part of an attitude control system of a spacecraft, this could mean that as an upper bound on the position accuracy, e_{norm} before the change was such that the error was $\pm 7.7^\circ$ ($57.3^\circ/\text{rad}$) and after the change was 12.1° , an intolerable situation. Depending on how the errors are "weighted" (shown here all the error was assumed

due to e_{position}), the contemplated change could possibly result in extremely sloppy position accuracy.

Now, the case of both state and input noise will be considered, i.e. $\underline{n} \neq 0$, $\underline{v} \neq 0$. The results will be found to be similar to (IV-2.B) thru (IV-9.B), although more involved. A sensitivity relationship for the error is developed similar to (IV-7.B)

$$\begin{aligned} \Delta e_{\text{norm}} = & \left[\frac{\partial e_{\text{norm}}}{\partial \eta_1} \Delta \eta_{1\text{max}} + \frac{\partial e_{\text{norm}}}{\partial \eta_2} \Delta \eta_{2\text{max}} + \dots + \frac{\partial e_{\text{norm}}}{\partial \eta_n} \Delta \eta_{n\text{max}} \right] \\ & + \left[\frac{\partial e_{\text{norm}}}{\partial \dot{\eta}_1} \Delta \dot{\eta}_{1\text{max}} + \frac{\partial e_{\text{norm}}}{\partial \dot{\eta}_2} \Delta \dot{\eta}_{2\text{max}} + \dots + \frac{\partial e_{\text{norm}}}{\partial \dot{\eta}_n} \Delta \dot{\eta}_{n\text{max}} \right] + \\ & + \left[\frac{\partial e_{\text{norm}}}{\partial v_1} \Delta v_{1\text{max}} + \frac{\partial e_{\text{norm}}}{\partial v_2} \Delta v_{2\text{max}} + \dots + \frac{\partial e_{\text{norm}}}{\partial v_r} \Delta v_{r\text{max}} \right] \end{aligned} \quad (\text{IV-11.B})$$

The partial derivatives can be determined by expanding (IV-1.B); from it,

$$\Gamma = \left\| \left| A_0 \underline{n} - \dot{\underline{n}} - B_m \underline{v} \right| \right\|_{\text{max}} = \left\| \begin{bmatrix} \eta_2 \\ \eta_3 \\ \vdots \\ \eta_n \\ -a_n \eta_1 - a_{n-1} \eta_2 \\ \dots - a_1 \eta_n \end{bmatrix} - \begin{bmatrix} \dot{\eta}_1 \\ \dot{\eta}_2 \\ \vdots \\ \dot{\eta}_n \end{bmatrix} - B_m \underline{v} \right\|$$

$$\Gamma = \sqrt{\left[\eta_2 - \dot{\eta}_1 - (b_{11}v_1 + b_{12}v_2 + \dots + b_{1r}v_r) \right]^2 + \left[\eta_3 - \dot{\eta}_2 - (b_{21}v_1 + b_{22}v_2 + \dots + b_{2r}v_r) \right]^2 + \dots + \left[\eta_n - \dot{\eta}_{n-1} - (b_{(n-1)1}v_1 + b_{(n-1)2}v_2 + \dots + b_{(n-1)r}v_r) \right]^2 + \left[(-a_n\eta_1 - a_{n-1}\eta_2 - \dots - a_1\eta_n) - \dot{\eta}_n - (b_{n1}v_1 + b_{n2}v_2 + \dots + b_{nr}v_r) \right]^2}$$

(IV-12.B)

also

$$\|\underline{\eta}\| = \sqrt{\eta_1^2 + \eta_2^2 + \dots + \eta_n^2}$$

(IV-13.B)

$$\frac{\partial e_{\text{norm}}}{\partial \eta_j} = \left\{ \begin{array}{l} c \left[\eta_j - \dot{\eta}_{j-1} - (b_{j1}v_1 + b_{j2}v_2 + \dots + b_{jr}v_r) \right] \\ -a_{n-j+1} \left[-a_n\eta_1 - a_{n-1}\eta_2 - \dots - a_1\eta_n - \dot{\eta}_n - (b_{n1}v_1 + b_{n2}v_2 + \dots + b_{nr}v_r) \right] \\ \hline \Gamma_{\text{nominal}} \end{array} \right\} \quad \text{if } j=2,3, \dots, n$$

$$\left\{ \begin{array}{l} c \left[-a_n \right] \left[(-a_n\eta_1 - a_{n-1}\eta_2 - \dots - a_1\eta_n) - \dot{\eta}_n - (b_{n1}v_1 + b_{n2}v_2 + \dots + b_{nr}v_r) \right] \\ \hline \Gamma_{\text{nominal}} \end{array} \right\} \quad \text{if } j=1$$

(IV-14.B)

$$\frac{\partial e_{\text{norm}}}{\partial \dot{\eta}_j} = \begin{cases} \frac{[-c \eta_{j+1} - \dot{\eta}_j - (b_{j1}v_1 + b_{j2}v_2 + \dots + b_{jr}v_r)]}{\Gamma_{\text{nominal}}} & \text{if } j=1,2, \dots (n-1) \\ \frac{[-c (-a_n \eta_1 - a_{n-1} \eta_2 - \dots - a_1 \dot{\eta}_n) - \dot{\eta}_n - (b_{n1}v_1 + b_{n2}v_2 + \dots + b_{nr}v_r)]}{\Gamma_{\text{nominal}}} & \text{if } j=n \end{cases} \quad (\text{IV-15.B})$$

$$\frac{\partial e_{\text{norm}}}{\partial v_j} = c \left\{ \sum_{i=1}^{n-1} \left[\eta_{i+1} - \dot{\eta}_i - (b_{i1}v_1 + b_{i2}v_2 + \dots + b_{ir}v_r) \right] \cdot (-b_{ij}) \right\} + \left[(-a_n \eta_1 - a_{n-1} \eta_2 - \dots - a_1 \dot{\eta}_n) - \dot{\eta}_n - (b_{n1}v_1 + b_{n2}v_2 + \dots + b_{nr}v_r) \right] \cdot (-b_{nj}) \left\{ \frac{\Gamma_{\text{nominal}}}{\Gamma_{\text{nominal}}} \right\} \quad \text{if } j=1,2, \dots r$$

where Γ_{nominal} is found by evaluating (IV-12.B) at the nominal operating condition (before a change occurs). Similarly as in (IV-9.B), a relative or % change in e_{norm} can be determined by dividing both sides of (IV-11.B) by e_{norm} evaluated at the nominal value. Inasmuch as (IV-11.B) thru (IV-16.B) appear so formidable, an example will be provided to illustrate their implementation in a practical problem.

Example:

The effect of using a new tracking radar system for altitude determination is being studied to determine what gross improvement in positional accuracy can be obtained. The system is to be part of a satellite launching missile inertial guidance system. From a study of the overall system, it has been determined that the standard deviation of position error can be reduced by half, although the new system costs 50% more than the old unit. The reduction in the overall error bound is desired to be found.

The basic missile information is as follows:

$$\begin{aligned} \dot{\underline{x}}_m &= \begin{bmatrix} 0 & 1 \\ -6 & -5 \end{bmatrix} \underline{x}_m + \begin{bmatrix} 0 \\ 1 \end{bmatrix} u && \text{Model} \\ \dot{\underline{x}}_p &= \begin{bmatrix} 0 & 1 \\ -4 & -5 \end{bmatrix} \underline{x}_p + \begin{bmatrix} 0 \\ 1 \end{bmatrix} u && \text{"Worst-case" plant} \end{aligned} \quad (\text{IV-17.B})$$

$u = 10^6 (1 - e^{-.005t})$, where u is to place the missile in a 10^6 feet (≈ 200 mile) high orbit.

$C = 1.4$ from a priori design of the Q matrix

Noise Statistics

$$v: \mu = 0, \sigma_v = 333.0 \text{ ft.}$$

$$\underline{\eta}: \mu_{\eta_1} = 0, \sigma_{\eta_1} = 1800 \text{ ft.}$$

$$\mu_{\eta_2} = 10 \text{ ft./sec.}, \sigma_{\eta_2} = 100 \text{ ft./sec.}$$

$$\begin{aligned} \dot{\eta}_1 &: \text{Bandwidth} \approx 0 \text{ Hz.} \\ \dot{\eta}_2 &: \text{Bandwidth} \approx 10 \text{ Hz.} \end{aligned}$$

The plant-model dynamics and the additive noises are shown in flow diagram of Figure IV-1.B. The basic earth-to-orbit configuration for the missile is shown in Figure IV-12.B.

Using (IV-12.B),

$$\begin{aligned} \Gamma_{\text{nominal}} &= \sqrt{310 - (=0) - (0)^2 + \left[(-4)(5400) - 5(+10 + 300) - 2\pi(10)(310) - 1000\right]^2} \\ &\approx 43,650 \end{aligned}$$

Using (IV-14.B),

$$\begin{aligned} \frac{\partial e_{\text{norm}}}{\partial \eta_1} &= \frac{(1.4)(-4) \left[(-4)(5400) - 5(310) - 2\pi(10)(310) - (1000)\right]}{\Gamma_{\text{nom}}} \\ &\approx 5.6 \end{aligned}$$

Using (IV-15.B)

$$\begin{aligned} \frac{\partial e_{\text{norm}}}{\partial \dot{\eta}_2} &= \frac{(1.4) \left[(-4)(5400) - 5(310) - 2\pi(10)(310) - (1)(1000)\right]}{\Gamma_{\text{nom}}} \\ &\approx 1.4 \end{aligned}$$

Using (IV-16.B)

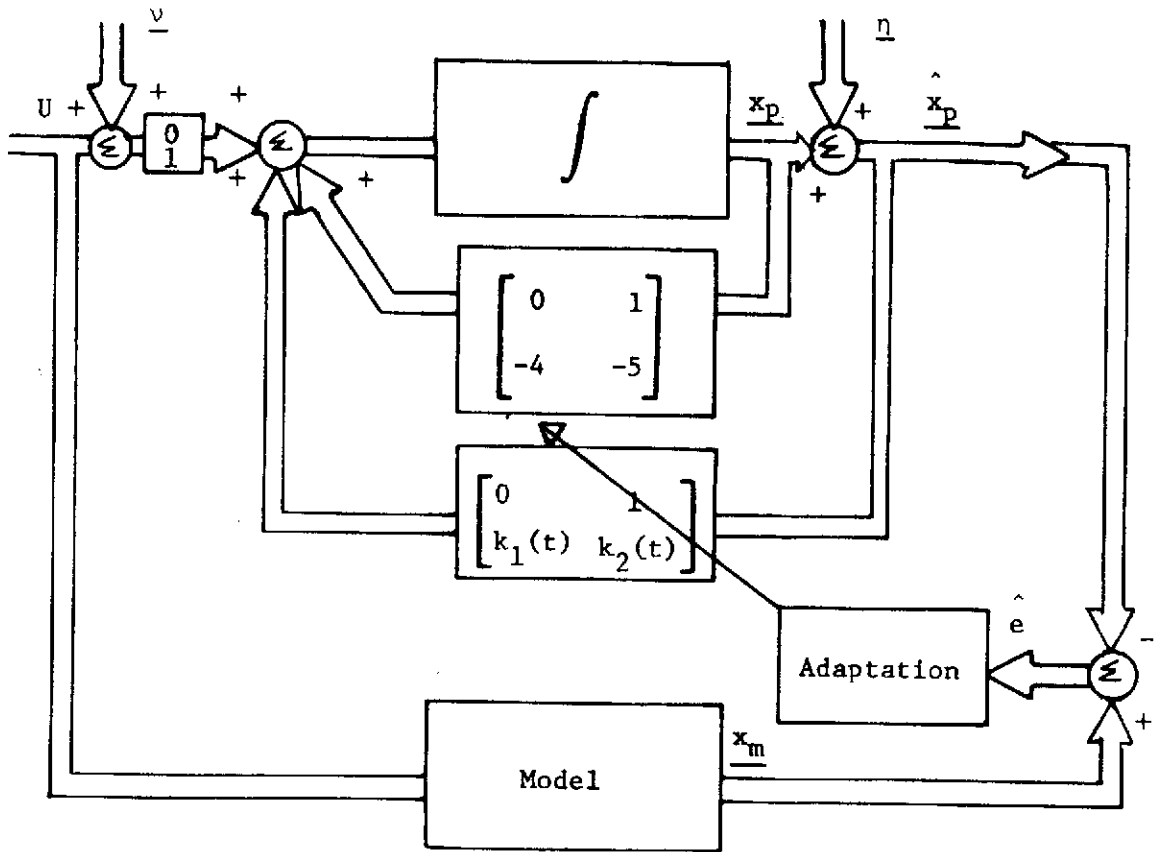


Figure IV-1.B. Model-Plant Layout for Example

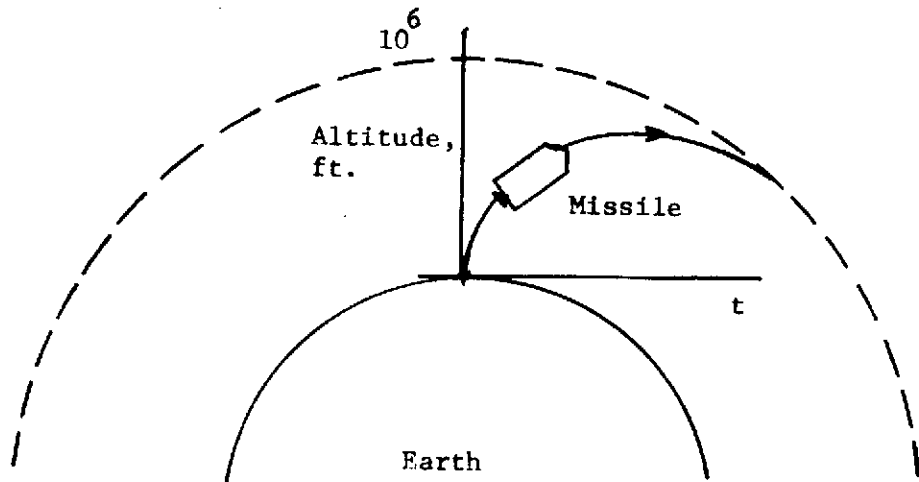


Figure IV-2.B. Earth to orbit Configuration for System in Figure IV-1.B.

$$\frac{\partial e_{\text{norm}}}{\partial v_1} \approx 1.4$$

With only η_1 improved,

$$\Delta e_{\text{norm}} = \frac{\partial e_{\text{norm}}}{\partial \eta_1} (\Delta \eta_1)$$

$$\Delta e_{\text{norm}} = (5.6)(-2700) = -15,100$$

Using (IV-2.B), the new e_{norm} is

$$e_{\text{norm}} = (1.4)(43,650) + \sqrt{(5400)^2 + (310)^2} - 15,100$$

$$\underline{e_{\text{norm}} \approx 51,300}$$

Assuming the error contributions to the error norm are proportional to the state noise standard deviations, the error in altitude measurement is improved from 62,800 ft. down to 48,400 ft.

Adding a new radar unit may necessitate a new computer and wiring system, resulting in σ_v increasing by 10% and σ_{η_2} by 5%, in which case

$$\Delta e_{\text{norm}} = \frac{\partial e_{\text{norm}}}{\partial \eta_1} (\Delta \eta_1) + \frac{\partial e_{\text{norm}}}{\partial \eta_2} (\Delta \eta_2) + \frac{\partial e_{\text{norm}}}{\partial v_1} (\Delta v_1) \quad (\text{IV-18.B})$$

$$\Delta e_{\text{norm}} = -15,100 + (1.4)(100) + (1.4)(2\pi)(15)(10) \approx \underline{-13,640}$$

which results in very little change in the error distribution from before.

C. Incomplete Adaptation and State Feedback

In many situations it may not be practical or possible to measure all the states of a system, or the available signals may be too noisy to use for feedback to the adaptive controller. In such cases incomplete state feedback, incomplete plant adaptation, replacement of certain plant states with model states, and state estimation are some of the remedies. However, the theoretical problems of stability then arise because, in most cases of the Lyapunov-designed type controllers discussed, the theory required all plant terms adapting and all plant states available. Any changes in the requirements of the states requires an analysis of the Lyapunov V and \dot{V} functions to ascertain stability. It should be pointed out that when developing adaptive controllers according to Lyapunov theory, modern stability theory such as the Circle criterion and Popov Criterion cannot be used directly on the plant but instead investigation of the V and \dot{V} functions and application of the Lyapunov stability theorems must be employed. Also, any results obtained will be a statement of fact or an overstatement of fact. The latter is because sufficient but not necessary conditions are obtained with Lyapunov theory.

In the case of incomplete adaptation, some work has been performed to determine bounds on the norm of the error. Results, however, are scarce.

For the adaptive rule in [5], an upper bound on the norm of the error has been developed [10] for a special case. Consider the single-input single-output system

$$\dot{\underline{x}}_p = A_p \underline{x}_p + B_p u + C_p r \quad (\text{plant}) \quad (\text{IV-1.C})$$

$$\dot{\underline{x}}_m = A_m \underline{x}_m + B_m u \quad (\text{model})$$

$$\underline{e} = \underline{x}_m - \underline{x}_p \quad (\text{error})$$

where

$$A_p = \begin{bmatrix} 0 & & I_{(n-1)} \\ a_{n1} & \dots & a_{nn} \end{bmatrix} \quad B_p = \begin{bmatrix} 0 \\ 0 \\ \vdots \\ b_n \end{bmatrix} \quad C_p = \begin{bmatrix} 0 \\ 0 \\ \vdots \\ c_n \end{bmatrix}$$

are constant unknown parameters

\underline{x} is an $n \times 1$ vector

r is a scalar input

u is an adaptive feedback signal

Using (IV-1.C),

$$\dot{\underline{e}} = A_m \underline{e} + \Delta \underline{x}_p + \delta r - B_p u \quad (\text{IV-2.C})$$

where

$$\Delta = \begin{bmatrix} \phi & & & \\ \delta_{n1} & \delta_{n2} & \dots & \delta_{nn} \end{bmatrix} = (A_m - A_p)$$

$$\delta = \begin{bmatrix} 0 \\ 0 \\ \vdots \\ \delta_n \end{bmatrix} = (B_m - C_p)$$

When all plant parameters are not adjusted, an upper bound on the norm of the error is

$$\| \underline{e} \| \leq \frac{\lambda(Q)_{\max}}{\lambda(Q)_{\min}} \left\{ \frac{2 \sqrt{n} \bar{q}_{in}^m |\bar{\delta}_{ni}| |\tilde{x}_{mi}| + |\bar{\delta}_n| |\tilde{r}|}{1 - 2 \sqrt{nm} \bar{q}_{in} |\bar{\delta}_{ni}|} \right\} \quad (\text{IV-3.C})$$

and $(1 - 2 \sqrt{nm} \bar{q}_{in} |\bar{\delta}_{ni}|) > 0$ is a sufficient condition for a region R_e guaranteeing boundedness of the tracking error. Where

$\lambda(Q)_{\max}, \lambda(Q)_{\min}$ are the maximum and minimum eigenvalues of Q (see Chapter II)

$$\bar{q}_{in} = \max_i \left\{ q_{in} \text{ of unadapted parameters } i \right\}$$

$$|\tilde{h}_i| = \max_{i,t} |h_i(t)|$$

$m =$ number of unadapted plant terms a_{ni} ; $m \leq n$

If there is complete adaptation then $m = 0$ and δ_n does not appear in (IV-3.C). Then $\| \underline{e} \| = 0$ in steady state and the error is asymptotically stable in \underline{e} .

In another study [9], a different adaptation rule was used than the one previously discussed and sufficient conditions developed to guarantee asymptotic stability when all of the plant states are replaced by corresponding model states. In general, results are scarce however.

D. An Adjustment Technique For Obtaining Time-Invariant Error Dynamics

In Chapter II a design procedure for selecting the various adaptive gain parameters for a class of model-reference systems was outlined.

This technique required that step inputs only be applied to the system, a severe restriction in terms of practical utility. However, simulation results have shown that for slowly time-varying inputs the method does have some design utility. In this section an appropriate modification is offered to obtain fixed error dynamics despite a wide range of input values. The method still guarantees asymptotic stability of the system error because all of the original Lyapunov stability conditions are maintained.

As given in Chapter II, the basic perturbed error characteristic equation is

$$1 + \frac{\left[\sum_{j=1}^n q_{jn} s^{j-1} \right] \left[\sum_{i=p}^p K_i s^{i-1} \right]}{s \Delta_m(s)} = 0 \quad (\text{II-16.B})$$

Similar to (II-11.B) and (II-16.B) it can be shown that, before substituting model states for plant states and setting $x_{jm}^0 = 0$, $j = 2, 3, \dots, n$, the lumped gains K_1 are of the form

$$\begin{aligned} K_1 &= \sum_{i=1}^n \left[\alpha_{ni} x_{ip}(t)^2 \right] + \sum_j^{\ell} \left[\psi_j(\gamma) U_j(t)^2 \right] \\ K_2 &= \sum_{i=1}^n \left[\beta_{ni} x_{ip}(t)^2 \right] + \sum_j^{\ell} \left[\psi_j(\delta) U_j(t)^2 \right] \\ K_3 &= \sum_{i=1}^n \left[\rho_{ni} x_{ip}(t)^2 \right] + \sum_j^{\ell} \left[\psi_j(\sigma) U_j(t)^2 \right] \end{aligned} \quad (\text{IV-1.D})$$

where

$\Psi_j \left((\cdot) \right)$ - represent a sum of terms of (\cdot) ; adaptive gain constant for j^{th} adapted input

x_{jm}^0 - represent steady state operating conditions on which the derivation is predicated

\sum_j^ℓ - means a sum of ℓ terms not necessarily in consecutive order (only adapted terms of B_ρ appear here)

U_j - j^{th} input

$\ell \leq r$, the number of inputs

and it has been assumed that $x_{ip}(t)$, $U_j(t)$ are functions of time. Note that for constant inputs the K_i in (IV-1.D) reduce to those expressions given in Chapter II, (IV-1.D) being a more general case. Factoring, the numerator of (II-16.B) becomes

$$\left[\sum_{j=1}^n q_{jn} s^{j-1} \right] \left[\sum_{k=1}^p K_i s^{i-1} \right] = k \prod_{i=1}^v (s + Z_i) \quad (\text{IV-2.D})$$

where

$v \leq n + 1$ (depends on type of adaptation)

Z_i - zero compensator location

k - root locus gain

(II-16.B) then becomes

$$1 + \frac{k \prod_{j=1}^v (s + Z_j)}{s \Delta_m(s)} = 0 \quad (\text{IV-3.D})$$

The Z_i are functions of the ratios of q_{in}/q_{nn} $i = 1, 2, \dots, n$ and of the

ratios K_1/K_2 , K_2/K_3 , etc. The root locus gain k is a function of q_{nn} and K_h

$$k = q_{nn} K_h$$

where K_h is either K_1 , K_2 , or K_3 depending on the adaptation method. The design theory says that, for a given set of constant inputs U_i^0 , there will be a set of error poles determined by (II-16.B) which tend to describe the error dynamics. For different input magnitudes, k will change and the closed loop roots will move along a fixed locus. Since the U_i 's are used to drive the system and will not be known a priori, the resulting K_h will vary in an unknown manner, determined by x_{ip} and the U_i . If it were possible to keep the closed loop error roots fixed while K_h varied, then time-invariant error dynamics would result.

There are two means of obtaining this result, both of which are illustrated in Figure IV-1.D. In (a) is shown a single set of loci, determined by the placement of the zeroes of (IV-2.D). Since K_h varies, if q_{nn} could be adjusted to keep in inverse proportion to K_h , then as long as the ratios q_{ij}/q_{nn} stayed constant, the closed loop poles would remain stationary on a fixed set of loci since k would remain constant. A second technique would allow for varying q_{ij} (and $\frac{\alpha}{\beta}$ type) ratios and magnitudes in order to keep the closed loop error roots as a solution of the root locus of some configuration of the form in (II-16.B). In order to effect this, some sort of "pseudo-identification" technique would be required to ascertain where the open-loop zeroes should be

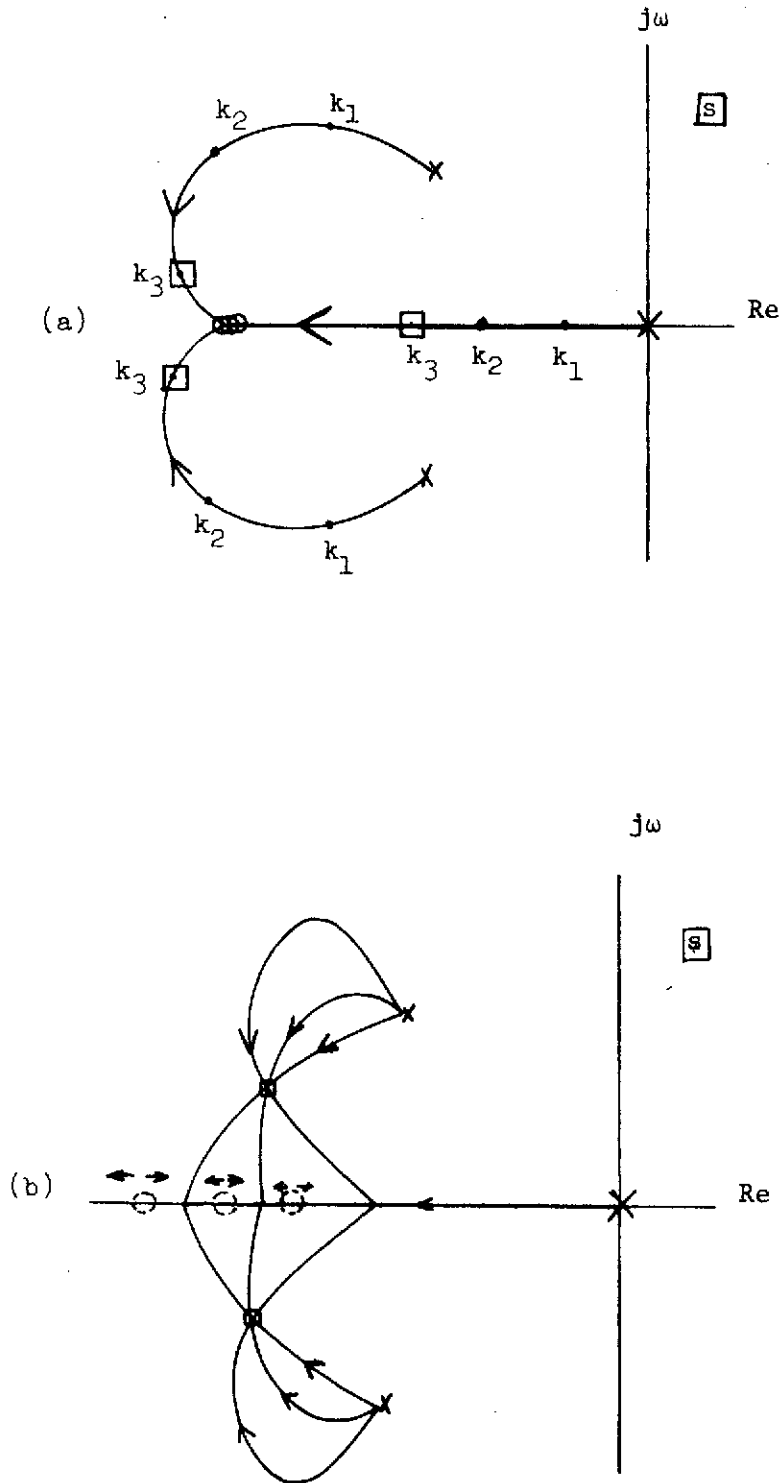


Figure IV-1.D. Two Means of Keeping Fixed Closed-Loop Error Dynamics
 (a) Keep the Zeros and Gain Constant (b) Vary the Zeros and Gain to Keep Roots Fixed.

located in order for the closed-loop error poles to be a valid solution of the loci.

The first of the two techniques is of interest here, both from a practical as well as theoretical standpoint. To illustrate why the second method is not a practical approach, a brief example will be given illustrating how the solutions of Figure IV-1.D were obtained.

Example:

$$1 + \frac{k(s+a)(s+b)(s+c)}{s\Delta_m(s)} = 0 \quad (\text{IV-4.D})$$

$$\Delta_m(s) = s^2 + 2s + 2$$

It is desired to force the closed-loop error roots to be at

$$p_1 = -4 \quad p_2 = -6.449 \quad p_3 = -1.551 \quad (\text{IV-5.D})$$

To do this it is necessary for (IV-4.D) to be the roots of

$$s^3 + \left(\frac{2 + ka + kb + kc}{1 + k} \right) s^2 + \left(\frac{2 + kab + kac + kbc}{1 + k} \right) s + \left(\frac{abc}{1 + k} \right) = 0 \quad (\text{IV-6.D})$$

where for this example two of the three zeroes in (IV-4.D) are due to ratios of α , β , ρ , γ , δ , and σ . Either one or more of the zeroes a , b , c must then be determined in order to keep (IV-4.D) as solutions to (IV-5.D) as k varies. The a , b , c can be found by iterative solution,

$$s^3 + ps^2 + qs + r = 0$$

$$a_{11} = \frac{1}{3} (3q - p^2) \qquad a_{12} = \frac{1}{27} (2p^3 - 9pq + 27r)$$

$$\frac{a_{12}^2}{4} + \frac{a_{11}^3}{27} < 0 \text{ for 3 real unequal roots}$$

$$A = \sqrt[3]{\frac{-a_{12}}{2} + \sqrt{\frac{a_{12}^2}{4} + \frac{a_{11}^3}{27}}} \qquad B = \sqrt[3]{\frac{-a_{12}}{2} - \sqrt{\frac{a_{12}^2}{4} + \frac{a_{11}^3}{27}}} \quad (\text{IV-7.D})$$

$$\left. \begin{aligned} s_1 &= A + B + \frac{p}{3} \\ s_2 &= \left\{ -\left(\frac{A+B}{2}\right) + \frac{p}{3} \right\} + j\left(\frac{A+B}{2}\right)\sqrt{3} \\ s_3 &= \left\{ -\left(\frac{A+B}{2}\right) + \frac{p}{3} \right\} - j\left(\frac{A+B}{2}\right)\sqrt{3} \end{aligned} \right\} \quad (\text{IV-8.D})$$

By computing k , a , b , and c are determined such that (IV-6.D) are equal to (IV-4.D). It is clear the technique requires an iterative non-linear technique to obtain a set of possibly non-unique zeroes a , b , c .

Complexity and computation time are severe drawbacks to this technique.

A more straightforward adjustment method is the first one discussed. It will be shown to involve a straightforward algebraic technique suitable for on-line computer use.

Using linear design techniques, an appropriate root locus gain k may be selected to obtain an acceptable transient error response. This gain in turn fixes the closed-loop error pole locations. Since $K_h(t)$ varies with the inputs, in order to keep k constant then q_{nn} must vary inversely to $K_h(t)$

$$q_{nn}(t) = \frac{k_{\text{desired}}}{K_h(t)} \quad (\text{IV-9.D})$$

where K_h is K_1 , K_2 or K_3 depending on the adaptation method. Since $x_{i_m}(t)$, $U_j(t)$ must be available to implement the basic adaptive gain equations, and the ψ_i are a priori fixed, then there is no difficulty with physical realizability of (IV-9.D), where K_h is given in (IV-1.D).

The case when K_h is zero, the regulator problem when all U_j are zero, must be considered. In this case (IV-9.D) would become singular and $q_{nn} = \infty$ would result, an impossible situation. A simple means of skirting this problem is to place a saturation operation so (IV-9.D) is replaced by

$$q_{nn}(t) = \frac{kd}{K_h(t)} \text{ sat}(q_s) \quad (\text{IV-10.D})$$

where q_s is an upper limit on q_{nn} , occurring at a value of $K_h = \epsilon$, $\epsilon > 0$. The limiting values of ϵ and q_s would be determined by the type of computational hardware employed.

Since the zeroes of (II-16.B) depend on the ratios

$$\frac{q_{jn}}{q_{nn}} \quad j = 1, 2, \dots, (n-1)$$

then if q_{nn} varies the q_{jn} must be altered also to keep the zeroes (due to the Q ratios) fixed. From (IV-2.D), the polynomial expansion is

$$q_{nn} \left(s^{n-1} + \frac{q_{n(n-1)}}{q_{nn}} s^{n-2} + \dots + \frac{q_{n1}}{q_{nn}} \right) \quad (\text{IV-11.D})$$

Defining the ratios as

$$\frac{q_{jn}}{q_{nn}} = a_j \quad j = 1, 2, \dots (n-1)$$

which are a priori chosen, then the necessary adjustment rule for the q_{ij} would be

$$q_{jn} = a_j q_{nn} \quad j = 1, 2, \dots (n-1) \quad (\text{IV-12.D})$$

The original Lyapunov theory on which the adaptive control theory discussed is based assumes Q is constant, so to insure this a sampled data adjustment law employing a zero-order hold for (IV-1.D) and (IV-10.D) is proposed. In this way, at any given instant the system will "see" only constant terms for the Q elements. The adjustment rules then become

$$K_h(kT) = \sum_{i=1}^n \Gamma_{ni} x_{im}(kT) + \sum_j^{\ell} \psi_j(\cdot) U_j(kT) \quad (\text{IV-13.D})$$

$$q_{nn}(kT) = \frac{k_d}{K_h(kT)} \text{sat}(q_s) \quad (\text{IV-14.D})$$

where

$k = 1, 2, \dots$ sample instants

$T =$ sample period, $\frac{1}{f}$

k_d - desired root locus gain value

q_s - saturation value for q_{nn}

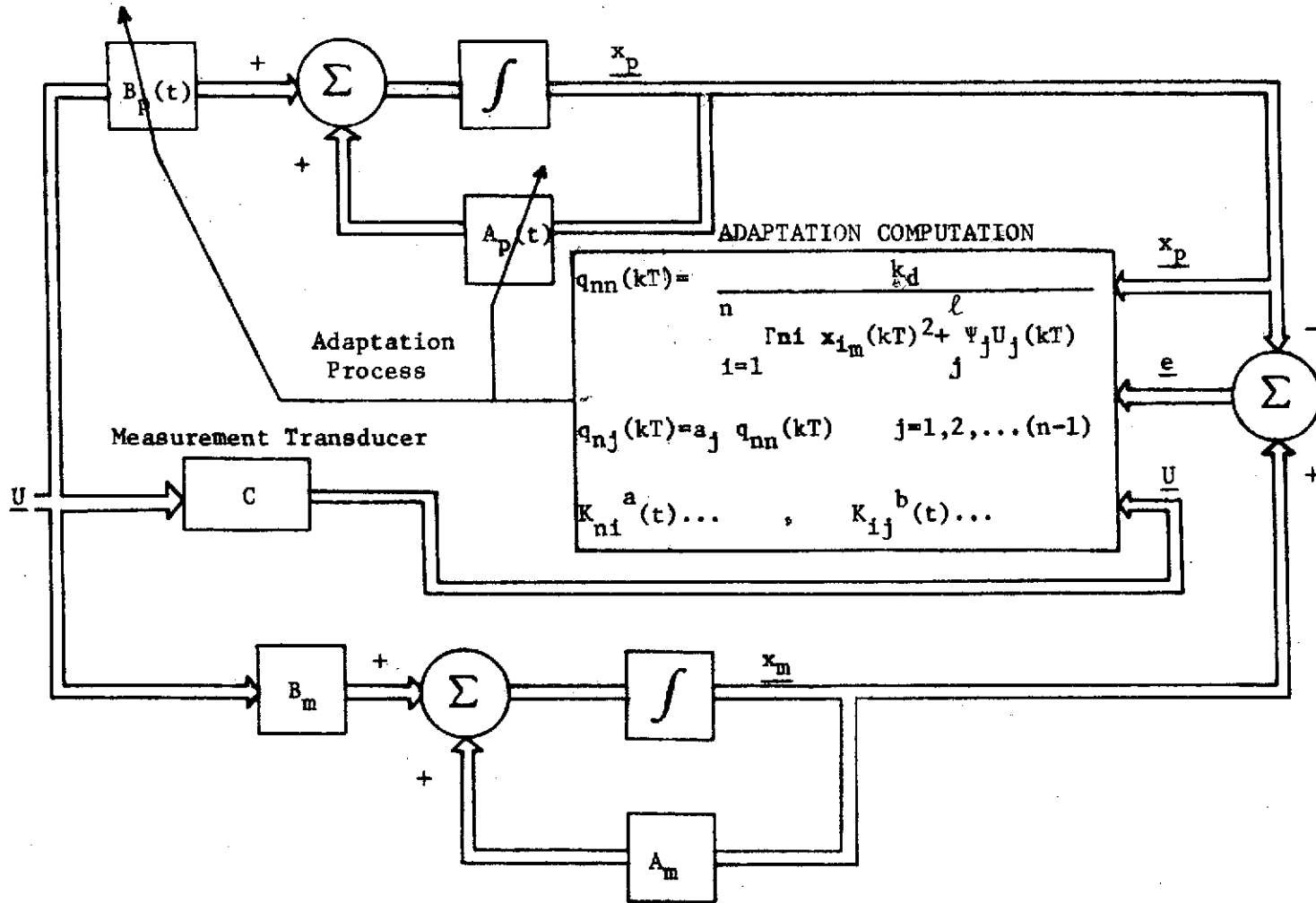


Figure IV-2.D. Adaptation Process Using Dynamic Error Adjustment Technique.

The question of transient response difficulties and the possible instability of the adapted system with the sampled-data adjustment law arises. The Lyapunov theory used guarantees that as $t \rightarrow \infty$, $\underline{e} \rightarrow 0$, one of the requirements being that Q be constant. If so, then $||\underline{e}(t)||$ will continuously decrease after starting at some peak value since $\dot{V}(\underline{e}, t) < 0$. This is illustrated in Figure IV-3.D (a), (b), (c) wherein different values of Q are applied at discrete time points. If adaptation is initiated at $t = t_1$ there will be a Q matrix $Q = Q^{(1)}$. If at time $t = t_2 > t_1$ a Q adjustment is performed, then

$$||\underline{e}(t_2 - \Delta t)|| < ||\underline{e}(t_2)|| < ||\underline{e}(t_2 + \Delta t)|| \quad (\text{IV-15.D})$$

and t_2 merely becomes a starting time for a new adaptive controller configuration. The sample rate for the Q adjustment is of no consequence as far as stability is concerned, the higher it being the better the approximation to time-invariant error dynamics. As an estimate of the lower bound for the sample rate one might invoke Shannon's Sample Theorem.

A continuous adjustment law using (IV-9.D) and (IV-10.D) cannot be employed and asymptotic stability be assured because by using the adaptive laws in [5, 6, 7], the resulting \dot{V} terms are sign indefinite. It could be that such a continuous adjustment law would be stable, since Lyapunov's theory provides only sufficient conditions, it is just that nothing definite can be said. It should be pointed out, however, that simulation results have revealed that the continuous adjustment law works well in practice.

Since the Q elements are adjusted, it is necessary to insure that the p.d. Q and n.d. $A_m^T Q + Q A_m$ conditions are met. Since all Q elements

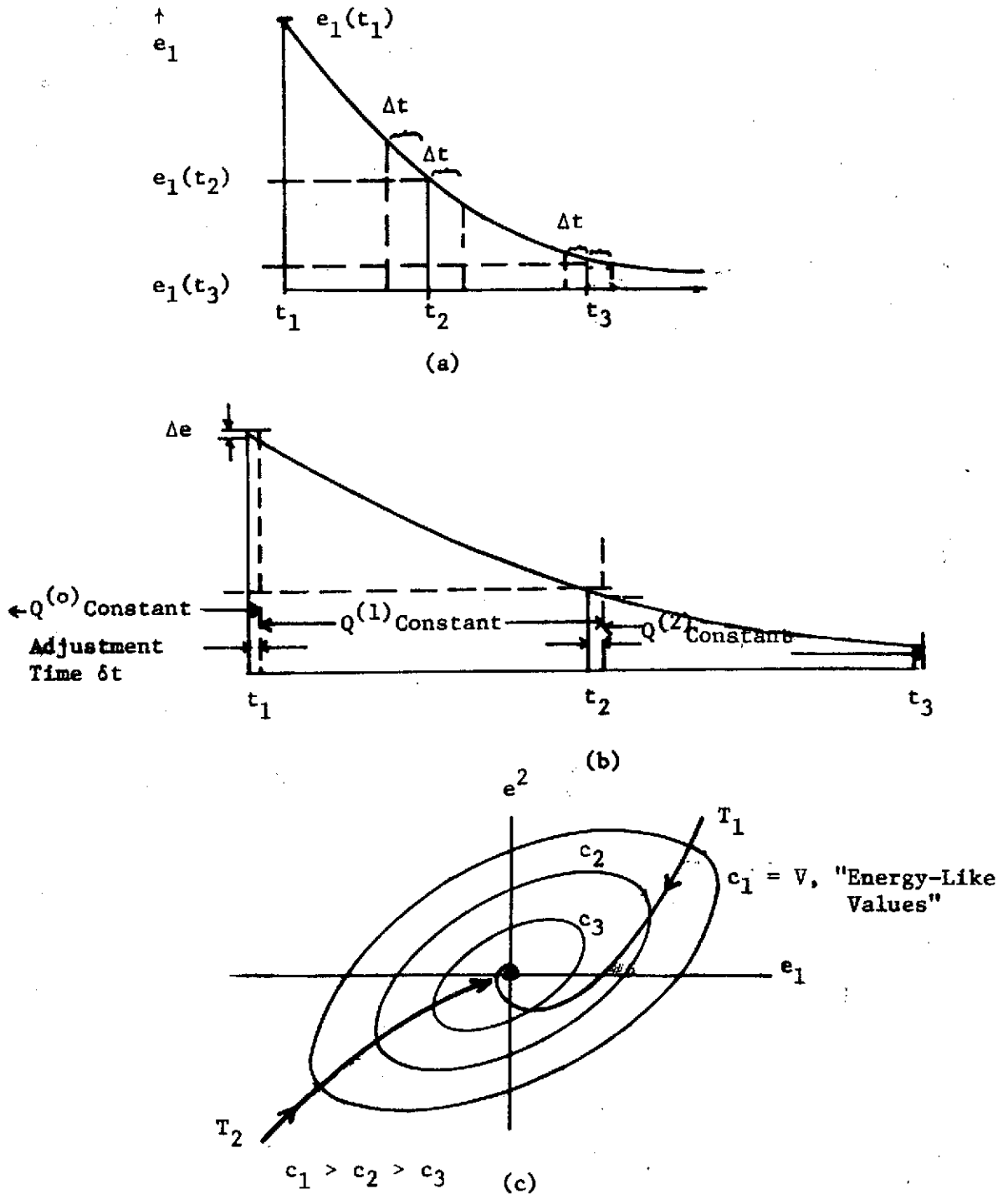


Figure IV-3.D. Error Reduction Using Lyapunov Adjustment Technique (a), (b) Timing and Error Reduction, (c) Typical Error Trajectory Illustrations.

are adjusted in the same proportion, if at $t = t_0$, $q_{nn} = q_{nn_0}$

$$Q|_{t_0} = \begin{bmatrix} q_{11}^0 & q_{12}^0 & \cdots & q_{1n}^0 \\ q_{21}^0 & q_{22}^0 & \cdots & q_{2n}^0 \\ \vdots & \vdots & \ddots & \vdots \\ q_{n1}^0 & q_{n2}^0 & \cdots & q_{nn}^0 \end{bmatrix}$$

and at $t = t_1$, $q_{nn} = q_{nn}^1$, then

$$Q|_{t_1} = C Q|_{t_0} \quad C > 0$$

$$A_m^T Q|_{t_1} + Q|_{t_1} A_m = C \left[A_m^T Q|_{t_0} + Q|_{t_0} A_m \right]$$

the p.d. and n.d. conditions are not changed by the adjustment technique (they are relatively changed, however).

For the case of step inputs of different values at different times, the necessary adjustment scheme is particularly simplified, as K_h then is in the form

$$K_h = \Gamma_{n1} x_{1m}^{o2} + \sum_j^{\ell} \psi_j U_j \quad (\text{IV-16.D})$$

but since

$$x_{1m}^o = \sum_{i=1}^r G(o) U_i^o \quad (\text{IV-17.D})$$

then the necessary adjustment equation for q_{nn} can be written as

$$q_{nn} = \frac{k_{\text{desired}}}{\left[\Gamma_{n1} \left(\sum_{i=1}^r G(o) U_i^o \right)^2 + \sum_j^{\ell} \psi_j U_j^{o2} \right]} \quad (\text{IV-18.D})$$

a particularly simple form to implement.

Example 1:

$$\frac{x_1}{U} = G_m(s) = \frac{2}{s^2 + 2s + 2} \quad G_p(s) = \frac{2}{s^2 + 2s + a_{21}^p}$$

Using the adaptive law in [6], an a priori determined acceptable error characteristic equation is

$$1 + \frac{10(s+2)^2}{s(s^2 + 2s + 2)} = 0 \quad (\text{IV-19.D})$$

The root locus of (IV-19.D) is shown in Figure IV-4.D. Since $x_{1m}^0 = G_m(o)U^0$, selecting $\alpha_{21} = 10$, $\beta_{21} = 5$, $q_{12} = 2q_{22}$ then

$$k = 5q_{22}U_o^2 \quad \text{and} \quad q_{22} = \frac{2}{U_o^2}$$

To account for $U^0 = 0$, a saturation value of $q_{22} = q_s = 1000$ was used. The resulting q_{nn} versus K_h characteristic is shown in Figure IV-5.D.

Shown in Figure IV-6.D is the result of using the adjustment scheme in (IV-18.D) for the cases $U = .06\mu(t)$, $U = 5\mu(t)$, $U = 3\mu(t)$. These results are compared with those obtained without the adjustment rule in (a), (b), (c) and the three input adjustment cases are compared with the desired response (based on the magnitude estimation technique). Note the excellent correlation between the adjustment results and the standard.

A time-varying example using (IV-13.D) and (IV-14.D) was also run using

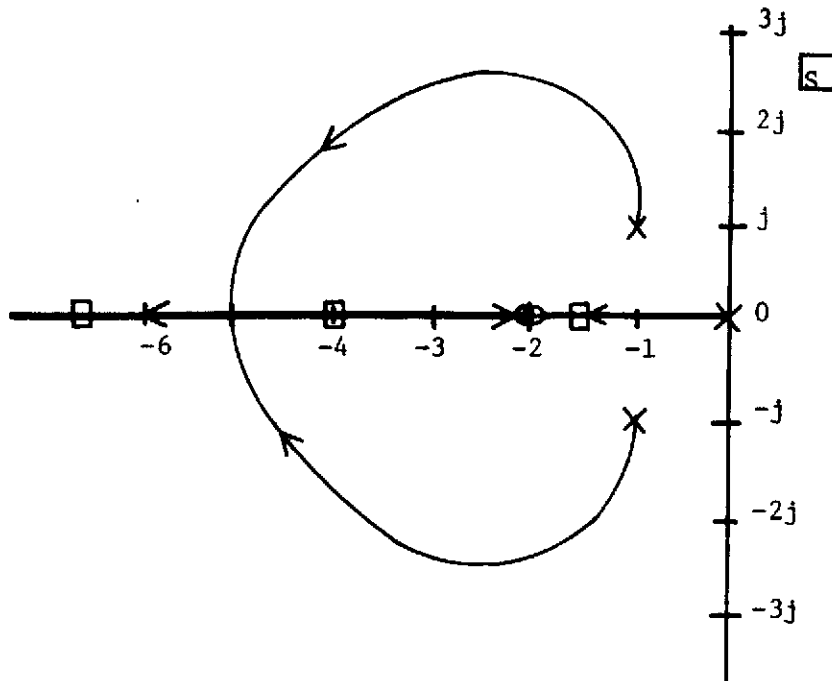


Figure IV-4.D. Root Locus Plot.

$$1 + \frac{K_2 q_{22} (s + q_{12}/q_{22}) (s + K_1/K_2)}{s(s^2 + 2s + 2)} = 0$$

$$q_{12}/q_{22} = 2 \qquad K_1/K_2 = 2$$

$$K_2 = \beta_{21} x_{1m}^2 = \beta_{21} U_o^2$$

For $k = q_{22} K_2 = 10$, the closed loop error roots are

$$p_1 = -4 \qquad p_2 = -6.449 \qquad p_3 = -1.551$$

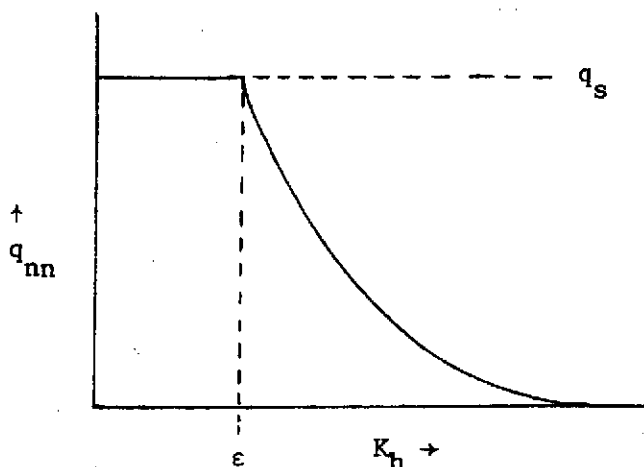


Figure IV-5.D. Saturation Curves for q_{nn} Adjustment.

$$U = \sin 3t$$

The results for various sample periods T are shown in Figure IV-7.D, where the initial error, $e_1 = .1$. The particular adjustment process used employs state measurements $x_{p1}(t)$ instead of $U_1(t)$ for the sampled-data update. Note that, even with need for q_s (since $\frac{1}{x_{p1}^2} \rightarrow \infty$ at a finite number of points), the time-varying adjustment process results in an error response similar to that predicted by the time-invariant linearization process.

One point to note, however, is that unless that sample period rate T is short enough, the error response will tend to exhibit characteristics of the forcing functions $U_j(t)$, i.e. $e(t)$ may exhibit a decaying sinusoidal characteristic if the inputs are sinusoidal.

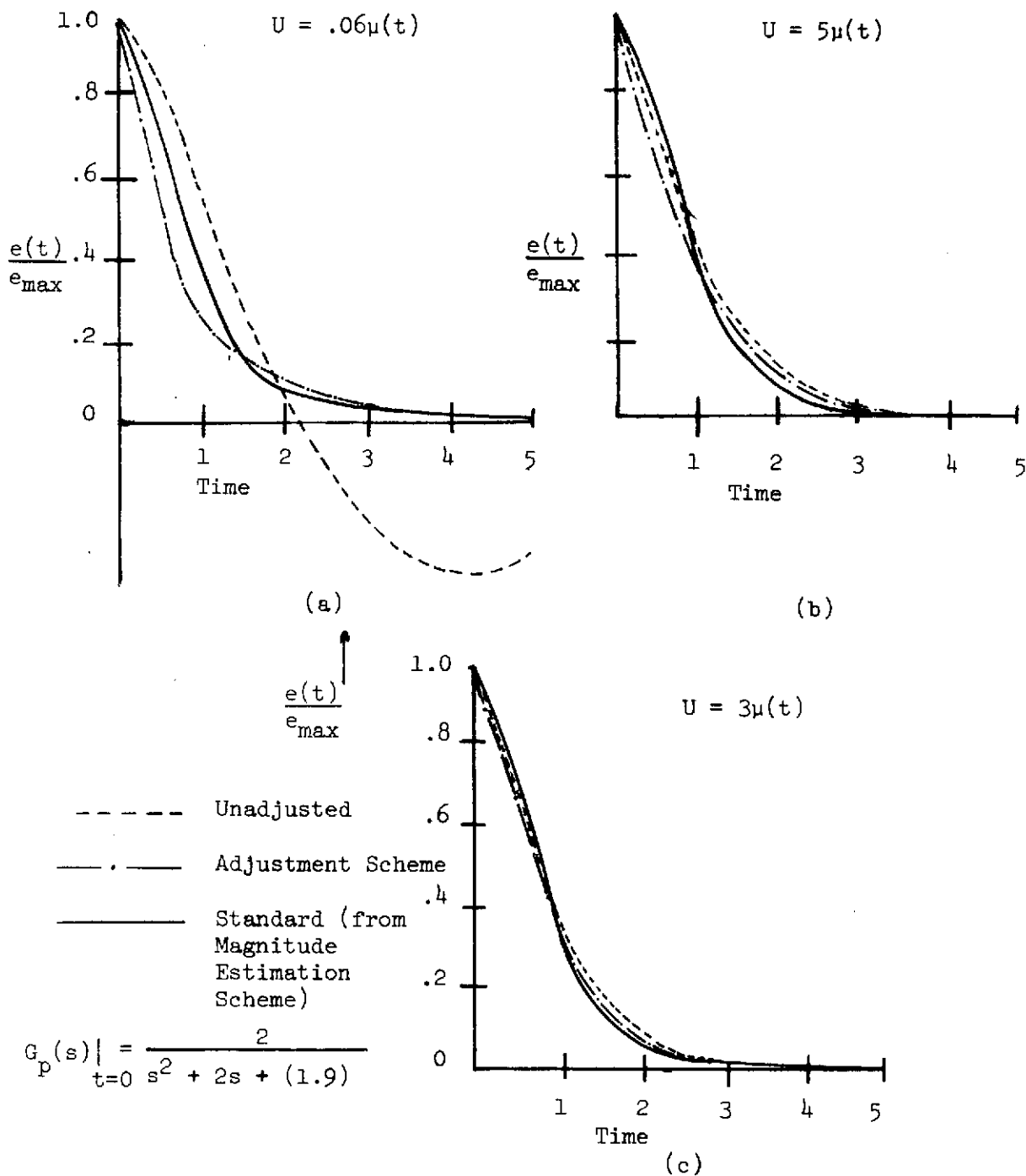


Figure IV-6.D Error Response Results From Adjustment Scheme For Various Step Inputs.

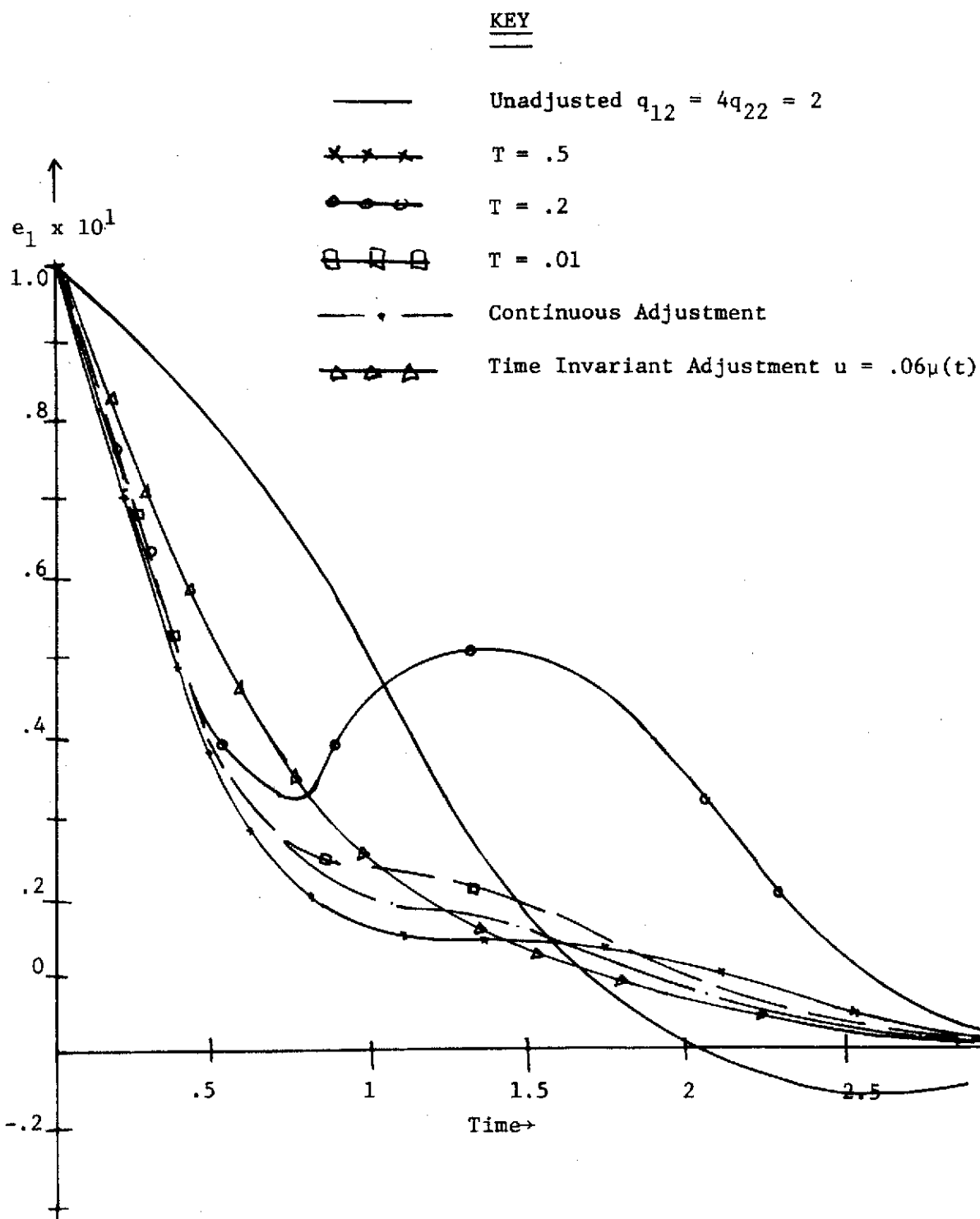


Figure IV-7.D. Error Response Using Adjustment Scheme With Sinusoidal Input.

V. RELATED TOPICS

The earlier chapters of this report have related various topics concerning the design of model-reference adaptive systems. Theoretical results for implementation difficulties such as stability bounds and noise error bounds have been presented. In this chapter, some simulation and numerical results for practical implementation difficulties where no exact mathematical results are presently available will be presented. These results give a qualitative indication of what the designer could expect an MRAS control system to look and operate like under real-world conditions.

A. Simulation Results For A Physically Realizable Space Shuttle Pitch-Axis Controller

An example was given in Chapter II relating the developed design theory of MRAS control to a hypothetical pitch axis controller. Neglected at that time was the problem of physical implementation. A simulation example will now be given where in practice the theory of adaptive control does not exactly fit the problem and hence exact analytical results regarding stability of such cases has as yet not been developed. However, from a practical approach, as long as the differences between theory and practice are not great, experience dictates that results should be expected to be similar.

In Figure V-1.A is shown a typical Shuttle-type aerodynamic control model-reference configuration. This contrasts with Figure II-4.D which disregards physical limitations. Note that in Figure V-1.A the summing junction Σ_1 is inside the dotted line which means that it is a mathematical junction and not a physical entity. The gains from the on-board computer are instead fed through an electrical junction Σ_2 where an error drive signal is developed to power a servo actuator to move the aerodynamic control surfaces. The resulting physical placement of the surfaces then causes forces and moments on the vehicle, and this is shown by α passing through b_{p_2} and δ_e through b_{p_2} . The crucial differences of Figure V-1.A from II-4.D are that

- (1) time varying, unknown input gains b_{p_1} and b_{p_2} are not adapted as in Figure II-4.D
- (2) the feedback adaptive gains K_{12}^a and K_{22}^a are fed back through b_{p_1} and b_{p_2}
- (3) an external mechanical servo is used to convert electrical drive signals to mechanical control

These differences alter the theory in the following manner. The basic attitude controller of Figure II-4.D has a transfer function of the form

$$\frac{\theta_p}{\delta_e}(s) = \frac{(K_{21}^b + b_{p_1})}{s^2 - (K_{22}^a + a_{22}^p)s - (K_{21}^a + a_{21}^p)} \quad (V-1.A)$$

where b_{p_1} , a_{p_2} , a_{p_1} are unknown, time-varying parameters. The basic adaptive control theory outlined in Chapter II relates to (V-1.A), where the adaptive gains are strictly additive with respect to corresponding

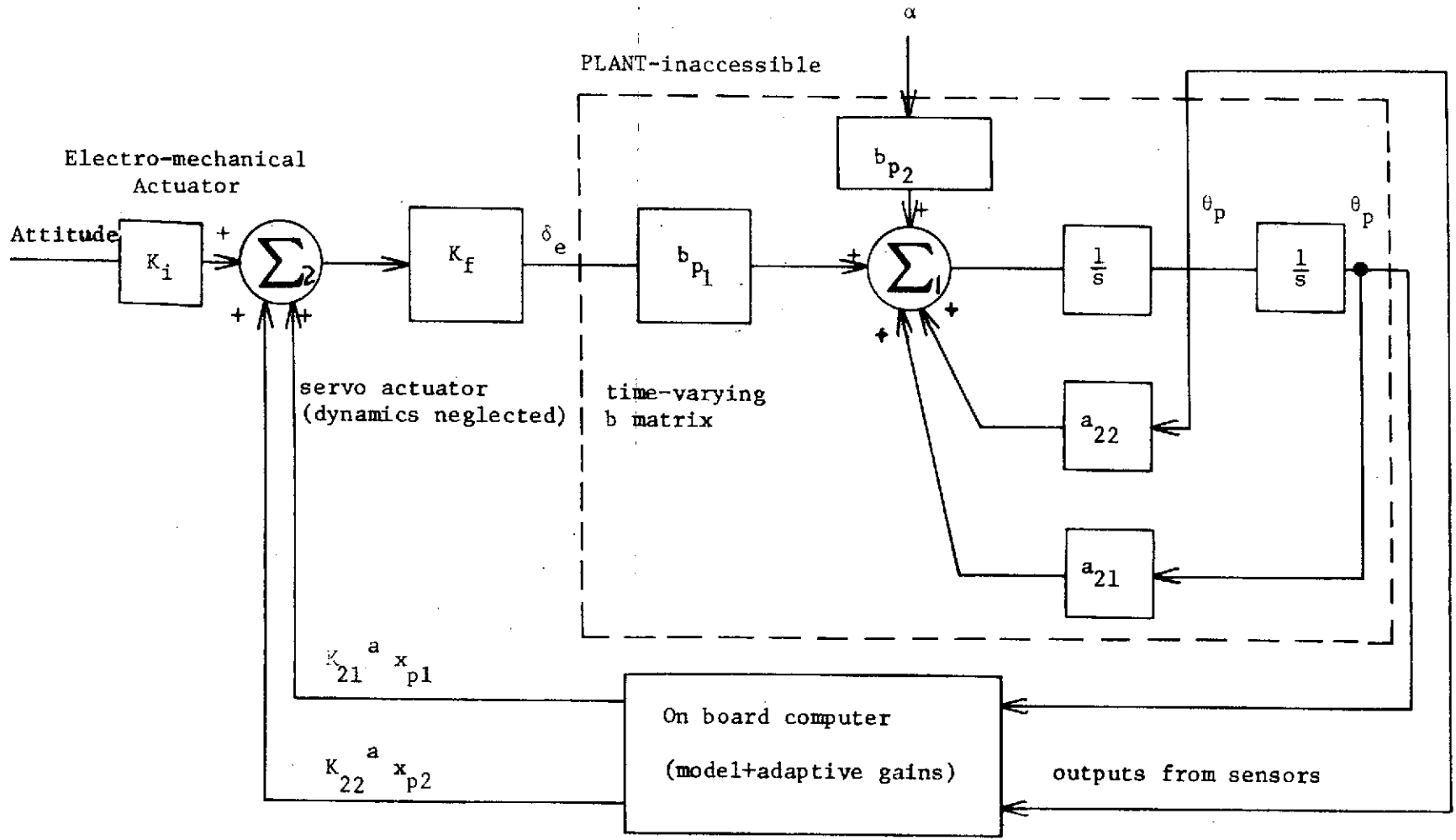


Figure V-1.A. Practical Implementation of a Shuttle-type Attitude Controller During Re-Entry Phase.

plant parameters. The equivalent transfer function from Figure V-1.A is

$$\frac{\theta_p}{\delta_e}(s) = \frac{K_{fb}b_{p1}}{s^2 - (K_{22}^a K_{fb}b_{p1} + a_{22}^p)s - (K_{21}^a K_{fb}b_{p1} + a_{21}^p)} \quad (V-2.A)$$

where

K_f - servo gain (dynamics neglected for illustrative purposes only)

In (V-2.A) the adaptive gains are effectively multiplied by $b_{p1} K_f$, an unknown quantity. This creates two problems

- (1) The effects of K_{21}^a , K_{22}^a must reach Σ_1 with an effective positive sign connected with them and if $K_{fb}b_{p1}$ is negative, then an appropriate sign change is called for at Σ_2 . Failure to do this will lead to instability of the MRAS controller. This implies that only some gross knowledge of the sign of $K_{fb}b_{p1}$ need be known.
- (2) $K_{fb}b_{p1}$ has the effect of "altering" the adaptive gains which were computed according to a theory which did not account for these terms. In effect this means that in the implementation problem, adaptive gains K_{21}^a and K_{22}^a should be used as feedback gains,

where

$$K_{21}^a = K_{21}^a / \tilde{K} \quad (V-3.A)$$

$$K_{22}^a = K_{22}^a / \tilde{K}$$

where

K_{21}^a , K_{22}^a represent adaptive gains computed according to (II-18.A) and (II-19.A)

K_{21}^a, K_{22}^a - actual electrical feedback adaptive gain signals
 \tilde{K} - best estimate of $K_f b_{p1}$ with both magnitude and sign taken into account

Another problem related to physical realizability is that of incomplete adaptation of even the K_{ij}^a gains. Due to costs and hardware complexity it may not be possible or desirable to construct all gains. In terms of the simple example in Figure V-1.A this would suggest that K_{22}^a might not be adapted.

In Figure V-2.A are shown simulation results for the control system of Figure V-1.A for the cases of incomplete adaptation and time-varying feedforward gains (i.e. $b_{p1} K_f$ of Figure V-1.A). The simulation conditions are listed in Table V-1. The parameters $\alpha, \beta, \gamma, \delta, q_{ij}$ are as defined in Section D of Chapter II.

$G_{m1}(s) = \frac{\theta_p(s)}{\alpha} = \frac{-0.05}{(s+1)(s+2)}$
$G_{m2}(s) = \frac{\theta_p(s)}{\text{attitude}(s+1)(s+2)} = \frac{-0.05}{\text{attitude}(s+1)(s+2)}$
$q_{12} = 3. \quad q_{22} = 1.$
$t_{\text{initial}} = 150 \text{ seconds (see Figure II-3.D)}$
$\alpha_{21} = 4000., \beta_{21} = 1000., \gamma_{21} = 400., \delta_{21} = 100.$
$\alpha_{22} = 4000., \beta_{22} = 1000., \gamma_{22} = 400., \delta_{22} = 100.$
$e_1 = \theta_m - \theta_p \quad e_2 = \dot{\theta}_m - \dot{\theta}_p$
$\alpha = 60^\circ, \text{attitude} = 65^\circ$

Table V-1. Simulation Data for Results Shown in Figure V-2.A.

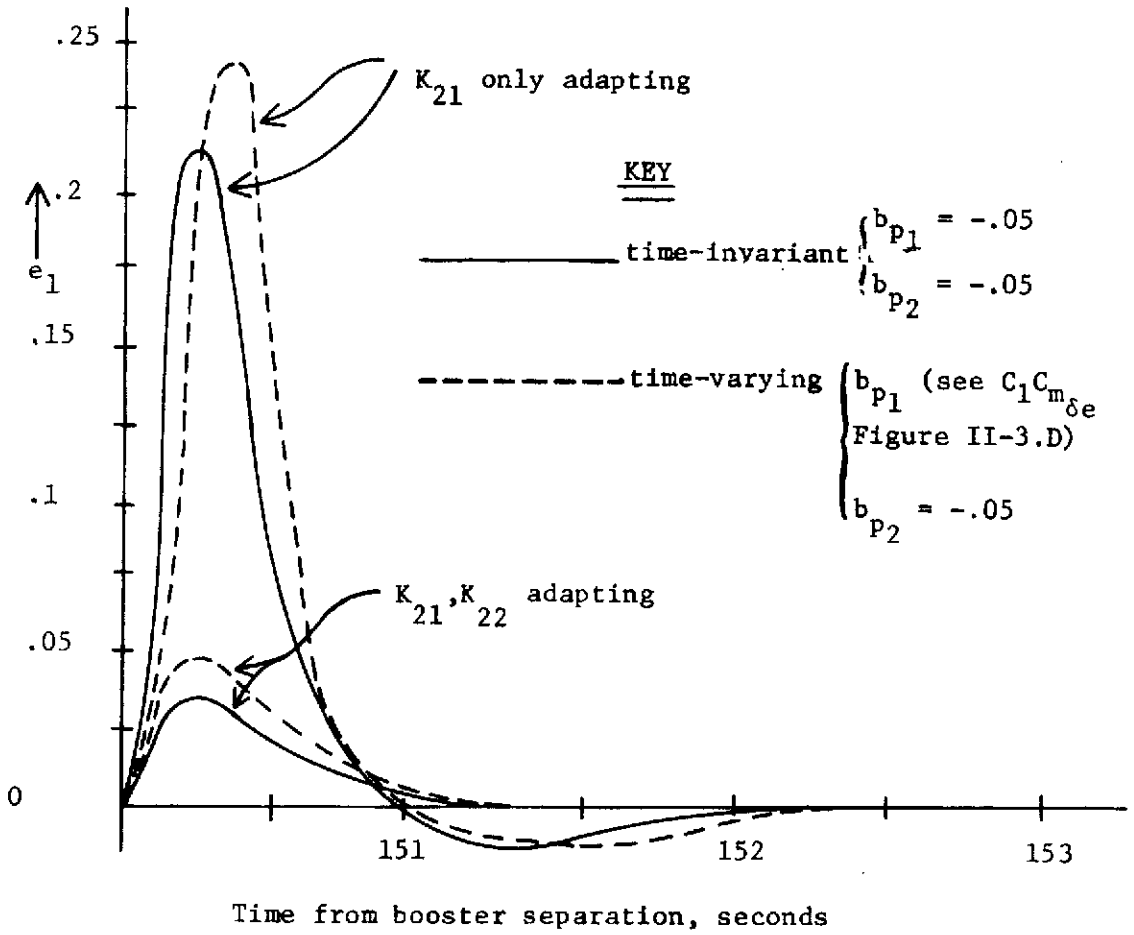


Figure V-2.A. Simulation Results for Incomplete Adaptation and Time-Varying Forward Gain

Note that, although exact theory is not available yet to describe the error dynamics for the adaptive controller subject to time-varying unadapted terms such as b_{p_1} , b_{p_2} of Figure V-1.A and incomplete adaptation (i.e. $K_{22}^a = 0$ in Figure V-1.A), the simulations reveal results similar to those expected from exact theory. With time varying b_{p_1} the errors were larger than from the exact methods, but the overall response was very similar. For the case of incomplete adaptation errors were larger than expected and there was a slight overshoot not predicted by the theory, but the overall "shape" of the response was as would be expected based on the linearization design of Chapter II.

This example illustrates that, from a practical standpoint, the Lyapunov MRAS adaptive system has merit even when many of the mathematical idealizations are not met in practice. Of course, simulation results can only provide a qualitative guide to stability, but indications are that practical implementation need not limit the adaptive control approach.

B. RCJ to MRAS Attitude Phase-Over Control During Re-Entry.

During the orbital flight phase, the Space Shuttle attitude is to be controlled by some form of reaction control jets. Such a control system allows a trade-off between attitude error (on the order of 2^0 - 3^0 usually) and low fuel consumption [23]. The control system for the RCJ package was designed assuming no aerodynamic forces would be present a very reasonable assumption at altitudes of 500 thousand feet or more. However, during re-entry aerodynamic forces begin to build up on the

vehicle, which, coupled with severe re-entry corridor attitude limits and unknown time-varying plant parameters, suggests that an MRAS controller might be used during the re-entry phase.

Unlike the Apollo and Gemini craft, the Shuttle has large wings for lift and it is exactly this lift capability which tends to nullify the stabilizing RCJ control torques during re-entry. This is because the moments due to aerodynamics very quickly become orders-of-magnitude greater than those available from conventional RCJ systems.

To facilitate the two different control modes, some sort of switch-over routine is needed. Some of the obvious alternative techniques for determining when to switch from RCJ to MRAS control during the re-entry profile include

- (1) perform a switchover from total RCJ to total MRAS control according to a fixed criterion (probably based on Monte Carlo-type simulation data), i.e. altitude, Mach number, dynamic pressure, attitude-hold capability
- (2) on-line manual pilot switch-over according to his "feel" of the controls
- (3) employ an automatic on-line technique for proportioning the control between RCJ and MRAS

It is (3) above which is of interest here.

The RCJ controller is of the form shown in Figure V-1.B, where only the pitch axis is shown, it being assumed decoupled from the roll-yaw axes. The coefficients A_1 and A_2 are time-varying coefficients due to aerodynamic parameters, T is the thruster force, I_y the vehicle pitch-axis inertia. In deep space the A_1 , A_2 are zero, but during re-entry these terms change to non-zero values. The actual values are unknown

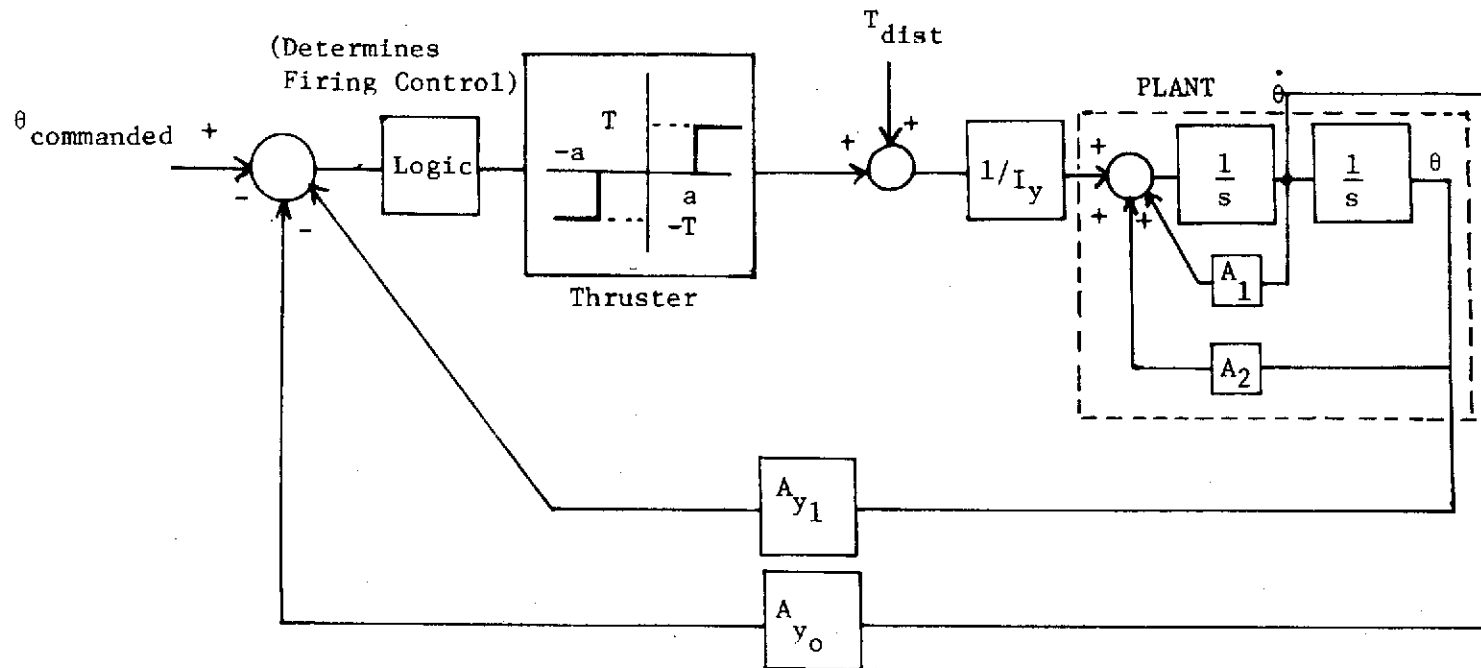


Figure V-1.B. RCJ Pitch Control System.

because of the indeterminate nature of the particular re-entry profile. With such a bang-bang controller, a reasonable trade-off between attitude deviation and fuel consumption is obtained. During re-entry, the aerodynamic coefficients alter the RCJ controller effectiveness and the need for aerodynamic control increases.

A basic adaptive attitude controller for the pitch axis is shown in Figure II-4.D. Given sufficient aerodynamic lift such a system can stabilize a re-entering Shuttle-type vehicle regardless of the actual plant parameters. As was illustrated by an example in Chapter II, the plant of the re-entering Shuttle can be unstable (without compensation), and without some form of adaptive control the vehicle could burn up.

Shown in Figure V-2.B is one possible physical implementation of a 'total' attitude control system. The heart of the system is the "controller proportioning device" which determines, on-line, which type of control, either RCJ or MRAS should be used at any given time.

Defining control effectiveness to be the amount of influence exerted on a space vehicle by a particular control system, the basic problem during re-entry is to optimize this "effectiveness" such that minimum attitude deviations occur. The control torque due to RCJ control is

$$T_{RCJ} = (L/2) \cdot F \quad (V-1.B)$$

where

T_{RCJ} = torque due to RCJ system

$L/2$ = effective moment arm for a single axis thruster

F = net thruster force

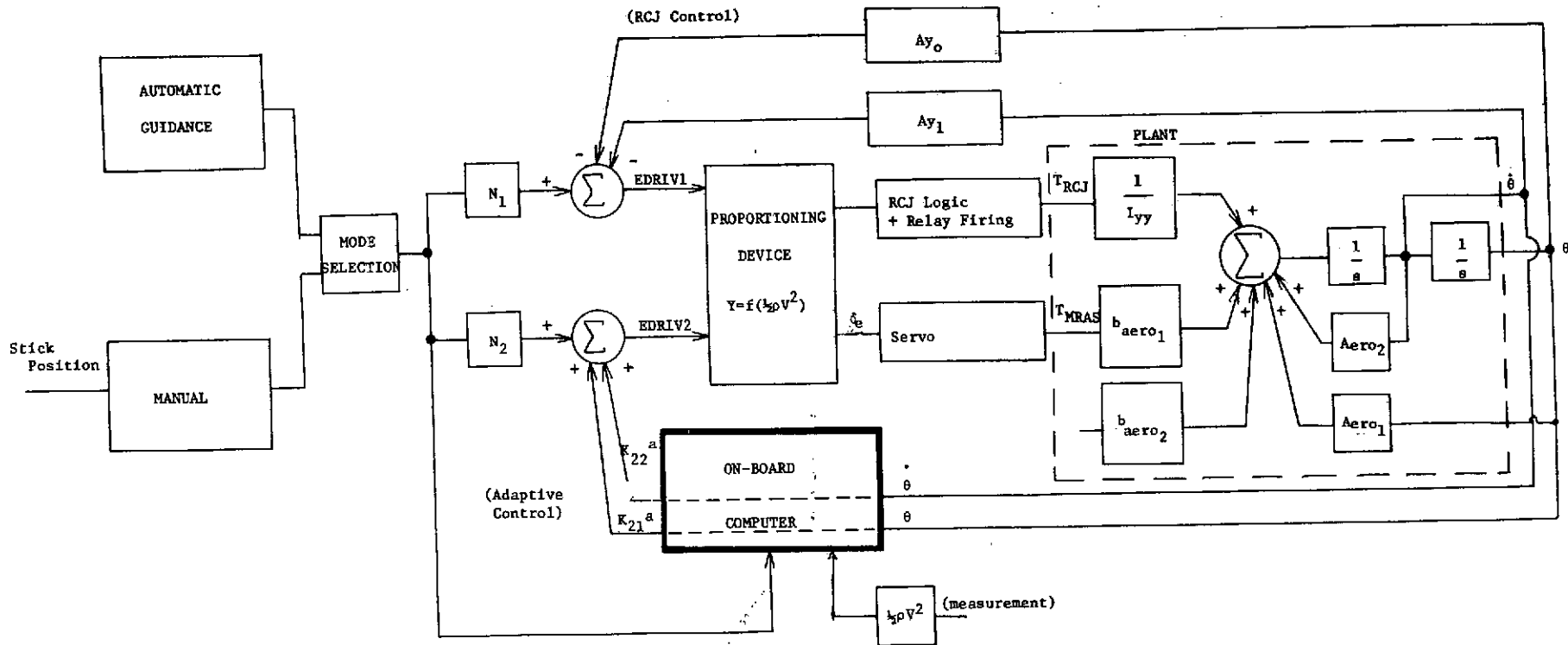


Figure V-2.B - Pitch Axis Control For RCJ to MRAS Phase-Over.

and the torque due to aerodynamic surfaces as

$$T_{MRAS} = (c)(\frac{1}{2}\rho V^2)(S_{ref})(C_{m\delta_e} \cdot \delta_e) + \frac{1}{2}\rho V S_{ref} c^2 C_{m\alpha} \alpha \quad (V-2.B)$$

T_{MRAS} = torque due to MRAS control

c = reference length

S_{ref} = wing effective reference area

$\frac{1}{2}\rho V^2$ = dynamic pressure

C_{m_z} = wing pitching moment derivative due to z .

A proportioning signal y representing the fraction of MRAS control as compared to RCJ is to be determined,

$$0 \leq y \leq 1$$

It is hypothesized that this phase-over control be a function of an on-line measurable parameter indicative of aerodynamic forces, so it is assumed that

$$y = f(\frac{1}{2}\rho V^2) \quad (V-3.B)$$

since the dynamic pressure ($\frac{1}{2}\rho V^2$) is related to aerodynamic control and is available. As a simple approach, y is assumed of the form of a polynomial in ($\frac{1}{2}\rho V^2$),

$$y = a_0 + a_1 x + a_2 x^2 + \dots + a_n x^n \quad (V-4.B)$$

where

$$x = \frac{1}{2}\rho V^2$$

$a_0, a_1, a_2, \dots, a_n$ are coefficients to be determined

This form of control is hypothesized because, in addition to being a function of an on-line measurable parameter, it is simple to implement, requires little computation time, and is a continuous function (so there will be no discontinuity in control). The amount of RCJ or MRAS control is then determined by the fraction of EDRIV1, and EDRIV2 shown in Figure V-2.B, available as a control signal

$$\begin{aligned} \text{amount RCJ control} &= (1-y) \cdot (\text{EDRIV1}) \\ \text{amount MRAS control} &= y \cdot (\text{EDRIV2}) \end{aligned} \tag{V-5.B}$$

The degree of the polynomial, n , is assumed to be at least of order two (to be explained later), but may be of any size, depending on the number of data points used.

There are at least three well-defined control points for a re-entering Shuttle-type vehicle (at least for the purposes of this presentation), and these three plus any additional points based some a priori selected criteria, may be used to determine the coefficients a_i . These three control points are

- (1) deep space-full RCJ control
- (2) atmospheric flight at $\approx 150,000$ feet-full MRAS control
- (3) the point in time at which $T_{\text{RCJ}} = T_{\text{MRAS}}$ - control is assumed 50% each mode

Other additional points could be defined on the basis of a given proportion of MRAS control for a given aerodynamic pressure. The control points then define a phase-over profile as a function of the dynamic pressure.

The simplest case is for $n = 2$, when

$$y = a_0 + a_1x + a_2x^2 \quad (V-6.B)$$

Using this approach a parabolic function of the form $y = x^2$ is obtained. Ideally y should be a single-valued function of x , and the simplest form is then

$$y = a_2x^2 \quad (V-7.B)$$

To further define the three control points, the following assumptions have been made:

- (a) x_{\min} is assumed to be zero
- (b) if $x < x_{\min}$, $y = 0$
- (c) $C_{m\delta_e}$ is constant during re-entry phase-over (this is approximately correct for the large (>5) Mach numbers and large ($\approx 60^\circ$) angle-of-attack encountered during re-entry)

In order to insure that only positive numbers are used for y , the y obtained from (V-4.B) is passed through a saturation device so that the actual y used as a controller signal is scaled to lie between 0 and 1.

This is shown in Figure V-3.B.

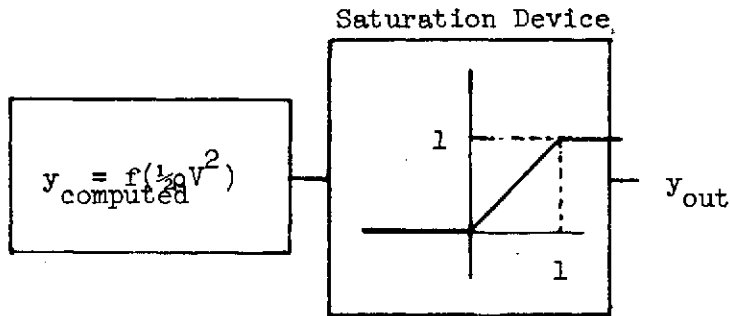


Figure V-3.B. Circuit to Insure That the Phase-Over Control y Lies Between 0 and 1.

Using (V-7.B) the three control points reduce to a 50% phase-over point and a 0% phase-over point, where the 50% point is defined as

$$\frac{T_{MRAS}}{T_{RCJ} + T_{MRAS}} = .5 \quad (V-8.B)$$

Equating the two torques and solving for ρ , the dynamic pressure $x_{50\%}$ can be obtained. This defines control point 2. Using (V-7.B) a particularly simple relation for point 3 is obtained. Using

$$y = a_2 x^2$$

$$y_2 = .5 @ x = x_2$$

$$y_3 = 1. @ x = x_3 = 2 x_2$$

So if x_2 is determined (using (V-8.B)), then x_3 is fixed. Computation of control phase-over is greatly simplified then, requiring only (V-8.B) and (V-7.B). An example will now be given to illustrate how this y function is computed for the simplest case, $n = 2$.

Example: $x = \frac{1}{2}\rho V^2 > 0$

Compatible Space Shuttle data

$$L/2 = 50 \text{ ft.}$$

$$F = 250 \text{ lb.}$$

$$c = 200 \text{ ft.}$$

$$S_{\text{ref}} = 10^4 \text{ ft.}^2$$

$$|C_{m_\alpha}| = |C_{m_{\delta_e}}| = .002/\text{degree}$$

$$|\delta_{e\text{nominal}}| = 1^\circ$$

$$\alpha = 60^\circ$$

$$V = 1.07 \times 10^4 \text{ ft./sec}$$

$x_{50\%}$ is found by equating (V-1.B) and (V-2.B) and solving for ρ

$$\begin{aligned} \rho &= \frac{(42) F}{\frac{1}{2} V S_{\text{ref}} c \frac{1}{2} |C_{m_\alpha}| \alpha + V |C_{m_{\delta_e}}| |\delta_e|} && \text{(V-13.B)} \\ &= \frac{(50)(250)}{\frac{1}{2}(1.07 \times 10^4)(10^4)(200) + \frac{1}{2}(200)(2 \times 10^{-3})(60) + (1.07 \times 10^4)(2 \times 10^{-2})(1)} \\ &\approx 5.16 \times 10^{-8} \text{ slug/ft.}^3 \end{aligned}$$

$$x_{50\%} = \frac{1}{2}\rho V^2 = .29 \text{ lb./ft.}^2 \quad y = a_2 x^2$$

from which

$$.5 = a_2 (.29)^2$$

$$a_2 = 5.95$$

Additional data points could be added by specifying y at a particular (estimated) aerodynamic force level, or some of the previously suggested control points could be redefined. The $n = 2$ case is attractive, however, as there are not local optima to contend with.

A simulation of the control system shown in Figure V-2.B was run with the control phaseover scheme discussed in the example and the results presented in Figure V-4.B. and V-5.B.

C. On-Board Control Computer Computational Requirements

Whenever one speaks of applying modern control theory to a practical problem, the age old questions of physical realizability and practical implementation arise. In the case of adaptive control, the concern generally rests with the complexity of the controller and the difficulty of real-time operation with limited computational hardware. In this section the computational requirements for implementing a model-reference system are discussed and some numerical results for a specific example presented to illustrate computation time as a function of the system order and the number of inputs processed.

The basic plant dynamics considered were of the form

$$\dot{\underline{x}}_p = \begin{bmatrix} 0 & 1 & 0 & \dots & 0 \\ 0 & 0 & 1 & \dots & 0 \\ \vdots & \vdots & \vdots & \ddots & \vdots \\ -a_0^p & -a_1^p & -a_2^p & \dots & -a_{n-1}^p \end{bmatrix} \underline{x}_p + \begin{bmatrix} 0 & 0 & \dots & 0 \\ 0 & 0 & \dots & 0 \\ \vdots & \vdots & \ddots & \vdots \\ b_{n_1} & b_{n_2} & \dots & b_{n_r} \end{bmatrix} \underline{U} \quad (\text{V-1.C})$$

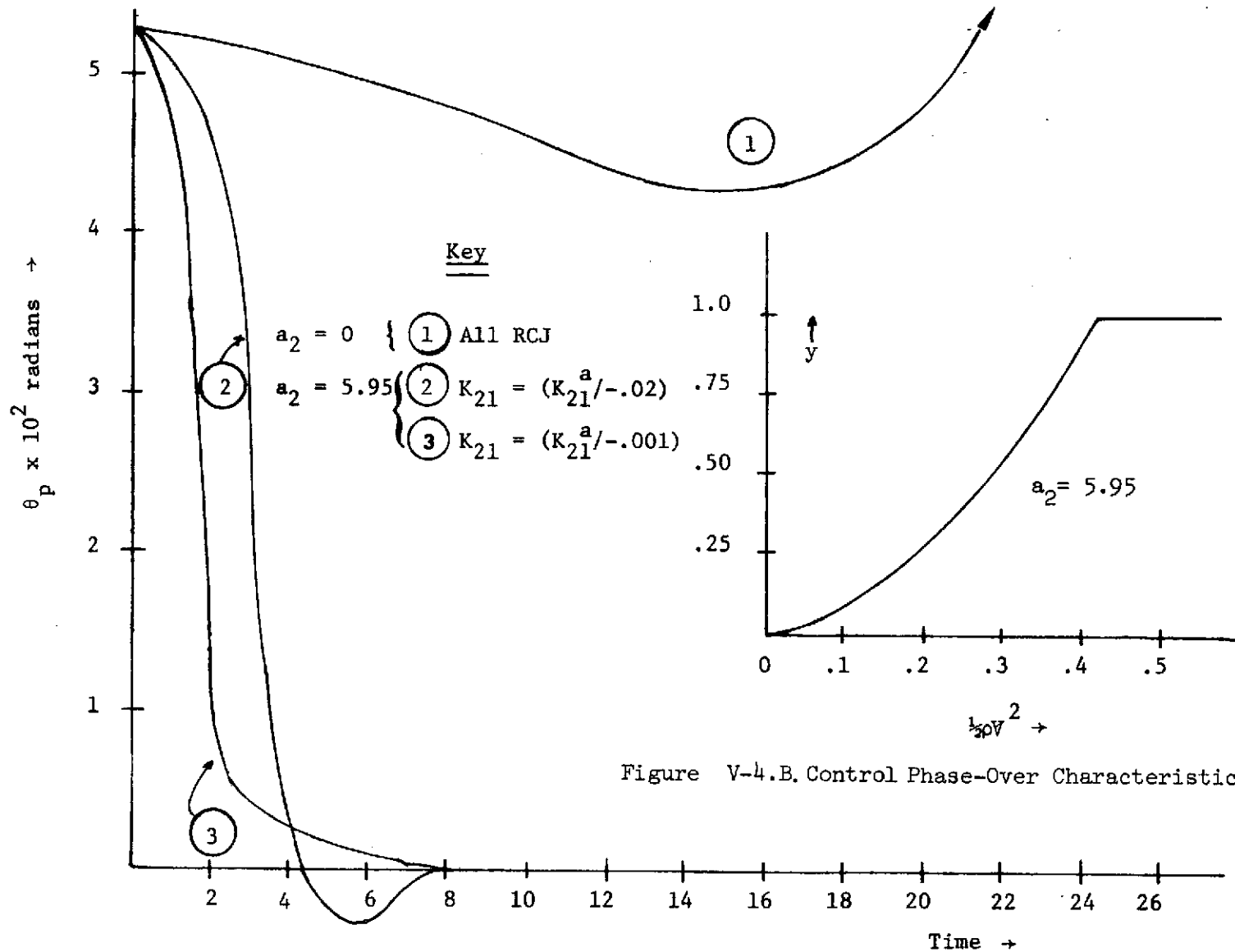


Figure V-5.B. Control Phase-Over Response.

Figure V-4.B. Control Phase-Over Characteristic.

where the terms are as defined previously. It is assumed that all terms are adapting so that "worst case" estimates will be available. The basic integration routine considered was the fourth-order Runge-Kutta and the differentiation process (used only with the Boland and Sutherlin method) was a basic 2nd order Lagrangion interpolation polynomial. Computational requirements were determined as a function of n (system order), r (number of inputs), plus computer add, subtract and multiply times.

The equations considered were

(II-18.A)	n of these
(II-19.A)	r of these
(II-2.A)	n of these
(II-1.A)	n of these
(II-5.A)	n of these

Using these and the numerical analysis methods mentioned, equations relating add, subtract and multiply times in terms of n and r were determined for the cases of [5,6,7]. The results are tabulated in Table V-2.

Type of Adaptation	Computation Time Function
1. Boland and Sutherlin [7]	$T_B = \left(5n^2 + 5rn + 48n + 5r^2 + 34r \right) M$ $+ \left(5n^2 + 5rn + 47n + 5r^2 + 28r \right) S$
2. Gilbert, Monopoli, and Price [6]	$T_G = T_B - 45n - 45r$
3. Winsor and Roy [5]	$T_W = T_B - 54n - 54r$
$S =$ subtract time (assumed equal to Add) $M =$ multiplication time $n =$ system order $r =$ number of inputs $T =$ computation time	

Table V-2. Computation Cycle-Time Equations

Using data for a particular class of aerospace computers [24], computer time requirements were determined using the data in Table V-2. and are presented as a series of graphs showing computation time per cycle versus system order with the number of inputs as a parameter.

Figure V-1.C shows the computation time, in order to perform a single set of computations for the adaptive gains at a given instant, for the Boland and Sutherlin adaptation technique. This method [7] represents the greatest computational load of the three methods discussed, but as shown in Figure V-2.C, this upper bound on the time is about equal to that for both [5] and [6]. The small differences between computation times for the various methods shown in Figure V-2.C means that computation time need not enter the consideration as to which technique to employ. Instead, such factors as the number of terms to adapt and model order might be of greater importance.

It should be pointed out that the cycle times listed are based upon a digital implementation of continuous systems equations. In actual practice, most likely a discrete-data set of equations would be implemented. In this way only summers, multipliers and delays would be needed to implement the adaptive equations. Most likely the indicated computational cycle time would be much smaller for a discrete-data implementation.

The reason an estimate of the discrete-data implementation was not given was that the adaptive control theory used in this report is based on continuous systems and thus far, very little concerning exact results for the discrete case is available. This is an area which has further research possibilities.

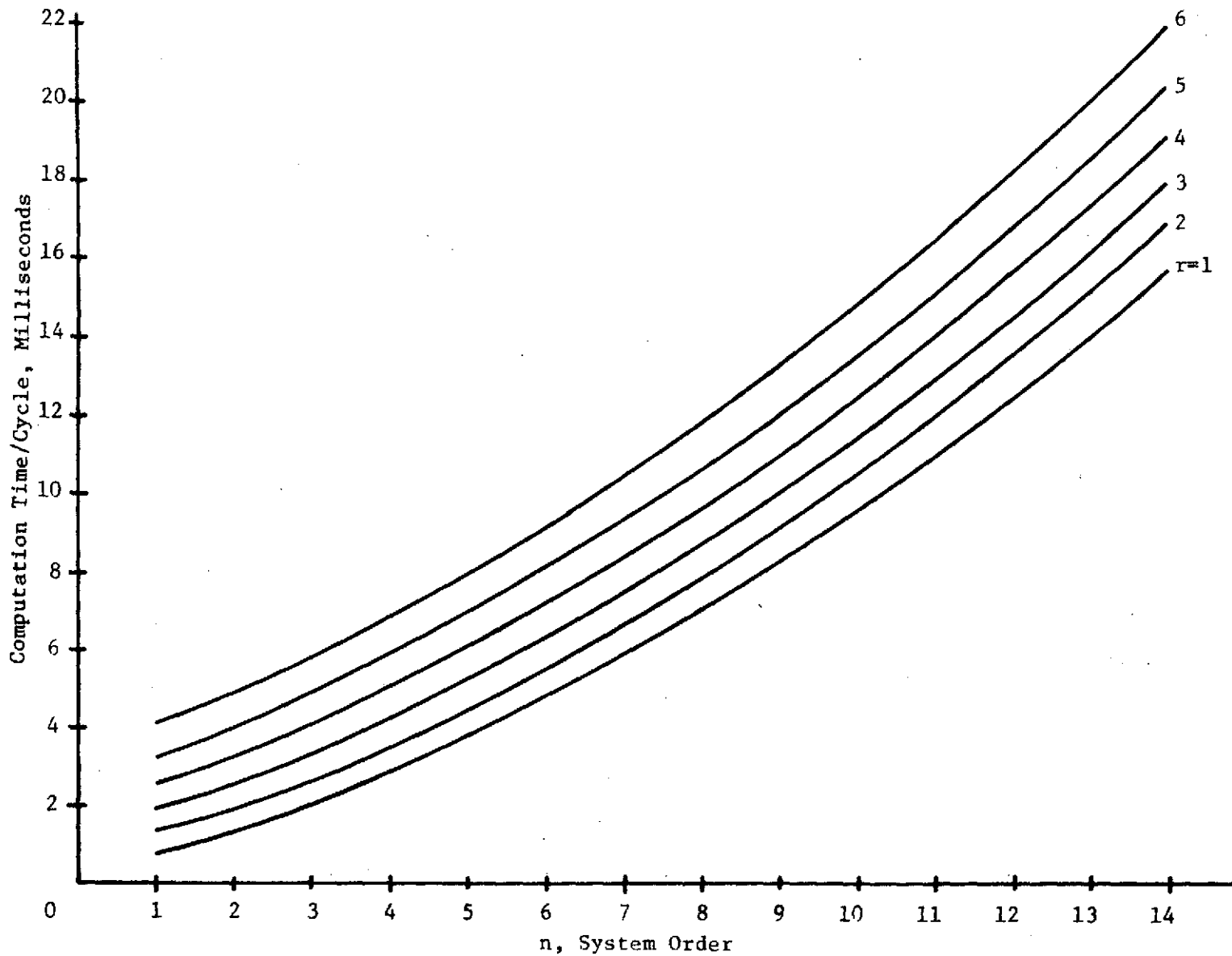


Figure V-1.C. Computation Time/Cycle for the Boland & Sutherland MRAS Implementation.

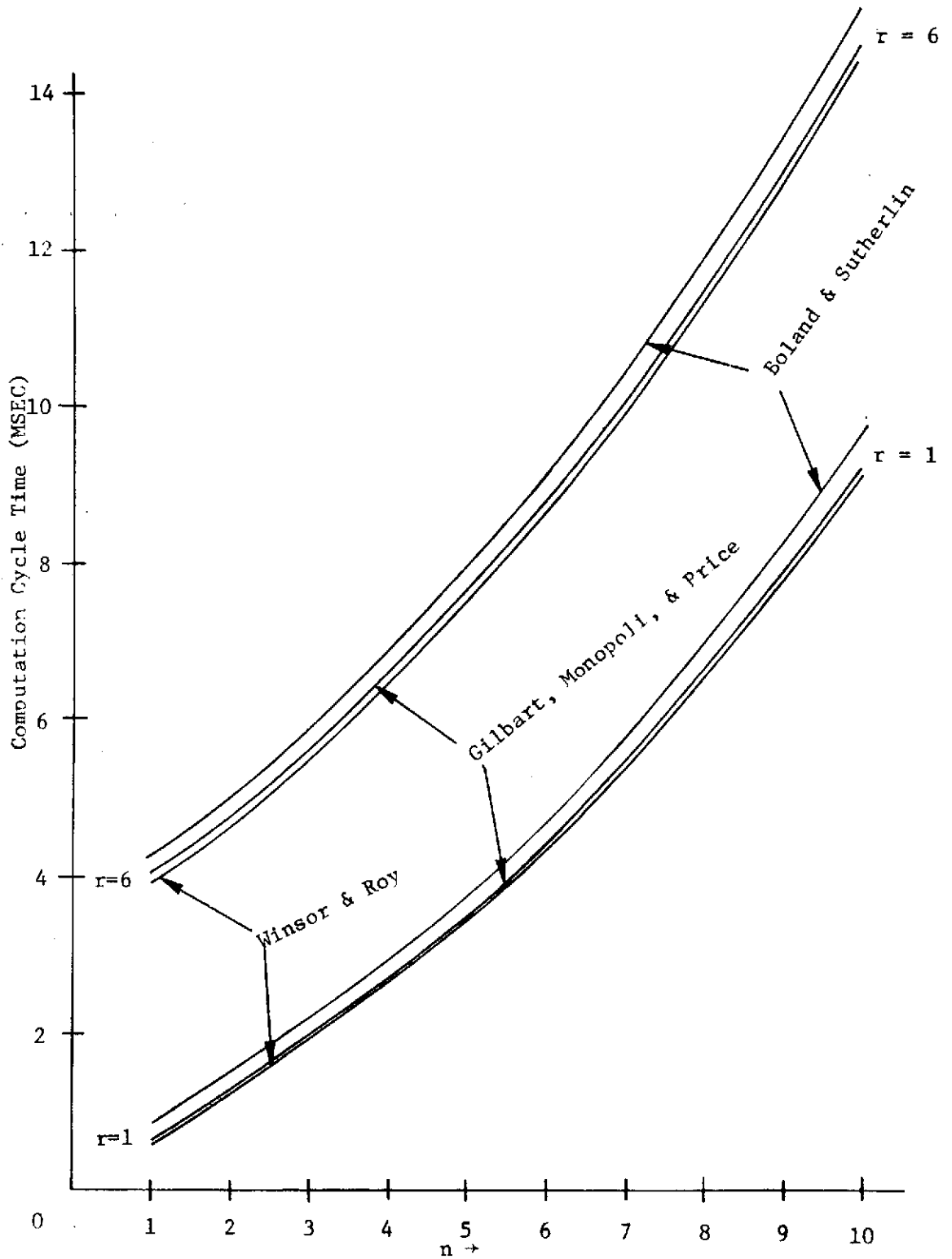


Figure V-2.C. Comparison of Computation Times for Three Adaptation Methods.

The previous results given are for the case when the on-board computer is all digital. In the case of present spacecraft controls, a hybrid or all analog approach is sometimes used, due to high reliability and simplicity. Figure V-3.C is an example of the actual adaptive equation implementation for an all-analog system, illustrating the difference between available measurements and actual required computations and adjustment controls.

D. Use of More Than One Model During Re-Entry

Because of various types of inputs and environment that a plant might be subjected to, it might be desirable to utilize different models for different plant operating conditions. The adaptive control theory discussed is based on time-invariant models, so some sort of switching routine would be required to change the plant response. During the transient phase when switching models, the error analysis techniques in Chapter II can be utilized (assuming constant inputs) to describe error transient response. This is because the analysis theory is based on the supposition of a jump change in a plant parameter. If, at $t = t_1^-$

$$G_m(s) = \frac{a^m}{s^n + a_{n-1}^m s^{n-1} + a_{n-2}^m s^{n-2} + \dots + a_0^m}$$

$$G_p(s) = \frac{a^p}{s^n + a_{n-1}^p s^{n-1} + a_{n-2}^p s^{n-2} + \dots + a_0^p}$$

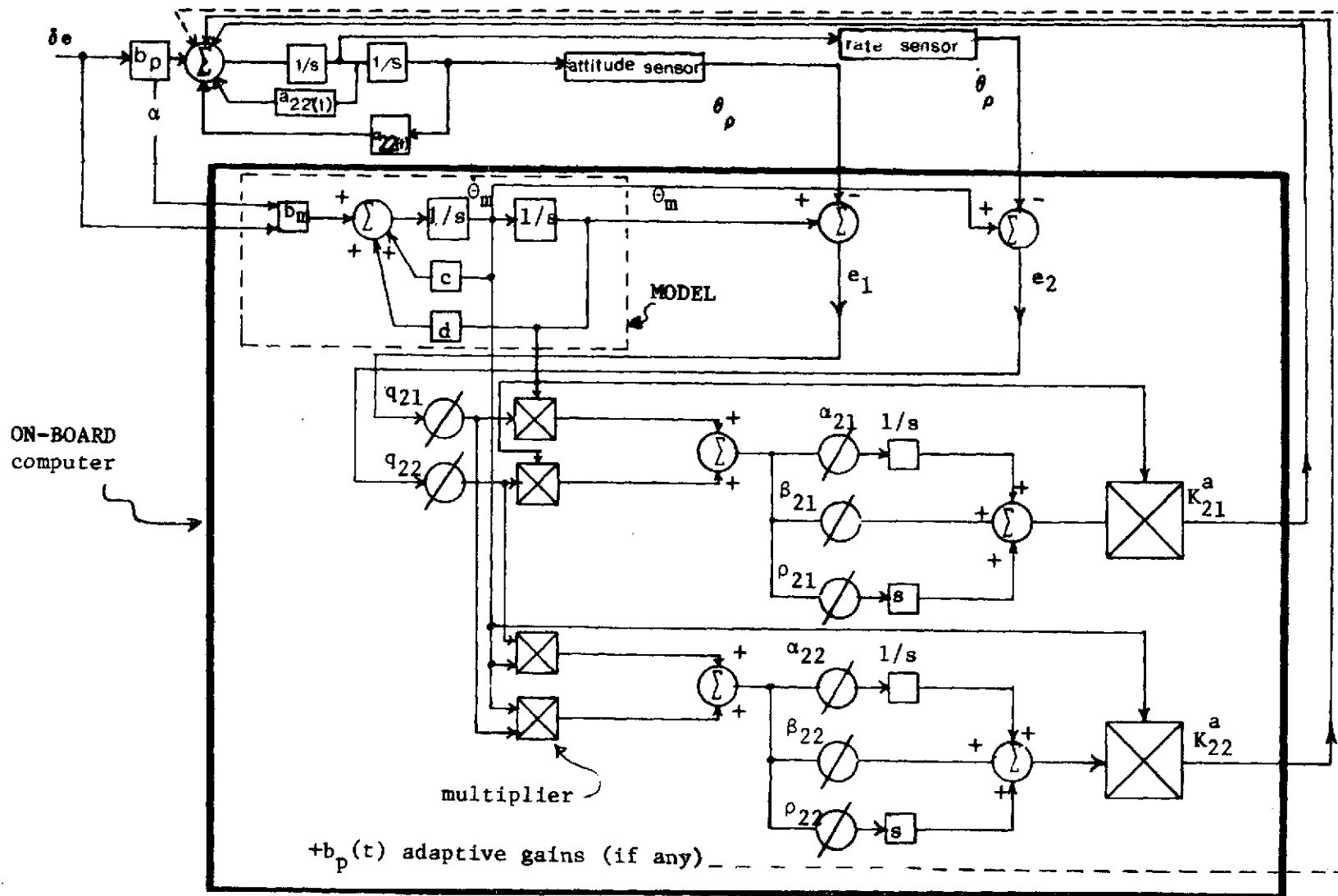


Figure V-3.C. MRAS Attitude Control System Showing the Internal Workings of an All Analog On-Board Computer.

and it is assumed

$$a_j^m(t_1^-) = a_j^p(t_1^-) \quad j = 1, 2, \dots (n-1)$$

and then at $t = t_1^+$ the a_j^m jump to new constant values, the plant transient response would be the same as if

$$a_j^m(t_1^-) = a_j^p(t_1^-)$$

where

$$a_j^m(t_1^-) = a_j^m(t_1^+) \quad a_j^p(t_1^-) \neq a_j^p(t_1^+)$$

and at $t = t_1^+$ the a_j^p jumped to values $a_j^p(t_1^+) = a_j^p(t_1^-)$.

Under such circumstances the new model at $t = t_1^+$ would be used as $\Delta_m(s)$ in (II-16.B). This shows then, that a step change in a model value has the same effect as a step change in a plant parameter. To the plant system the unchanged plant parameters appear as step changes with respect to the new model parameter values.

VI. SUMMARY AND CONCLUSIONS

A. Summary

A large number of generally related topics of stability, analysis, design, and implementation of a class of MRAS controllers were presented. In order to employ these techniques in one grand design package, the following design synopsis is presented.

With a plant and model in the form

$$\dot{\underline{x}} = \hat{A}\underline{x} + \hat{B}\underline{u}$$

where \hat{A} , \hat{B} are given by (II-15.B) a basic error characteristic equation, given in (II-16.B) was derived for the adaptive gains given in (II-18.A) and (II-19.A) for the system defined in (II-1.A), (II-2.A), (II-3.A), (II-4.A), and (II-5.A). Using these, and given a knowledge of the q_{ij} ratios, the fixed adaptive gain parameters α , β , ρ , γ , δ , σ may be selected. In case \hat{B} terms as well as \hat{A} terms of the plant are adapted, (II-11.C) should be employed. To estimate the maximum error e_1 and the time increment which passes after a plant disturbance before this maximum occurs, (II-5.E), (II-6.E), (II-12.E), (II-15.E), and (II-16.E) are employed.

To determine "zero" placements of $s^{n+q_{(n-1)n}/q_{nn}}s^{n-1} + \dots + q_{1n}/q_{nn}$ the technique outlined in section III.C may be used, along with the computer program QRANGE. Exact analytical results for a 2nd order

system were given for (III-2.E) in (III-6.E). An extended stability bounding criteria, subject to the restrictions given in section III.B is given in (III-6.B). Although restrictive in when it may be applied, such a technique does allow the designer more freedom in the transient error selection.

The effects of stochastic noise on both inputs and states simplify to the need to minimize (IV-10.A). Error sensitivity under noise reduces to an evaluation of (IV-7.B) and (IV-8.B).

In section IV.D an adjustment technique to insure time invariant error dynamics was presented. The major results are presented in (IV-10.D), (IV-12.D), (IV-13.D), (IV-14.D), and (IV-18.D).

Using the equations outlined in this section, a control engineer with only a background in classical control design could easily design an adaptive controller.

B. Conclusions

1. The non-linear time-varying adaptive gains can be analyzed in a linear fashion such that only classical control knowledge is required.
2. The basic design and analysis of MRAS controllers can be reduced to a series of simple computer programs suitable for interactive terminal use, relegating drudgery work to computer aided design (CAD) studies and allowing for maximum flexibility and design by the design engineer.
3. Analysis of stochastic noise effects can be easily handled and an upper bound on the error norm obtained.

4. Analytical results from Chapter IV and simulation results from Chapter V indicate that even when many of the necessary conditions (i.e. model and plant of the same order, all states adapting, etc.) are not met in practice, overall response characteristics and the resulting plant stability are at worst only slightly affected, suggesting that adaptation offers a viable solution to unknown (and possibly time-varying) plant control.

5. Very little applied research has been performed in regard to practical implementation difficulties and there is much room for additional study in these areas.

Some of the possible areas for additional study include the use of state estimation for reconstructing missing plant states, CAD of the design phase, decoupling of multi-variable adaptive systems, and effects of various classes of nonlinearities (especially saturation) on Lyapunov stability constraints.

REFERENCES

- [1] Osborn, P. V., Whitaker, H. P., Keezer, A., "New Development In The Design of Adaptive Control Systems," IAS Paper No. 61-39.
- [2] Shackcloth, B. and Butchart, R., "Synthesis of Model Reference Adaptive Systems By Liapunov's Second Method," Proceedings of 1965 IFAC Symposium on Adaptive Control.
- [3] Parks, P. C., "Liapunov Redesign of Model-Reference Adaptive Control Systems," IEEE Transactions on Automatic Control, Vol. AC-14, pp. 362-367, July, 1966.
- [4] Phillipson, P. H., "Concerning Liapunov Redesign of Model Reference Adaptive Control Systems," IEEE Transactions on Automatic Control (Correspondence), Vol. AC-12, p. 625, October, 1967.
- [5] Winsor, C. A., Roy, R. J., "Design of Model-Reference Adaptive Control Systems by Liapunov's Second Method," IEEE Transactions Automatic Control (Correspondence) Vol. AC-13, p. 204, April, 1968.
- [6] Gilbert, J. W., Monopoli, R. V., and Price, C. F., "Improved Convergence and Increased Flexibility in the Design of Model-Reference Adaptive Control Systems," 1970 IEEE Symposium on Adaptive Processes, Decision and Control, Austin, Texas, December, 1970.
- [7] Boland, J. S. and Sutherlin, D. W., "Model-Reference Adaptive Control System Design Technique," ASME Journal on Dynamic Systems Measurement and Control, to be published December, 1973,
- [8] Gilbert, J. W. and Monopoli, R. V., "Parameter Adaptive Control Of A Class Of Time-Varying Plants," Fifth Annual Princeton Conference on Information Sciences and Systems, Princeton, New Jersey, March, 1971.
- [9] Schooley, D. J., "Model-Referenced Adaptive Control of Plants With Noise and Inaccessible State Vector," Ph.D. Dissertation, University of Missouri - Rolla, 1970.
- [10] Lindorff, D. P., "Effects of Incomplete Adaptation and Disturbance in Adaptive Control," 1972 Joint Automatic Control Conference, Stanford University, August, 1972.

- [11] Boland, J. S. and Colburn, B. K., "Adaptive Attitude Control of the Re-Entering Space Shuttle Vehicle," The Applications of Control Theory to Modern Weapons Systems, Naval Weapons Center, China Lake, California, May, 1973.
- [12] Shahein, H. I. H., Ghonaimy, M. A. R., and Shen, D. W. C., "Accelerated Model-Reference Adaptation via Lyapunov and Steepest Descent Techniques," IEEE Transactions on Automatic Control (Short Paper) Vol. AC-17, pp. 125-128, February, 1972.
- [13] Kudva, P. and Narendra, K., "An Identification Procedure For Linear Multivariable Systems," Becton Center Technical Report CT-48, Department of Engineering and Applied Science, Yale University, New Haven, Connecticut.
- [14] "Luders, G. and Narendra, K., "An Adaptive Observer and Identifier For a Multivariable Linear System," Becton Center Technical Report CT-54, Department of Engineering and Applied Science, Yale University, New Haven, Connecticut.
- [15] Kalman, R. E. and Bertram, J. E., "Control Systems Analysis and Design Via the 'Second Method' of Lyapunov, Part I: Continuous Time Systems," Transactions ASME, Vol. 82, Series D, No. 2., pp. 371-393. June, 1960.
- [16] Porter, B. and Tatnall, M. L., "Performance Characteristics of Multi-Variable Model-Reference Adaptive Control Systems Synthesized by Liapunov's Direct Method," International Journal on Control, Vol. 10, No. 3, pp. 241-257, 1969.
- [17] DeRusso, Roy, Close, State Variables For Engineers, John Wiley and Sons, Inc., New York, 1965, pp. 519-520.
- [18] Hsu, Meyer, Modern Control Principles and Applications, McGraw-Hill, New York, 1968, pp. 349-352.
- [19] Kleinman, D. L., "An Iterative Technique For Ricatti Equation Computation," Bolt Beronek and Newman Inc., Technical Memorandum No. DLK-1, June 30, 1970.
- [20] Morgan, B. S., "Sensitivity Analysis and Synthesis of Multivariable Systems," IEEE Transactions on Automatic Control (Correspondence), Vol. AC-13, pp. 129-131, February, 1968.
- [21] Asseo, S. J., "Phase-Variable Canonical Transformation of Multicontroller Systems," IEEE Transactions on Automatic Control (Correspondence), Vol. AC-13, pp. 129-131, February, 1968.

- [22] Luenberger, D. G., "Canonical Forms For Linear Multivariable Systems," IEEE Transactions on Automatic Control (Short Paper), Vol. AC-12, pp. 290-293, June, 1967.

- [23] Boland, J. S. and Drinkard, K. M., "Comparison of Thruster Configurations in Attitude Control Systems", Fourth Technical Report, Contract NAS8-26580, Engineering Experiment Station, Auburn University.

- [24] Mendel, J. E., "Computational Requirements For A Discrete Kalman Filter", IEEE Transactions on Automatic Control, vol. AC-16, no. 6, Dec. 1971, pp. 748-758.

APPENDICES

APPENDIX A

Derivation of Defining Equation for Determining Bounds on the q_{ij} Elements

Using (III-2.C), repeated below, a matrix equation will be developed for determining bounds on the q_{ij} elements.

$$A_m^T Q + Q A_m = - \begin{bmatrix} 2c_{11} & \phi & & \\ \phi & 2c_{22} & & \\ & & \dots & \\ & & & 2c_{nn} \end{bmatrix} \quad \text{(III-2.C)}$$

The c_{ii} entries are all greater than zero and can take on values in the range of 0^+ to ∞ . The case where the q_{ij} 's are not necessarily equal will now be used to obtain generalized ratios of q_{ij}/q_{nn} and these ratios compared with those values obtained from a Routh-Hurwitz array. With A_m in the phase variable form (III-2.C) is computed as

$$\begin{bmatrix} 0 & 0 & 0 & \dots & -a_{n1}^m \\ 1 & 0 & 0 & \dots & -a_{n2}^m \\ 0 & 1 & 0 & \dots & \cdot \\ \cdot & \cdot & \cdot & \cdot & \cdot \\ \cdot & \cdot & 1 & \cdot & \cdot \\ \cdot & \cdot & \cdot & \cdot & \cdot \\ 0 & 0 & 0 & \dots & 1 - a_{nn}^m \end{bmatrix} \begin{bmatrix} q_{11} & q_{12} & \dots & q_{1n} \\ q_{21} & q_{22} & \dots & q_{2n} \\ \cdot & & & \cdot \\ \cdot & & & \cdot \\ \cdot & & & \cdot \\ \cdot & & & \cdot \\ q_{n1} & q_{n2} & \dots & q_{nn} \end{bmatrix} +$$

$$\begin{bmatrix} q_{11} & q_{12} & \dots & q_{1n} \\ q_{21} & q_{22} & \dots & q_{2n} \\ \vdots & \vdots & \ddots & \vdots \\ q_{n1} & q_{n2} & \dots & q_{nn} \end{bmatrix} \begin{bmatrix} 0 & 1 & 0 & 0 & \dots & 0 \\ 0 & 0 & 1 & 0 & \dots & \\ 0 & 0 & 0 & 1 & \dots & 0 \\ \vdots & \vdots & \vdots & \vdots & \ddots & \vdots \\ -a_{n1}^m & -a_{n2}^m & \dots & -a_{nn}^m \end{bmatrix} = -C \tag{A-1}$$

Expanding, (A-1) simplifies to (A-2) shown on the following page. The left hand side forms a symmetric matrix, so when equating the matrices term by term there are only $n(n+1)/2$ linearly independent equations. Using the fact that

$$A_m^T Q + QA_m = [b_{ij}]$$

where $b_{ij} = b_{ji}$

the equations are

$$\left. \begin{aligned} -2q_{1n} a_{n1}^m &= -2c_{11} \\ q_{11} - q_{1n} a_{n2}^m - q_{2n} a_{n1}^m &= 0 \\ q_{12} - q_{1n} a_{n3}^m - q_{3n} a_{n1}^m &= 0 \\ q_{13} - q_{1n} a_{n4}^m - q_{4n} a_{n1}^m &= 0 \\ \vdots & \\ q_{1(n-1)} - q_{1n} a_{nn}^m - q_{nn} a_{n1}^m &= 0 \end{aligned} \right\} n \text{ terms} \tag{A-3}$$

$$\begin{bmatrix}
 -q_{n1} a_{n1}^m & -q_{n2} a_{n1}^m & \dots & -q_{nn} a_{n1}^m \\
 q_{11} - q_{n1} a_{n2}^m & q_{12} - q_{n2} a_{n2}^m & \dots & q_{1n} - q_{nn} a_{n2}^m \\
 q_{21} - q_{n1} a_{n3}^m & q_{22} - q_{n2} a_{n3}^m & \dots & q_{2n} - q_{nn} a_{n3}^m \\
 \vdots & \vdots & & \vdots \\
 q_{(n-1)1} - q_{n1} a_{nn}^m & q_{(n-1)2} - q_{n2} a_{nn}^m & \dots & q_{(n-1)n} - q_{nn} a_{nn}^m
 \end{bmatrix} +$$

$$\begin{bmatrix}
 -q_{1n} a_{n1}^m & q_{11} - q_{1n} a_{n2}^m & \dots & q_{1(n-1)} - q_{1n} a_{nn}^m \\
 -q_{2n} a_{n1}^m & q_{21} - q_{2n} a_{n2}^m & \dots & q_{2(n-1)} - q_{2n} a_{nn}^m \\
 -q_{3n} a_{n1}^m & q_{31} - q_{3n} a_{n2}^m & \dots & q_{3(n-1)} - q_{3n} a_{nn}^m \\
 \vdots & \vdots & & \vdots \\
 -q_{nn} a_{n1}^m & q_{n1} - q_{nn} a_{n2}^m & \dots & q_{n(n-1)} - q_{nn} a_{nn}^m
 \end{bmatrix} = \begin{bmatrix}
 2c_{11} & & & \\
 & 2c_{22} & & \emptyset \\
 & & \emptyset & 2c_{33} \\
 & & & \ddots \\
 & & & & 2c_{nn}
 \end{bmatrix}$$

(A-2)

$$b^T = \begin{bmatrix} q_{11} & q_{12} & q_{13} & \dots & q_{22} & q_{23} & q_{24} & \dots & 0 & \dots & q_{nn} \\ -c_{11} & 0 & 0 & \dots & -c_{22} & 0 & 0 & \dots & 0 & \dots & -c_{nn} \end{bmatrix} \quad (A-6)$$

For the general case, the entries in the A and b matrices of (A-4) are very detailed, hence an explanation is in order.

A may be partitioned into n sub-matrices, the sub matrices decreasing in size from $n \times m$ to $1 \times m$ in steps one 1,

$$A = \begin{bmatrix} A^{(1)} \\ \text{---} \\ A^{(2)} \\ \text{---} \\ \vdots \\ \text{---} \\ A^{(m)} \end{bmatrix}$$

$$A^{(3)} = \begin{bmatrix} (n-2) \times m & q_{11} & \dots & q_{1n} & \dots & q_{23} & \dots & \dots & q_{2n} & \dots & q_{3(n-1)} & q_{3n} & \dots & q_{nn} \\ 0 & 0 & & 1 & 1 & & & & \dots & \dots & & -a_{n3}^m & \dots & 0 \\ \vdots & & & & & & & & & & & -a_{n4}^m & & \\ \vdots & & & & & & & & 1 & 1 & & \vdots & & \\ \vdots & & & & & & & & & & & -a_{nn} & & -a_{n3}^m \end{bmatrix}$$

$$A^{(n)} = \begin{bmatrix} \vdots \\ \vdots \\ \vdots \end{bmatrix}$$

These $A^{(k)}$ sub-matrices may be generated according to 4 basic rules. To simplify the explanations, elemental locations will be referred to in terms of the row number of the k th sub matrix and the column location by the location of the q_{ij} th element, i.e.

$$\begin{array}{cccccccc}
 q_{11} & q_{12} & q_{13} & \cdots & q_{1n} & \cdots & q_{2n} & \cdots & q_{3n} & \cdots & q_{nn} \\
 & & & & A^{(1)} & & & & & & \\
 & & & & & & A^{(2)} & & & & \\
 & & & & & & \cdot & & & & \\
 & & & & & & \cdot & & & & \\
 & & & & & & \cdot & & & & \\
 & & & & & & & & A^{(n)} & & \\
 & & & & & & & & & &
 \end{array}$$

The q_{ij} th element in \underline{x} can be determined from

$$x_{(p)} = q_{ij} \quad , \quad p = (j - i + 1) + \sum_{\ell=0}^{i-2} (n-\ell)$$

where $\sum_{\ell=0}^{-1} (n-\ell) \triangleq 0$ by definition

The four rules for construction of the $A^{(k)}$ are:

(1) diagonal of 1's starting in row 2 of q_{kk} , $k = 2, 3, \dots, n$

(2) diagonal of 1's starting in $q_{(k-1)k}$, $k = 1, 2, \dots, n$

where q_{01} is disregarded

(3) in q_{kn} column, sequence of $-a_{nj}^m$ $j = k, k+1, \dots, n$

(4) "diagonal like" array of $-a_{nk}^m$ from q_{kn} entry to q_{nn} entry.

As an example of this technique, for the fourth order plant-model system, where

$$A_m = \begin{bmatrix} 0 & 1 & 0 & 0 \\ 0 & 0 & 1 & 0 \\ 0 & 0 & 0 & 1 \\ -a_{41}^m & -a_{42}^m & -a_{43}^m & -a_{44}^m \end{bmatrix}, \quad Q_{4 \times 4} \text{ Symmetric}$$

the resulting "A" matrix of $A\underline{x} = \underline{b}$ is given on the following page.

	q_{11}	q_{12}	q_{13}	q_{14}	q_{22}	q_{23}	q_{24}	q_{33}	q_{34}	q_{44}
$A^{(1)}$	$\begin{bmatrix} 0 \\ 1 \\ 0 \\ 0 \end{bmatrix}$	$\begin{bmatrix} 0 \\ 0 \\ 1 \\ 0 \end{bmatrix}$	$\begin{bmatrix} 0 \\ 0 \\ 0 \\ 1 \end{bmatrix}$	$\begin{bmatrix} -a_{41}^m \\ -a_{42}^m \\ -a_{43}^m \\ -a_{44}^m \end{bmatrix}$	$\begin{bmatrix} 0 \\ 0 \\ 0 \\ 0 \end{bmatrix}$	$\begin{bmatrix} 0 \\ 0 \\ 0 \\ 0 \end{bmatrix}$	$\begin{bmatrix} 0 \\ -a_{41}^m \\ 0 \\ 0 \end{bmatrix}$	$\begin{bmatrix} 0 \\ 0 \\ 0 \\ 0 \end{bmatrix}$	$\begin{bmatrix} 0 \\ 0 \\ -a_{41}^m \\ 0 \end{bmatrix}$	$\begin{bmatrix} 0 \\ 0 \\ 0 \\ -a_{41}^m \end{bmatrix}$
$A^{(2)}$	$\begin{bmatrix} 0 \\ 0 \\ 0 \end{bmatrix}$	$\begin{bmatrix} 1 \\ 0 \\ 0 \end{bmatrix}$	$\begin{bmatrix} 0 \\ 1 \\ 0 \end{bmatrix}$	$\begin{bmatrix} 0 \\ 0 \\ 1 \end{bmatrix}$	$\begin{bmatrix} 0 \\ 1 \\ 0 \end{bmatrix}$	$\begin{bmatrix} 0 \\ 0 \\ 1 \end{bmatrix}$	$\begin{bmatrix} -a_{42}^m \\ -a_{43}^m \\ -a_{44}^m \end{bmatrix}$	$\begin{bmatrix} 0 \\ 0 \\ 0 \end{bmatrix}$	$\begin{bmatrix} 0 \\ -a_{42}^m \\ 0 \end{bmatrix}$	$\begin{bmatrix} 0 \\ 0 \\ -a_{42}^m \end{bmatrix}$
$A^{(3)}$	$\begin{bmatrix} 0 \\ 0 \end{bmatrix}$	$\begin{bmatrix} 0 \\ 0 \end{bmatrix}$	$\begin{bmatrix} 0 \\ 0 \end{bmatrix}$	$\begin{bmatrix} 0 \\ 0 \end{bmatrix}$	$\begin{bmatrix} 0 \\ 0 \end{bmatrix}$	$\begin{bmatrix} 1 \\ 0 \end{bmatrix}$	$\begin{bmatrix} 0 \\ 1 \end{bmatrix}$	$\begin{bmatrix} 0 \\ 1 \end{bmatrix}$	$\begin{bmatrix} -a_{43}^m \\ -a_{44}^m \end{bmatrix}$	$\begin{bmatrix} 0 \\ -a_{43}^m \end{bmatrix}$
$A^{(4)}$	$\begin{bmatrix} 0 \end{bmatrix}$	$\begin{bmatrix} 0 \end{bmatrix}$	$\begin{bmatrix} 0 \end{bmatrix}$	$\begin{bmatrix} 0 \end{bmatrix}$	$\begin{bmatrix} 0 \end{bmatrix}$	$\begin{bmatrix} 0 \end{bmatrix}$	$\begin{bmatrix} 0 \end{bmatrix}$	$\begin{bmatrix} 0 \end{bmatrix}$	$\begin{bmatrix} 1 \end{bmatrix}$	$\begin{bmatrix} -a_{44}^m \end{bmatrix}$

APPENDIX B

Phase Variable Transformation

The derivation of the perturbed error characteristic equation given in (II-16.B) requires that the plant and model state matrices be in the phase variable canonical form

$$A_m = \begin{bmatrix} 0 & 1 & 0 & \dots & 0 \\ 0 & 0 & 1 & \dots & 0 \\ \vdots & \vdots & \vdots & \ddots & \vdots \\ -a_{n0}^m & -a_{n1}^m & -a_{n2}^m & \dots & -a_{n(n-1)}^m \end{bmatrix} \quad (B-1)$$

where

$$s^n + a_{n(n-1)}^m s^{n-1} + a_{n(n-2)}^m s^{n-2} + \dots + a_{n1}^m s + a_{n0}^m = 0 \quad (B-2)$$

represents the characteristic equation of the model. The conditions under which a transformation exists which will result in a coordinate transformation from one state space into another is given in this Appendix, along with the transformation.

Consider the time-invariant n^{th} order model

$$\underline{\dot{z}} = K\underline{z} + D\underline{u} \quad (B-3)$$

where

\underline{u} is $r \times 1$ input vector

K is $n \times n$ matrix not in the form of (B-1)

D is $n \times r$ matrix

\underline{z} - $n \times 1$ state vector

D can be written in the form

$$D = \begin{bmatrix} | & | & \dots & | \\ d_1 & d_2 & \dots & d_r \\ | & | & & | \end{bmatrix} \quad (B-4)$$

where the d_i $i = 1, 2, \dots, r$ are the column vectors of D . It is desired to determine the transformation matrix T , such that

$$\underline{z} = T\underline{x} \quad (B-5)$$

and the conditions under which T exists. A necessary and sufficient condition for (B-3) to be transformed to the form

$$\underline{x} = A\underline{x} + B\underline{u} \quad (B-6)$$

where A is in the form of (B-1), is that the system be controllable.

This is true if at least one of the matrices Q_i has rank n ,

where

$$Q_i = \begin{bmatrix} | & | & | & \dots & | & | \\ d_i & Kd_i & K^2d_i & \dots & K^{(n-1)}d_i & d_i \\ | & | & | & & | & | \end{bmatrix} \quad i = 1, 2, \dots, r \quad (B-7)$$

and Q_i is the controllability matrix of the system in (B-3). If one of the Q_i has rank n , then a transformation matrix T will exist such

that

$$\underline{z} = T\underline{x}$$

and T will transform a system in the form of (B-3) into the form of (B-6), where the matrices K, A and D, B are related by

$$A = T^{-1}KT \quad B = T^{-1}D \quad (\text{B-8})$$

The B matrix is of the form

$$B = \begin{bmatrix} b_{11} & b_{12} & \dots & b_{1r} \\ b_{21} & b_{22} & \dots & b_{2r} \\ \vdots & & & \\ \vdots & & & \\ b_{n1} & b_{n2} & \dots & b_{nr} \end{bmatrix} = \begin{bmatrix} | & | & \dots & | \\ b_1 & b_2 & \dots & b_r \\ | & | & & | \end{bmatrix} \quad (\text{B-9})$$

where in general at least one of the column vectors b_i is of the form

$$b_i = \begin{pmatrix} 0 \\ 0 \\ \vdots \\ \vdots \\ 1 \end{pmatrix} \quad i = 1, 2, \dots, r \quad (\text{B-10})$$

A straightforward technique for computing T is given in [20].

If (B-3) is such that K is in the form of (B-1), then no transformation is required. In this case, D (or B) may consist of any combination of $n \times r$ terms. In general, when the plant model dynamics are such that the system matrix is in phase-variable form, then the system flow model will appear as in Figure (B-1).

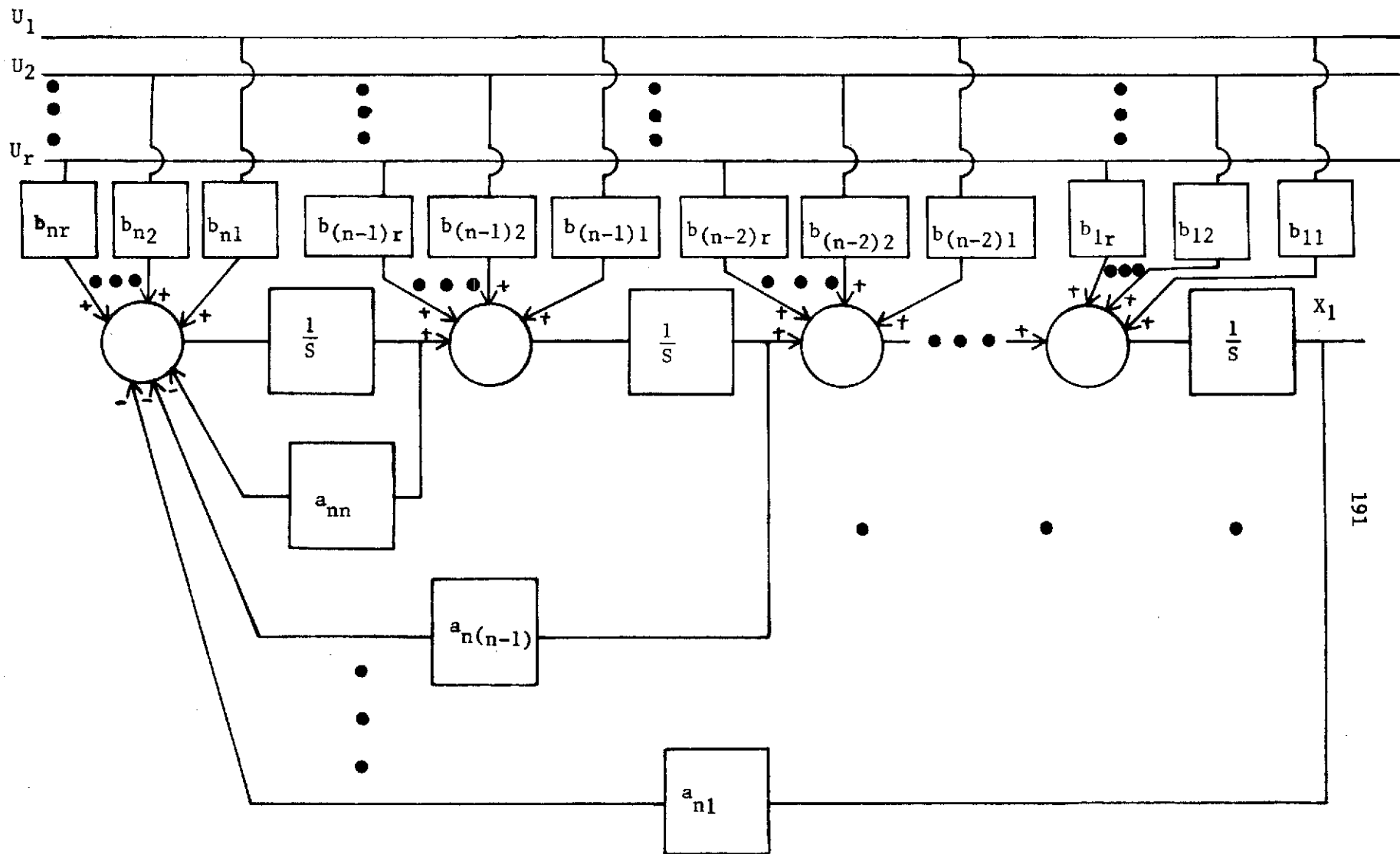


Figure (B-1) Flow Diagram of a phase-variable canonical form.

In order to possess physical meaning, the artificial states \underline{x} must have a one-to-one relationship with those of the original state space. Assuming that one particular state of the original system is the major "output" (e.g., an aerospace vehicle attitude, the flow rate of a chemical in a refinery, etc.) and

$$T = \begin{bmatrix} -t_{1r}- \\ -t_{2r}- \\ \cdot \\ \cdot \\ -t_{nr}- \end{bmatrix} \quad (B-11)$$

is such that

$$t_{1r} = (1 \quad 0 \quad 0 \cdots 0) \quad (B-12)$$

then there will be a one-to-one correspondence between the actual state z_1 and the artificial state x_1 . In a more practical sense, if the "0" elements of (B-10) were very small (with respect to 1) non-zero numbers, the design results using the error characteristic equation with the artificial states should provide reasonable engineering results for the actual state z_1 . Note, however, that there need not be any simple relation between z_i and x_i if $i \geq 2$.

A positive aspect of using the configuration given in (B-1) and (B-9) is that a well defined transformation matrix T can, in general, be determined for a multivariable system such that the system matrix is in the phase variable Frobenius form. In most application work involving multivariable systems, a constraint on the "B" matrix as to the

particular form it may possess severely limits the form the "A" matrix may take on [21, 22]. The linearization procedure for the error equation, however, places no restrictions on the form of the B matrix. The resulting transformation is non-unique, as is to be expected with multivariable systems, but is straightforward in application.

APPENDIX C

Derivation of an Error Bound with State and Input Noises Present

The noisy plant discussed in Chapter IV is the basis for the derivation of the following gross error bound. The model and plant equations are

$$\underline{x}_m = A_m \underline{x}_m + B_m \underline{r}(t) \quad (C-1)$$

$$\underline{x}_p = A_0 \underline{x}_p + K(t) \hat{\underline{x}}_p(t) + B_p \underline{u}(t) \quad (C-2)$$

$$\hat{\underline{e}} = \underline{x}_m - \hat{\underline{x}}_p(t) = \underline{e} - \underline{\eta}(t) \quad (C-3)$$

Differentiating (C-3) with respect to time and substituting in (C-2) and (C-1),

$$\dot{\hat{\underline{e}}} = A_m \dot{\underline{x}}_m + B_m \dot{\underline{r}}(t) - [A_0 \dot{\underline{x}}_p + K(t) \dot{\hat{\underline{x}}}_p(t) + B_p \dot{\underline{u}}(t) + \dot{\eta}(t)] \quad (C-4)$$

Defining

$$A_p = A_0 + K(t) \quad (C-5)$$

$$\underline{u}(t) = \underline{r}(t) + \underline{v}(t) \quad (C-6)$$

$$\hat{\underline{x}}_p(t) = \underline{x}_p + \underline{\eta}(t) \quad (C-7)$$

(C-4) can be written as

$$\begin{aligned} \dot{\hat{\underline{e}}} = & A_m \dot{\underline{x}}_m + B_m \dot{\underline{r}}(t) - [A_p \dot{\hat{\underline{x}}}_p + B_p \dot{\underline{r}}(t) + B_p \dot{\underline{v}}(t) - A_0 \dot{\underline{\eta}}(t) + \dot{\underline{\eta}}(t)] \\ & + A_m \dot{\underline{x}}_p - A_m \dot{\hat{\underline{x}}}_p \end{aligned} \quad (C-8)$$

Combining terms, (C-8) simplifies to

$$\dot{\underline{e}} = \underline{A}_m \underline{e} + [\underline{A}_m - \underline{A}_p] \underline{\hat{x}}_p + [\underline{B}_m - \underline{B}_p] \underline{r}(t) - \underline{B}_p \underline{v}(t) + \underline{A}_0 \underline{\eta}(t) - \underline{\eta}(t)$$

$$\dot{\underline{e}} = \underline{A}_m \underline{e} + \underline{A} \underline{\hat{x}}_p + \underline{B} \underline{r}(t) + (-\underline{B}_p \underline{v}(t) + \underline{A}_0 \underline{\eta}(t) - \underline{\eta}(t)) \quad (\text{C-9})$$

(C-9) is the noise-presence equivalent to the noise free case of (II-7.A), where now the external input is $\underline{r}(t)$ instead of $\underline{u}(t)$.

The Lyapunov function for the Boland and Sutherland [7] method is now modified so as to be p.d. in \underline{e} , $\underline{u}(t)$, and $\underline{\hat{x}}_p$, the available error, input and plant states

$$\begin{aligned} V = & \underline{\hat{e}}^T Q \underline{\hat{e}} + \sum_{i=1}^n \sum_{j=1}^n \frac{1}{\alpha_{ij}} \left\{ a_{ij} + \beta_{ij} \sum_{k=1}^n \hat{e}_k q_{ki} \hat{x}_{pj} \right. \\ & \left. + \rho_{ij} \frac{d}{dt} \sum_{k=1}^n \hat{e}_k q_{ki} \hat{x}_{pj} \right\}^2 + \sum_{i=1}^n \sum_{j=1}^n \rho_{ij} \left[\sum_{k=1}^n \hat{e}_k q_{ki} \hat{x}_{pj} \right]^2 \\ & + \sum_{i=1}^n \sum_{j=1}^r \frac{1}{\gamma_{ij}} \left\{ b_{ij} + \delta_{ij} \sum_{k=1}^n \hat{e}_k q_{ki} u_j + \sigma_{ij} \frac{d}{dt} \sum_{k=1}^n \hat{e}_k q_{ki} u_j \right\}^2 \\ & + \sum_{i=1}^n \sum_{j=1}^r \sigma_{ij} \left[\sum_{k=1}^n \hat{e}_k q_{ki} u_j \right]^2 \end{aligned} \quad (\text{C-10})$$

where the notation is analogous to that in Chapter II. The time derivative of V is

$$\dot{V} = \underline{\hat{e}}^T \dot{Q} \underline{\hat{e}} + \underline{\hat{e}}^T Q \dot{\underline{\hat{e}}} + 2 \sum_{i=1}^n \sum_{j=1}^n \frac{a_{ij} \dot{a}_{ij}}{\alpha_{ij}}$$

$$\begin{aligned}
& + 2 \sum_{i=1}^n \sum_{j=1}^r \frac{\sigma_{ij}}{\gamma_{ij}} b_{ij} \frac{d^2}{dt^2} \sum_{k=1}^n \dot{e}_{k^q_{ki} u_j} \\
& + 2 \sum_{i=1}^n \sum_{j=1}^r \frac{\delta_{ij} \sigma_{ij}}{\gamma_{ij}} \left[\frac{d}{dt} \sum_{k=1}^n \dot{e}_{k^q_{ki} u_j} \right]^2 \\
& + 2 \sum_{i=1}^n \sum_{j=1}^r \frac{\delta_{ij} \sigma_{ij}}{\gamma_{ij}} \sum_{k=1}^n \dot{e}_{k^q_{ki} u_j} \frac{d^2}{dt^2} \sum_{k=1}^n \dot{e}_{k^q_{ki} u_j} \\
& + 2 \sum_{i=1}^n \sum_{j=1}^r \frac{\delta_{ij}^2}{\gamma_{ij}} \sum_{k=1}^n \dot{e}_{k^q_{ki} u_j} \frac{d}{dt} \sum_{k=1}^n \dot{e}_{k^q_{ki} u_j} \\
& + 2 \sum_{i=1}^n \sum_{j=1}^r \frac{\sigma_{ij}^2}{\gamma_{ij}} \frac{d}{dt} \sum_{k=1}^n \dot{e}_{k^q_{ki} u_j} \frac{d^2}{dt^2} \sum_{k=1}^n \dot{e}_{k^q_{ki} u_j} \\
& + 2 \sum_{i=1}^n \sum_{j=1}^n \rho_{ij} \sum_{k=1}^n \dot{e}_{k^q_{ki} x_{pj}} \frac{d}{dt} \sum_{k=1}^n \dot{e}_{k^q_{ki} x_{pj}} \\
& + 2 \sum_{i=1}^n \sum_{j=1}^n \sigma_{ij} \sum_{k=1}^n \dot{e}_{k^q_{ki} u_j} \frac{d}{dt} \sum_{k=1}^n \dot{e}_{k^q_{ki} u_j} \tag{C-11}
\end{aligned}$$

With \dot{a}_{ij} and b_{ij} chosen to implement physically realizable controls,

$$\begin{aligned}
\dot{a}_{ij} &= -\alpha_{ij} \sum_{k=1}^n \dot{e}_{k^q_{ki} x_{pj}} - \beta_{ij} \frac{d}{dt} \sum_{k=1}^n \dot{e}_{k^q_{ki} x_{pj}} \\
&\quad - \rho_{ij} \frac{d^2}{dt^2} \sum_{k=1}^n \dot{e}_{k^q_{ki} x_{pj}} \tag{C-12}
\end{aligned}$$

$$\begin{aligned}
& + 2 \sum_{i=1}^n \sum_{j=1}^n \frac{\beta_{ij}}{\alpha_{ij}} \sum_{k=1}^n \dot{e}_{kq_{ki}} x_{pj} \\
& + 2 \sum_{i=1}^n \sum_{j=1}^n \frac{\rho_{ij}}{\alpha_{ij}} a_{ij} \frac{d}{dt} \sum_{k=1}^n \dot{e}_{kq_{ki}} x_{pj} \\
& + 2 \sum_{i=1}^n \sum_{j=1}^n \frac{\rho_{ij}}{\alpha_{ij}} a_{ij} \frac{d^2}{dt^2} \sum_{k=1}^n \dot{e}_{kq_{ki}} x_{pj} \\
& + 2 \sum_{i=1}^n \sum_{j=1}^n \frac{\beta_{ij} \rho_{ij}}{\alpha_{ij}} \left[\frac{d}{dt} \sum_{k=1}^n \dot{e}_{kq_{ki}} x_{pj} \right]^2 \\
& + 2 \sum_{i=1}^n \sum_{j=1}^n \frac{\beta_{ij} \rho_{ij}}{\alpha_{ij}} \sum_{k=1}^n \dot{e}_{kq_{ki}} x_{pj} \frac{d^2}{dt^2} \sum_{k=1}^n \dot{e}_{kq_{ki}} x_{pj} \\
& + 2 \sum_{i=1}^n \sum_{j=1}^n \frac{\beta_{ij}^2}{\alpha_{ij}} \sum_{k=1}^n \dot{e}_{kq_{ki}} x_{pj} \frac{d}{dt} \sum_{k=1}^n \dot{e}_{kq_{ki}} x_{pj} \\
& + 2 \sum_{i=1}^n \sum_{j=1}^r \frac{\rho_{ij}^2}{\alpha_{ij}} \frac{d}{dt} \sum_{k=1}^n \dot{e}_{kq_{ki}} x_{pj} \frac{d^2}{dt^2} \sum_{k=1}^n \dot{e}_{kq_{ki}} x_{pj} \\
& + 2 \sum_{i=1}^n \sum_{j=1}^r \frac{\dot{b}_{ij} b_{ij}}{\gamma_{ij}} + 2 \sum_{i=1}^n \sum_{j=1}^r \frac{\delta_{ij}}{\gamma_{ij}} \dot{b}_{ij} \sum_{k=1}^n \dot{e}_{kq_{ki}} u_j \\
& + 2 \sum_{i=1}^n \sum_{j=1}^r \frac{\delta_{ij}}{\gamma_{ij}} b_{ij} \frac{d}{dt} \sum_{k=1}^n \dot{e}_{kq_{ki}} u_j \\
& + 2 \sum_{i=1}^n \sum_{j=1}^r \frac{\sigma_{ij}}{\gamma_{ij}} \dot{b}_{ij} \frac{d}{dt} \sum_{k=1}^n \dot{e}_{kq_{ki}} u_j
\end{aligned}$$

$$\begin{aligned} \dot{b}_{ij} = & -\gamma_{ij} \sum_{k=1}^n \dot{\epsilon}_{kq_{ki}} u_j - \delta_{ij} \frac{d}{dt} \sum_{k=1}^n \epsilon_{kq_{ki}} u_j \\ & - \sigma_{ij} \frac{d^2}{dt^2} \sum_{k=1}^n \epsilon_{kq_{ki}} u_j \end{aligned} \quad (C-13)$$

Substituting a_{ij} and b_{ij} into V results in

$$\begin{aligned} V = & \underline{\hat{e}}^T (A_m^T Q + Q A_m) \underline{\hat{e}} + \underline{\hat{x}}_p^T (A_m - A_p)^T Q \underline{\hat{e}} + \underline{\hat{e}}^T Q (A_m - A_p) \underline{\hat{x}}_p \\ & + \underline{r}^T (B_m - B_p)^T Q \underline{\hat{e}} + \underline{\hat{e}}^T Q (B_m - B_p) \underline{r} - \underline{v}^T B_p^T Q \underline{\hat{e}} \\ & - \underline{\hat{e}}^T Q B_p \underline{v} + \underline{\eta}^T A_0^T Q \underline{\hat{e}} + \underline{\hat{e}}^T Q A_0 \underline{\eta} - \underline{\eta}^T Q \underline{\hat{e}} - \underline{\hat{e}}^T Q \underline{\eta} \\ & - 2 \sum_{i=1}^n \sum_{j=1}^n a_{ij} \sum_{k=1}^n \epsilon_{kq_{ki}} \hat{x}_{pj} - 2 \sum_{i=1}^n \sum_{j=1}^n \beta_{ij} \left(\sum_{k=1}^n \epsilon_{kq_{ki}} \hat{x}_{pj} \right)^2 \\ & - 2 \sum_{i=1}^n \sum_{j=1}^r b_{ij} \sum_{k=1}^n \epsilon_{kq_{ki}} u_j - 2 \sum_{i=1}^n \sum_{j=1}^r \delta_{ij} \left(\sum_{k=1}^n \epsilon_{kq_{ki}} u_j \right)^2 \end{aligned}$$

which reduces to

$$\begin{aligned} V = & \underline{\hat{e}}^T (A_m^T Q + Q A_m) \underline{\hat{e}} - 2 \sum_{i=1}^n \sum_{j=1}^n \beta_{ij} \left(\sum_{k=1}^n \epsilon_{kq_{ki}} \hat{x}_{pj} \right)^2 \\ & - 2 \sum_{i=1}^n \sum_{j=1}^r \delta_{ij} \left(\sum_{k=1}^n \epsilon_{kq_{ki}} u_j \right)^2 + 2 \underline{\hat{e}}^T Q [A_0 \underline{\eta} - \underline{\eta} - B_m \underline{v}] \end{aligned} \quad (C-14)$$

This function, without further information, is of an indefinite form.

By using a bounding process [9], (C-14) can be written as

$$\begin{aligned}
V \leq & + \underline{\hat{e}}^T (A_m + Q + QA_m) \underline{\hat{e}} - 2 \sum_{i=1}^n \sum_{j=1}^n \beta_{ij} \left(\sum_{k=1}^n \hat{e}_k q_{ki} x_{pj} \right)^2 \\
& - 2 \sum_{i=1}^n \sum_{j=1}^r \delta_{ij} \left(\sum_{k=1}^n \hat{e}_k q_{ki} u_j \right)^2 + ||Q\underline{\hat{e}}|| \Gamma \quad (C-15)
\end{aligned}$$

where Γ is defined by (IV-7.A), $(A_m^T Q + QA_m)$ forms a symmetric matrix, so equating

$$H^T H = -(A_m^T Q + QA_m)$$

then

$$\Gamma ||Q\underline{\hat{e}}|| = \Gamma ||QH^{-1}H\underline{\hat{e}}|| \leq \Gamma ||QH^{-1}|| ||H\underline{\hat{e}}|| \quad (C-16)$$

If

$$||H\underline{\hat{e}}|| > \Gamma ||Q|| ||H^{-1}|| \geq \Gamma ||QH^{-1}|| \quad (C-17)$$

then

$$\Gamma ||Q\underline{\hat{e}}|| \leq \Gamma ||QH^{-1}|| ||H\underline{\hat{e}}|| < ||H\underline{\hat{e}}||^2 = -\underline{\hat{e}}^T (A_m^T Q + QA_m) \underline{\hat{e}} \quad (C-18)$$

and V will consequently be negative definite.

If A is an $n \times n$ matrix and \underline{x} an $n \times 1$ vector, the norm of $A\underline{x}$ will be defined to be

$$||A\underline{x}|| \leq M ||\underline{x}|| \quad (C-19)$$

where M is the smallest positive number for which (C-19) holds, where $||\underline{x}||$ is the Euclidean norm. Using (C-18)

$$\lambda^{\frac{1}{2}} (-A_m^T Q - QA_m)_{\min} ||\underline{\hat{e}}|| \leq ||H\underline{\hat{e}}|| \leq \lambda^{\frac{1}{2}} (-A_m^T Q - QA_m)_{\max} ||\underline{\hat{e}}|| \quad (C-20)$$

where $\lambda(A)$ is an eigenvalue of the matrix A. Defining

$$\begin{aligned} ||Q|| &= \lambda(Q)_{\max} \\ ||H^{-1}|| &= \frac{1}{\lambda^{\frac{1}{2}}(-A_m^T Q - QA_m)_{\min}} \end{aligned} \quad (C-21)$$

From (C-19) thru (C-21), (C-17) can be used to obtain

$$||\underline{\hat{e}}|| > \frac{\lambda(Q)_{\max}}{\lambda(-A_m^T Q - QA_m)_{\min}} \quad \Gamma = p \quad (C-22)$$

This represents an upper bound on the norm of the error vector $\underline{\hat{e}}$ in order to guarantee V is negative definite (n.d.). Very possibly $||\underline{e}||$ could be less than indicated by (C-22) and V still be n.d.; it is simply that nothing can be said then. Similarly, if for some $||\underline{\hat{e}}|| < p$ \dot{V} became positive definite then the equilibrium state would be unstable in the sense of Lyapunov and the plant would be driven such that the error $\underline{\hat{e}}$ increased to the point where \dot{V} was n.d..